Secretory granule exo-endocytosis studied in the neuroendocrine cell line PC12

Holroyd, Phillip

Award date:
2002

Awarding institution:
University of Bath

Max-Planck-Institute
for
Biophysical Chemistry

University of Bath
Dept. of
Biology and Biochemistry

Secretory Granule Exo-endocytosis Studied in the Neuroendocrine Cell Line PC12

Submitted by Phillip Holroyd

For the degree of PhD
Of the University of Bath
2002

ProQuest LLC
789 East Eisenhower Parkway
P.O. Box 1346
Ann Arbor, MI 48106-1346

Dedicated to:

"my family

and

other animals"

Contents

1. Summary

During exocytosis, secretory granules fuse with the plasma membrane and discharge their content into the extracellular space. To maintain cellular membrane balance the exocytosed membrane is then internalised by endocytosis in a co-ordinated fashion. While endocytosis by clathrin-coated vesicles is essential for membrane internalisation in neurones and secretory cells, the role and extent to which direct retrieval mechanisms are involved is still debated.

To investigate this, exo-endocytosis of single secretory granules was monitored in a cell-free assay (Avery et al., 2000). Plasma membrane sheets with attached secretory granules were prepared from PC12 cells and imaged by epi-fluorescence microscopy. Secretory granules were labelled using either acridine orange dye or GFP-labelled neuropeptide Y and imaged as bright fluorescent spots. Acridine orange provided a rapid and simple stain for secretory granules allowing exocytosis to be monitored as an "all or nothing" loss of fluorescent spots. A further characterisation of this system and several new approaches to monitor exocytosis are presented. Finally, as an alternative fluorescent marker, GFP labelled neuropeptide Y was used. Exocytosis was observed as a surprising pattern of fluorescence intensity changes, which suggest incomplete release of the labelled peptide upon exocytosis.

Further investigation revealed that a significant population of docked secretory granules fuse with the plasma membrane, take up fluid phase markers and are retrieved at the same position*. Thus, fusion

allows for complete discharge of small molecules (e.g. acridine orange) whereas GFP-labelled neuropeptide Y ($M_w \approx 35$ kDa) is only partially released. Such retrieved granules were preferentially associated with dynamin. Furthermore, re-capture is inhibited by GTPγS and by peptides known to block dynamin function. It is concluded that secretory granules can be re-captured by spatially coupled endocytosis without undergoing full fusion. Endocytosis requires dynamin and thus is biochemically distinct from SNARE-dependent exocytosis (Holroyd et al., 2002).

* Note – see also the work of Taraska et al. (2003) in living PC12 cells.

2. Foreword

It is something we can all relate to, the heightened sense of awareness, and racing of the heart that comes with having a shocking experience. When our brain receives sensory inputs, which are interpreted as danger, the hypothalamus stimulates (through nerve impulses) the adrenal glands. As a consequence, the cells of the adrenal glands co-ordinate the controlled release of chemical signals into the blood stream. It is these endocrine hormones that are responsible for the familiar fight or flight response. This is just one of many instances in which cells release signalling molecules in a rapid and highly regulated process.

At a cellular level these molecules, be they neurotransmitters, peptides or large proteins, are stored in a concentrated form within small membrane bound organelles or secretory granules. In order for their contents to be released these organelles must first move into a close apposition with the plasma membrane. This subsequently allows fusion of both plasma and vesicle membranes in response to external stimuli. The underlying process is the result of the highly conserved cellular mechanism of regulated exocytosis. In a separate, but closely linked, process the cell is able to compensate for increases in its surface area due to exocytosis. Here, membrane and protein are retrieved, in vesicles endocytosed from the plasma membrane, into the cytoplasm allowing it to be recycled.

3. Introduction

3.1 Exo- endocytosis - constitutive and regulated pathways

Exocytosis is the term used to describe the process of cellular secretion, or more specifically the release of (macro)-molecules mediated by the fusion of vesicles with the plasma membrane. It is possible to further distinguish exocytosis into constitutive and regulated activities (for review see Burgess and Kelly, 1987).

Constitutive secretion is an essential function of all eukaryotic cells and is vital to their viability. Molecules or material designated, as constitutive cargo is sorted in the Golgi apparatus, before leaving the trans-Golgi network in neatly packaged membrane bound vesicles. In order to reach the cell periphery these vesicles are actively transported via the microtubular cytoskeleton to their final destination at the sub-plasmalemma. Here the vesicles fuse (bilayer mixing) to the plasma membrane, integrating with it and, releasing their content. Thus, a constant flow of material is supplied to the cell membrane (protein and lipid) and extra-cellular environment. Although a net gain in cell surface area is required for growth, excess lipid and protein must be removed from the plasma membrane by constitutive endocytosis. Thus, these two processes acting in concert allow a constant turnover of cellular membranes. Together these housekeeping activities are vital to the functional health of the cell and tissue in which it resides.

Unlike its constitutive cousin, regulated exocytosis is tightly coupled to extracellular stimuli and is not found ubiquitously among cell types. Cells with a regulated secretory pathway include, among others, exocrine and endocrine cells, mast cells, lymphocytes, neutrophils, and neurones (Burgess and Kelly, 1987). The varied physiological stimuli that trigger regulated exocytosis depend on the cell type. Typically these stimuli lead to an increase in intracellular calcium and/ or other second messengers. In electrically excitable cells, like nerve and neuroendocrine cells, intracellular calcium concentrations increase by an influx of ions through voltage sensitive channels. In cells which lack such systems, hormones act via G-protein coupled receptors to generate second messenger molecules which lead to a release of calcium from intracellular stores (Hille, B. et al., 1999). Alternatively, the stimuli can lead to changes in protein phosphorylation states, which lead to a triggering of exocytosis. As with constitutive exocytosis, lipid and protein added to the plasma membrane must be recycled. This occurs through the tightly coupled process of compensatory endocytosis.

3.2 The secretory granule life cycle

3.2.1 Biogenesis

The organelles of the regulated secretory pathway are called secretory granules. The formation of mature secretory granules involves a series of discrete and unique events such as protein sorting, formation of immature secretory granules, pro-hormone processing and finally

homotypic fusion and re-modelling (for a review see Tooze et al., 2001). Proteins destined for regulated secretion become associated with specialised areas of the lumenal membrane in the *trans*-Golgi network. Here the proteins aggregate to form large multimers. At the points of aggregation the Golgi membrane coats and buds, eventually to be "pinched" off into the cytoplasm to form an immature secretory granule. During this process, membrane proteins required for the later maturation and function of the granule are incorporated. The immature secretory granules undergo homotypic fusion forming larger structures from which mature granules are subsequently re-modelled. In this final series of steps, excess membrane and proteins are removed leaving the secretory products packed tightly together as a typical dense core.

In a recent publication Kim et al. (2001) presented evidence that the secretory granule marker protein chromogranin A (CGA) is itself responsible for regulating secretory granule biogenesis. The use of anti-sense RNAs to down-regulate CGA expression in PC12 cells led to a profound lost of secretory granules. Further, over-expression of CGA in a mutant PC12 cell line lacking both CGA and a secretory pathway restored the secretory phenotype.

The mature granules are transported (as described for constitutive vesicles) to the cell periphery. Here large numbers of such vesicles gather in the cytoplasm at close proximity to the plasma membrane. Thus in response to a stimulus, such cells are able to discharge large amounts of material over a short period of time.

3.2.2 Exocytosis

The regulated exocytosis of secretory granules can be described as a cascade of protein-protein and protein-lipid interactions that finally lead to the fusion of granule and plasma membrane bilayers. Indeed, the number of proteins and interactions described in the literature has grown tremendously in the past decade. These include several highly conserved protein families believed to be required for all eukaryotic fusion events e.g. the SNAREs (SNAP (soluble N-ethylmaleimide-sensitive factor attachment protein) receptors), Sec1/Munc-18 related, and Rab proteins (for review see Jahn and Südhof, 1999). However, despite the large number of proteins implicated, the exact order of molecular steps that lead to exocytosis remains to be solved (see figure 1).

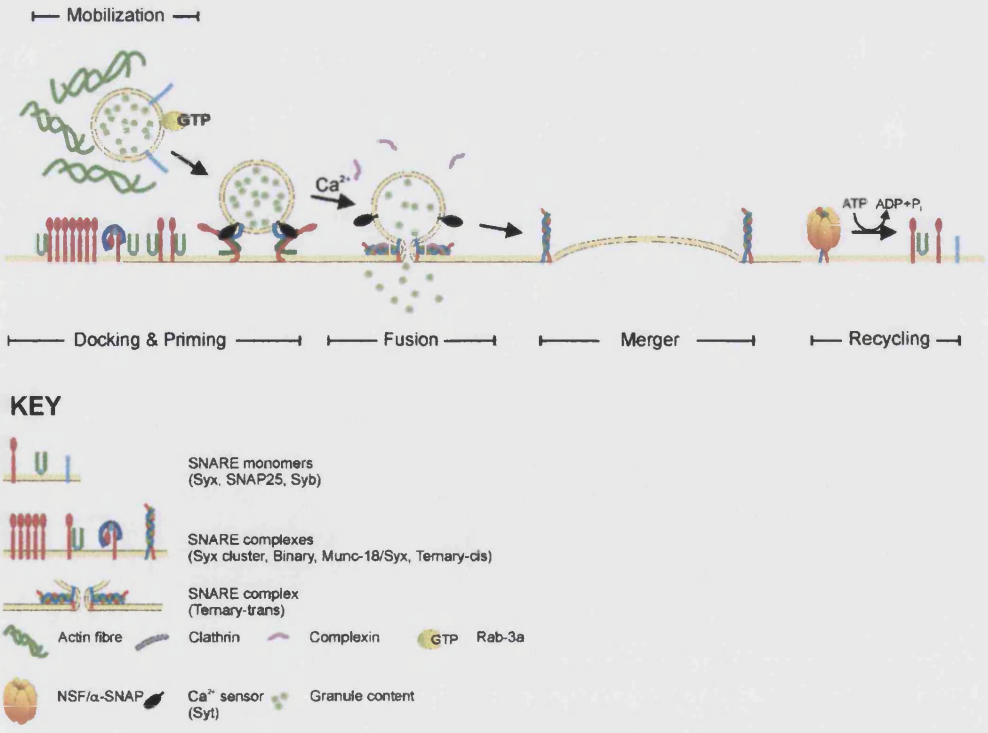

◄ ***Figure 1. Late steps in regulated neuronal exocytosis***

A detailed description of the steps shown here is given in the text. Abbreviations; Syx (syntaxin), Syb (synaptobrevin), Syt (synaptotagmin)

The challenge therefore, is to integrate this complex network of interactions into a coherent pathway. Thus, for purposes of description it is perhaps useful to classify the later steps of the regulated secretory pathway.

Mobilisation - After they mature, secretory granules gather in large numbers in the cytoplasm of the cell periphery. Before they can reach the plasma membrane granules must first navigate the actin cortex - a meshwork of filamentous and bundled actin which criss-crosses the sub-plasmalemma region. The actin network is thought to regulate the availability of vesicles for subsequent steps and is often viewed as a barrier that hinders the movement of vesicles to the plasma membrane (Cheek and Burgoyne, 1986; Sontag et al., 1988; Vitale et al., 1991).

In neurones it has been proposed that synaptic vesicles are attached to the actin cytoskeleton by synapsin crossbridges (Turner et al., 1999). Upon activation (during an action potential), synapsins are phosphorylated at multiple sites by calcium and cAMP dependent kinases. The resulting reduction of the binding affinities releases the vesicles from the cytoskeleton.

The role of the actin cortex in the regulated exocytosis of neuroendocrine secretory granules has also been investigated. In a recent

study (Lang et al., 2000) a microscopic approach was used to investigate the relationship of actin cortex dynamics to secretory granule motion in PC12 cells. The majority of granule movements were random and much slower than expected. Such motions were inhibited by withdrawal of MgATP, blockade of F-actin re-modelling by phalloidin, or in the presence of myosin inhibitors. This suggests that granules within 500 nm of the plasma membrane are probably restricted by an amorphous filamentous cage of actin, and might be cross-linked to it via myosin. However, small numbers of granules were observed to move in a directed fashion over longer distances. Such motions could also be blocked in a similar manner to the random movements. These probably represented granules that had met a conveniently orientated actin bundle (stress fibre) along which they were then transported. Thus, the actin cortex probably functions as a barrier to granule progression to the plasma membrane. However, due to its dynamic nature it is not impenetrable. This feature provides a mechanism for transfer of its own movements onto embedded granules, or allows it to form tracks along which granules can be transported.

Docking - Once mobilised, granules have the opportunity to approach the plasma membrane. The initial contact between the vesicle and plasma membrane (docking or tethering) is mediated by protein complexes that appear to be essential for ensuring that only the appropriate membranes fuse. Currently, little is known about the factors involved in the docking of vesicles to the plasma membrane. As a model system the homotypic

docking of intracellular transport vesicles has been well studied, with the mechanism involved likely to be similar. A key role has been assigned to Rab proteins, a family of Ras-related small GTPases. A specific family member that resides on the vesicle membrane controls each fusion step. Like Ras, Rabs operate as molecular switches that are active in the GTP- and inactive in the GDP-bound form. Active Rabs recruit a variety of structurally diverse effector proteins to the vesicle that may then bridge the membranes destined to fuse. Alternatively, Rabs may also co-ordinated the downstream reactions that lead to *trans*-SNARE complex formation after the vesicle is tethered to the target membrane (for review see Waters and Hughson, 2000).

The spatial organisation of proteins in the plasma membrane may also play an important role in the docking of secretory vesicles and for subsequent steps in the exocytotic pathway. Indeed, it has been widely demonstrated that many proteins and lipids involved in membrane trafficking and signalling processes are organised into macromolecular assemblies critical for their correct function. For instance, syntaxin 1A has been demonstrated to form clusters in the plasma membrane of PC12 neuroendocrine cells the integrity of which are essential for exocytotic competence (Chamberlain et al., 2001; Lang et al., 2001).

At synapses vesicles are seen to dock at a specialised region, called the active zone, which lies in register with the post-synaptic density (an organised network of ion channels, cytoskeleton, signal transduction components, and adhesion receptors). This dense matrix of proteins or

"pre-synaptic web" is likely to play an important role in regulating vesicle docking, while at the same time co-ordinating this with priming, fusion, and recycling (see below). Electron microscopy has revealed that vesicles at the active zone of the neuro-muscular junction are positioned at the membrane within a regular protein scaffold (Harlow et al., 2001). Research into identifying the individual components of this pre-synaptic scaffold has been hampered by the lack of biochemical methods for the purification of this structure. However, in a recent paper Phillips et al. (2001) have described a procedure for the isolation of these entities and went on to identify the proteins present. The most abundant included components of the endocytic machinery (e.g. clathrin, dynamin), the cytoskeleton (actin/spectrin), and proteins involved in exocytosis (Munc18/NSF). Amongst the minor components were the active zone proteins RIM (see below) and Bassoon.

Priming - Priming is a complex series of poorly defined, reversible reactions that are thought to require a variety of soluble and membrane bound factors together with MgATP (Parsons et al., 1995). The exact number of intermediate stages, their stability and life times are unknown. Priming is a process of stepwise maturation, bringing vesicles into a state where their fusion with the membrane can be rapidly triggered by calcium. Using fast electrophysiological measurements it has been possible to define several kinetic phases during the stimulation response. The interpretation is that these represent distinct, functionally interconnected

vesicle "pools" that reflect different and subsequent steps in vesicle maturation and priming (for a review see Neher, 1998). However, various unknowns such as calcium channel and buffer distributions and a lack of molecular information confound the situation.

A number of recent studies of the active zone in neurones, that combined genetic, biochemical, and electrophysiological methods, have provided insight into the roles of two active zone proteins – RIM and Munc13 (for review see Martin, 2002). Munc13 was originally identified as the *unc13* gene product in *C.elegans* and found to contain a diacylglycerol/phorbol ester binding domain (Maruyama and Brenner, 1991). Phorbol esters have been widely reported to enhance neurotransmitter release and where thought to act via protein kinase C. However, the recent work of Rhee and colleagues (Rhee et al., 2002) on knock-in mice has shown that the major functionally relevant phorbol ester receptors in hippocampal neurones are Munc13 proteins. Munc13 also binds to syntaxin (Brose et al., 2000) and is thought to regulate the formation of ternary *trans*-SNARE complexes by promoting the "open" conformation of syntaxin. Consistent with this is the bypass of transmission defects in loss-of-function *Unc13* mutants in *C. elegans* by expression of a mutational stabilised "open" form of syntaxin (Richmond et al., 2001). This maybe balanced by the efforts of another soluble protein, Munc18 (Hata et al., 1993), which through its interaction with syntaxin promotes the "closed" conformation of this molecule preventing its entry into the SNARE complex (Yang et al., 2000). The Munc13-1 isoform also

binds to RIM through an N-terminal isoform specific interaction (Betz et al., 2001). RIM is itself essential for presynaptic function. It interacts with the vesicle proteins Rab3 (hence RIM – Rab3 interacting molecule) and synaptotagmin, the plasma membrane protein SNAP25, and Ca^{2+} channels. That both Munc13 and RIM are involved in priming and not docking are strongly supported by two observations: (i) Ablation of the protein leads to no reduction in the number and morphology of docked vesicles at the active zone but, (ii) a dramatic reduction of synaptic responses corresponding to vesicles of the readily releasable pool.

Fusion - Membrane fusion itself is probably the most understood step in the sequence of events leading to exocyotosis. However, many open questions remain. The secretion of catocholamines by chromaffin cells can occur with a minimal delay of 50 ms. This implies that the underlying protein machinery is brought to a point that requires only a few additional molecular steps to make vesicles fuse with the plasma membrane. Essential for fusion are the SNAREs, a super-family of small membrane proteins. In the middle of the 1980's Rothman and co-workers were able to reconstitute vesicular transport within the Golgi apparatus in a cell-free system (Balch et al., 1984). It was observed that this process required ATP and was inhibited by N-Ethylmaleimide (NEM) (Glick and Rothman, 1987). This led to the isolation of the NEM-sensitive factor (NSF), a soluble cytosolic protein (Block et al., 1988). In addition it was also possible to isolate three other soluble proteins that interact with NSF (α,β,

and γ-SNAP) (Whiteheart et al., 1993). In binding assays with α-SNAP and NSF it was possible to isolate a complex with a sedimentation coefficient of 20S from bovine brain extract (Söllner et al., 1993a). This complex contained, in addition to α-SNAP and NSF, three proteins – the so-called SNAP receptor (SNARE) proteins.

To date the best characterised SNAREs are those that regulate the fusion of synaptic vesicles in neurones and secretory granules in neuroendocrine cells. They include the plasma membrane proteins syntaxin 1A and SNAP-25 together with the vesicle protein synaptobrevin (also referred to as VAMP). Structural and functional studies of these proteins have provided a conceptual framework around which the mechanistic role of SNAREs in membrane fusion can be rationalised. The following lines of evidence support the hypothesis that the SNARE proteins are essential for vesicular transport and membrane fusion:

- In total eight different clostridial neurotoxins have been identified: Tetanus toxin (TeNT) and seven Botulinum toxins (BoNT/A, B, C1, D, E, F and G) (reviewed in Schiavo et al., 2000). These are homologous, heterodimeric proteins. The heavy chain functions to modulate the entry of the toxin into the pre-synaptic nerve terminal. The light chain is responsible for the selective and specific proteolysis of the neuronal SNARE proteins (Jahn and Niemann, 1994; Montecucco and Schiavo, 1994). This leads to an irreversible blockade of synaptic vesicle

exocytosis.

- Proteins of the Bakers yeast (*S. cerevisiae*), that are homologues of the neuronal SNAREs, are involved in the excyotosis of vesicles from the secretory pathway of this organism (Ferro-Novick and Jahn, 1994). The yeast SNAREs build a complex, which is remarkably similar to that of the neuronal SNAREs (Rossi et al., 1997).
- A multitude of other SNARE proteins have now been discovered and characterised that play roles in intracellular fusion processes (for a review see Jahn and Südhof, 1999; Chen and Scheller, 2001).
- *In-vitro* the SNARE proteins alone have been shown to be necessary and sufficient to fuse synthetic liposomes into which they are separately reconstituted (Weber et al., 1998; Nickel et al., 1999).

Both syntaxin and synaptobrevin are anchored into the membrane by carboxyl-terminal transmembrane domains, while SNAP-25 is attached to the membrane by palmitoyl side chains. The SNAREs contain membrane proximal heptad repeats (SNARE motifs) that interact to form a core complex, or four-helix bundle. This complex displays exceptional thermal stability and dissociates first at a temperature of 90 °C (Fasshauer et al., 1997b). The complex is also SDS resistant. In the presence of MgATP, α-SNAP and through the enzymatic activity of NSF the complex

can be dissociated into the individual components (Söllner et al., 1993b). The role of this reaction *in vivo* is probably required for a post-fusion recycling of the SNARE proteins.

Within the SNARE complex the helices lie in parallel forming a stable rod-like structure 100-120 Å in length (Sutton et al., 1998). It is assumed that this structure forms when the SNAREs bridge the gap between vesicle and plasma membrane, "zippering" from the initial N-terminal contacts towards their membrane proximal C-termini (*trans*-complex formation). This process is speculated to provide the energy that overcomes the repulsive electrostatic forces between vesicle and plasma membrane. However, it is still unclear whether this process is the driving force of membrane fusion or if the SNAREs act as workhorses needed to pull the membranes close enough together, with fusion performed by an unknown downstream factor (Bruns and Jahn, 2002).

Indeed, Peters et al. (2001) have identified VO, the membrane integral sector of the vacuolar H^+-ATPase, as a target of calmodulin in yeast vacuoles. The authors propose that VO-subunits assemble into gap-like junction channels that may connect the fusing membranes. In addition, the fusion of vacuoles was revealed to be un-inhibited by the dissociation of SNARE complexes shortly before fusion (Ungermann et al., 1999). Such findings have re-opened an old debate that a proteinaceous fusion channel rather than an external scaffold of proteins (around a lipid pore) are at the heart of the fusion mechanism (Lindau and Almers, 1995).

The "zipper" model of SNARE function postulates that the proteins

might partially assemble before fusion. Indeed, several studies present data in support of this argument (Weber et al., 1998; Fiebig et al., 1999; Xu et al., 1999; Scales et al., 2000; Chen et al., 2001; Margittai et al., 2001). The presence of such intermediates would provide a possible explanation for the different effects of the clostridial neurotoxins. For example, in crayfish neuromuscular junction the effects of tetanus and botulinum D toxins are stimulus dependent, whereas that of botulinum toxin B is not (Hua et al., 1999). The proteolytic sites of toxin action are well mapped in the primary structures of SNARE proteins. Thus, one may propose the existence of an intermediate SNARE complex in which these cleavage sites are differentially accessible. Such intermediates also present further possibilities for modulation of the exocytotic process by control proteins (e.g. complexin, synaptotagmin). In fact, this is where regulated secretion differs markedly from other exocytotic events and is subject to a further layer of control proteins. Synaptotagmin 1, for example is found on the outer membrane of synaptic vesicles it is thought to function as a calcium sensor in neurotransmitter release (Perin et al., 1990; Perin et al., 1991; Geppert and Südhof, 1998). It has been observed that synaptotagmin 1 binds in a calcium dependent manner to syntaxin 1A (Chapman et al., 1995), SNAP-25 (Schiavo et al., 1997) and with the SNARE complex (Davies et al, 1999). In addition the protein binds calcium-dependently to phospholipids (Brose et al., 1992).

3.2.3 Endocytosis

In order to maintain their net surface area and recycle membrane proteins and lipids, cells must retrieve material added to the plasma membrane during secretion. In neurones and neuroendocrine cells this process must be fast and efficient due to the high rate of membrane addition during regulated exocytosis. To distinguish this from the constitutive process of endocytosis this mechanism is referred to as compensatory endocytosis. In the now classical work of Heuser and Reese (1973) firm evidence was obtained that synaptic vesicle recycling involves clathrin coated vesicles. This was later confirmed by genetic evidence in Drosophila (Koenig et al., 1983; Gonzalez-Gaitan and Jackle, 1997). According to this model the machinery required for compensatory endocytosis is essentially identical with that required for constitutive endocytosis, with adaptations that allow tighter spatial and temporal regulation. Indeed nerve terminals are enriched in many of the proteins known to be involved in constitutive endocytosis e.g. AP2, clathrin, amphiphysin, and synaptojanin, or the neurone specific isoforms of others e.g. AP180, dynamin 1, and syndapin 1. The process has been well studied in neurones allowing it to be classified into several distinct morphological and biochemical stages (see also figure 2).

Figure 2. Steps in clathrin mediated endocytosis ►

A detailed description of the steps shown here is given in the text.

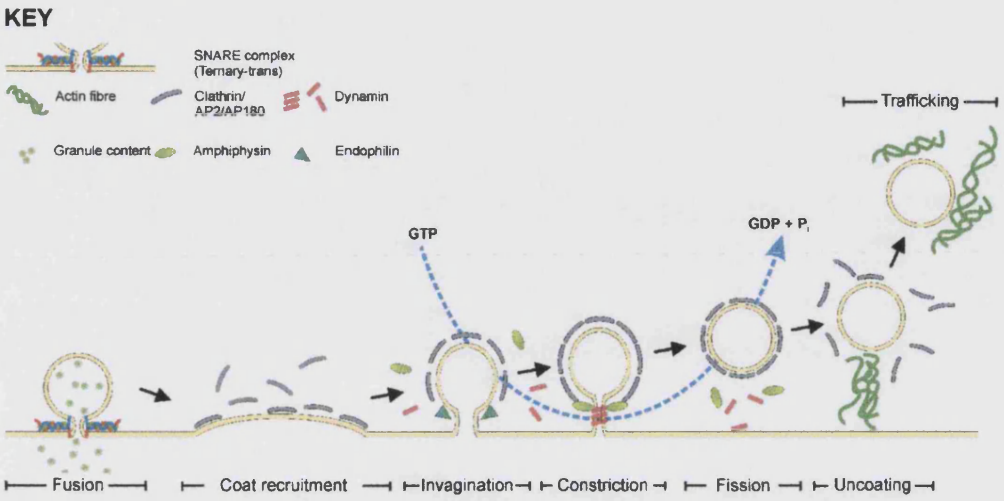

Coat recruitment – Endocytosis is initiated when the synaptic vesicle membrane integrates into the plasma membrane following exocytosis. Currently, a mixing of synaptic vesicle and plasma membrane components is believed to be retarded by the differing cholesterol and lipid compositions of the bilayers (Thiele et al., 2000). Thus the synaptic vesicle proteins are thought to remain in a "raft" to which AP2 adaptor complex recruits clathrin and AP180 coat proteins. This possibly occurs by recognition of binding motifs within the vesicle protein synaptotagmin (Zhang et al., 1994). Coat recruitment is also known to involve phosphoinositides. AP2, AP180, and synaptotagmin have been identified as major binding proteins for such inositol phospholipid species (for review see Cremona and De Camilli, 2001).

Invagination – Recruitment of AP2, AP180 and clathrin to phosphatidylinositol-4,5-biphosphate (PIP_2) containing liposomes *in-vitro* appears sufficient to initiate invagination with the formation of shallow coated pits. The increased curvature of these structures appears to be dependent on AP2 (Ford et al., 2001). Micro-injection studies in the lamprey giant synapse demonstrate that additional factors are required for the formation of invaginated coated pits, and that the coat proteins alone are insufficient. In a study by De Camilli and co-workers (Ringstad et al., 1999) antibodies against endophilin were shown to arrest invagination at the stage of a shallow coated pit. However, the authors were unable to see an effect of endophilin on coat formation *in-vitro*. These findings suggested that endophilin acts directly on the membrane, playing a vital role in promoting its invagination. This idea is supported by the fact that endophilin is a Lysophophatidic acid acyltransferase (LPAAT) and is critical for synaptic vesicle biogenesis *in-vitro* (Schmidt et al., 1999). Thus endophilin is speculated to influence membrane geometry by modifying lipids at the neck of the invaginated pit.

Constriction – The process subsequent to invagination involves narrowing the neck of the coated pit. Such structures are rarely seen in normal synapses. However, in the temperature sensitive *Drosophila* mutant *shibire* (Kosaka and Ikeda, 1983), or in lamprey giant nerve terminals micro-injected with the SH3 domain of amphiphysin (Gad et al., 2000) they can be readily observed. In such preparations, a collar of electron dense

material is seen around the constricted neck of the coated vesicle. This collar is known to be composed of the large GTPase dynamin (Hinshaw, 2000). The structure and function of dynamin together with its interactions have been extensively studied (reviewed in Hinshaw, 2000 and Sever et al., 2000). Dynamin is a multi-domain protein. In addition to the three domains associated with its GTPase activity and self-assembly, dynamin contains pleckstrin homology (PH) and proline rich domains (PRD) important for PIP_2 binding, membrane targeting and SH3 interactions. Dynamin self-assembles into higher order structures that resemble rings and helical stacks of rings though interaction mediated by its GTPase and GTPase effector domain (GED). Self assembly is promoted in the presence of the non-hydrolysable analogues GTPγS and GDP:AlF_4^- *in-vitro* (Carr and Hinshaw, 1997). Dynamin also self assembles onto a template vesicle membrane forming helical oligomers which tubulates the lipid. Such self assembly is associated with a 1000 fold increase in GTPase activity together with a conformational change, seen as an increase in helical pitch of the lipid bound oligomers (Stowell et al., 1999). These structures have the same dimensions as and are believed to be analogous to those seen at the constricted necks of coated pits in s*hibire* flies.

In addition to dynamin, several other proteins are thought to play a role in constriction. Chief among these is amphiphysin. Alongside its ability to bind to membranes (enhanced in the presence of phosphoinositides, Cremona et al., 1999), amphiphysin binds to clathrin (McMahon et

al.,1997; Slepnev et al., 1998), AP2 (Wang et al., 1995; Slepnev et al., 1998), the polyphosphoinositide phosphatase synaptojanin (McPherson et al., 1996), and dynamin (David et al., 1996). Thus, amphiphysins may act to link the clathrin coat to a recruitment of dynamin at the neck region (Shupliakov et al., 1997; Takei et al., 1999; Slepnev et al., 2000).

Fission – Free CCVs are generated in a fission reaction that severs the vesicle and plasma membranes. A prime candidate for mediating this nano-mechanical event is dynamin. The dynamin-dynamin self-assembly process, which drives membrane constriction, is speculated to be followed by a rapid fission of the narrowed neck region with assembly stimulated GTP hydrolysis providing the necessary driving energy. This idea is supported by *in-vitro* and *in-vivo* data that demonstrate that GTP hydrolysis by dynamin is (i) required for the conformational changes of self assembled dynamin helices (Marks et al., 2001) and (ii) for vesiculation of dynamin coated lipid membranes (Sweitzer and Hinshaw, 1998).

However, the exact coupling of constriction and fission mechanics to the timing of GTP hydrolysis is unknown (emphasised by the blue arrow in Fig. 2). Indeed, at least five models of dynamin function in the fission reaction have been proposed (for a review see Sever et al., 2000). Of these the "pinchase" (or "molecular garrote") and "poppase" (or "molecular spring") models have gained wider interest. The "pinchase" model was the first proposed to describe the mechanism of dynamin action (Hinshaw and Schmid, 1995; Warnock et al., 1996). Nucleotide free dynamin or

dynamin:GDP would be targeted to a newly formed coated pit. Subsequent GTP binding promotes self assemble of the dynamin into a helical collar, constricting the neck of the pit. The rapid and co-ordinated hydrolysis of GTP would trigger a second concerted conformational change, tightening the collar and pinching the membranes together. This mechanical force would eventually result in fission of the membranes. In the "poppase" model dynamin would assemble at the neck of a newly formed coated pit in a manner similar to that proposed above. However, the observation that the conformation of dynamin helices assembled on lipid nanotubes was subject to an abrupt change on GTP hydrolysis (the pitch of the helix increases in a concerted manner). This led to the hypothesis that the force of the extending dynamin spring could shear the membranes and "pop" the CCV vesicle off into the cytoplasm (Stowell et al., 1999).

Alternatively, it has been speculated that dynamin may act as a regulatory GTPase in the fission process. Such a model of dynamin function was suggested by the observation that over-expression of dynamin mutants, specifically defective in assembly stimulated GTPase activity, was found not to inhibit, but to stimulate endocytosis (Sever et al., 1999). In analogy with the classical role for GTPases in the cell, the active GTP bound conformation of dynamin was suggested to recruit downstream partner(s) that are involved in the formation of CCVs.

Uncoating – After the fissile release of CCVs a process of un-coating is initiated. The dephosphorylation of phosphoinositides by synaptojanin is essential for this process. Indeed the nerve terminals of synaptojanin knock-out mice are characterised by an accumulation of CCVs (Cremona et al., 1999). If the phosphatase activity of synaptojanin plays a role in un-coating, this would essentially represent a reversal of the coat recruitment process. The AP2 binding protein auxilin appears to be required for the actual removal of the clathrin coat. Auxilin recruits hsc70 heat shock protein and stimulates its ATPase activity, indeed overexpression of hsc70 mutants deficient in ATPase activity blocks un-coating of CCVs *in vivo* (Newmyer and Schmid, 2001). However, a link between the activities of synaptojanin and Auxilin/hsc70 has not been demonstrated.

3.3 The Heuser-Ceccarelli debate

Despite many years of intense investigation and considerable progress in identifying the molecular players involved, it is still a controversial matter as to which mechanism the compensatory endocytotic pathway follows.

The description of endocytosis, which was presented above, represents the most widely accepted model first described 30 years ago by the laboratory of John Heuser (see Heuser and Reese, 1973). Heuser's model has gained wide acceptance becoming a dogma familiar to every graduate of the biological sciences. This is in part due to the close

resemblance it has to constitutive endocytic mechanisms found in non-neuronal tissues and the extent to which it has been characterised (see for example: Brodin et al., 2000; Wakeham et al., 2000; Slepnev and De Camilli, 2001).

An alternative pathway, termed "kiss and run", was proposed at around the same time by Ceccarelli and co-workers (reviewed in Ceccarelli and Hurlburt, 1980; Heuser, 1989). Ceccarelli´s model attempted to explain the apparent lack of correlation between the rate of synaptic vesicle exocytosis, and the numbers/ appearance of clathrin coated vesicles within the synapse. In the “kiss and run” senario vesicles would not fully fuse with the plasma membrane and their retrieval appeared to be clathrin independent. Thus, vesicle integrity would be maintained during fusion, and the transmitter content discharged by means of a fusion pore, which transiently opened. While little direct evidence for kiss and run recycling has been found in synapses, the findings of many groups have suggested its existence. For example, the use of the lipophilic dye FM1-43 reveals a discrepancy between how much dye escapes from pre-labelled terminals and the amount of neurotransmitter exocytosis (Klingauf et al., 1998). The interpretation is that the membrane bound dye can not dissociate rapidly enough to escape those vesicles, which undergo the rapid kiss and run process. This difference has been used to estimate the percentage of exocytotic events that are a result of kiss and run – in hippocampal neurones the value is around 20 %. Recently, in good agreement with this, it has been shown

that mutant endophilins in *Drosphila* result in a complete block of clathrin mediated endocytosis at synapses. However, vesicle recycling must persist as mutants sustain 15-20% of neurotransmitter release during repetitive stimulation (Verstreken et al., 2002). This strongly suggests the presence of an alternative vesicle recycling pathway operating in nerve terminals.

While the speed of neuronal exo-endocytotic cycling may have been achieved though the evolution of specialised mechanisms, a significant body of evidence points to the existence of a rapid recycling process in endocrine cells, that is different from and functions in parallel with endocytosis via clathrin coated vesicles. When monitoring exocytosis in mast cells by patch-clamp analysis (Alvarez de Toledo et al., 1993), or in chromaffin cells by patch-clamp amperometry (Albillos et al., 1997; Ales et al., 1999) the stepwise rises in capacitance were often balanced by step-decreases in the trace. Such events are interpreted to represent an endocytotic reversal of the fusion event. The time intervals between the upward and downward steps of the traces ranged between hundreds of milliseconds to several seconds. This interval, or "open" time, was found to be influenced by the concentration of Ca^{2+} or various pharmacological agents (e.g. see the work of Henkel et al., 2001b).

Capacitance measurements have not only provided insight into individual fusion - fission events, but have also demonstrated that compensatory endocytosis involves both large and small endocytic vesicles (Henkel et al., 2001a), and that the process follows distinct kinetic

phases (Neher and Zucker, 1993; Artalejo et al., 1995; Smith and Neher, 1997). Thus, it appears that in chromaffin cells two pathways of membrane retrieval operate during compensatory endocytosis. The first is believed to involve large vesicles that have a size roughly equal to that of secretory granules, possess a dense core and are capable of trapping the fluid phase maker horse radish peroxidase. The second correspond well to the size of clathrin coated vesicles (Henkel et al., 2001a). It is unclear if these types of vesicle operate simultaneously or act at different phases of endocytosis. A further possibility is that these vesicles represent endocytotic pathways for different populations of granule membrane and so perform different functions during or after stimulation of exocytosis.

Artalejo and co-workers have studied the kinetics of endocytosis following exocytosis in chromaffin cells (Artalejo et al., 1995; Elhamdani et al., 2001). Contrary to the findings described above they found that compensatory endocytosis did not require clathrin, and was blocked completely by anti-dynamin antibodies or GTPγS. They proposed that recycling of secretory granules occurs exclusively through a dynamin dependent mechanism for which clathrin is not required. This is consistent with the idea that secretory granules do not collapse into the membrane following exocytosis and thus, do not require the membrane deformation activities of clathrin to be recaptured. More recent findings (Elhamdani et al., 2001; Graham et al., 2002) suggest that dynamin may also regulate the size of catecholamine quanta from individual granules. However, this is at odds with the data from other groups in which no evidence for a

partial release of small transmitter molecules were found (Bruns and Jahn, 1995; Ales et al., 1999; Bruns et al., 2000).

Secretory granules are of course also responsible for the release of peptide hormones. These larger molecules, as elegantly demonstrated by Barg and colleagues (2002), appear to require long time intervals and a greater dilation of the fusion pore to escape the granule during fusion (seconds to tens of seconds). In pituitary lactotrophs the dense cores of secretory granules are suggested to remain exposed to the external milieu for extended time periods before becoming recaptured (Angleson et al., 1999). Thus for secretory granules membrane fusion is not a direct measure of peptide release. In fact the two processes appear to be temporally separated and may present a possibility for a post-fusion control over secretion. The molecular mechanisms that may regulate these functions are unknown. The speed of this process suggests that a kiss and run-like paradigm as suggested for synaptic vesicles is not required, and that alternative direct endocytotic process may be responsible.

3.4 Post-exocytotic fates of the secretory granule

Current cell biological dogmas of membrane trafficking are epitomised by their broad acceptance of the vectorial nature of membrane transport. Indeed vesicular traffic within the secretory pathway can be broken down into elementary steps that occur in many variations in every eukaryotic cell:

- Vesicle formation via budding from a precursor organelle or membrane
- Transport to their cellular destination
- Docking and fusion with the target membrane

These steps are biologically irreversible - a prerequisite for ordered and directed transport. In accordance with this, the molecular machines for budding and fusion, at least as far as is known, are completely different. Families of evolutionary conserved proteins, as has already been discussed, including SNAREs, Rabs Sec1/Munc-18 related proteins mediate fusion. In contrast, budding and fission, i.e. the reversal of vesicle fusion normally involves the formation of specialised protein coats (clathrin or COP), together with a host of adapter and accessory proteins (adaptors, amphiphysins, dynamin, ADP-ribosylation factors (ARFs), etc (for review see Kirchhausen, 2000).

Despite this wealth of molecular knowledge, little is known about the fate of the membranes and components of vesicles during individual rounds of exo-endocytosis. While it is difficult to exclude that lipid mixing occurs upon bilayer fusion, there is evidence to suggest that vesicle components (proteins and associated lipid species) remain together after the fusion event (as rafts, which then act as nucleation sites for the endocytosis machinery). However, the fact that cholesterol, a lipid that is highly enriched in synaptic vesicles (Jahn and Südhof, 1999), interacts with the synaptic vesicle protein synaptophysin (Thiele, 2001) could

suggest that proteins from newly fused synaptic vesicles stay concentrated in microdomains at the plasma membrane.

Given the size of regulated secretory organelles (for a PC12 cell a LDCV is ≈ 120 nm in diameter) and the rates at which they fuse with the plasma membrane one is faced with the following question: Why is it not more efficient for the cell to prevent the membranes from integrating i.e. vesicle collapse? The kiss and run model as originally suggested would seem to provide a mechanism by which such efficiency could be achieved. However, although the evidence (as discussed above) for a kiss and run mechanism is substantial such models can not account for all of the recycling that takes place. Additionally, the kiss and run idea is at odds with current models of membrane trafficking in which biochemical reversibility plays no role.

Assuming two such models for vesicle recycling a further important question is: How is the site of exocytosis related to that of endocytosis? Most models of clathrin mediated endocytosis are consistent with the idea that endocytosis occurs at a spatially separate position to that of exocytosis. The data from several groups demonstrates that the biochemical apparatus for endocytosis is located outside the active zone in neurones (see Heuser and Reese, 1973; Roos and Kelly, 1999).

As discussed briefly above, capacitance studies of secretory granule exocytosis suggest transient opening during exocytosis. The group of Palfrey and Artalejo have presented data that such events involve dynamin (but not clathrin) to recapture (close) vesicles after fusion (or

even to regulate the quantal size of individual events) (Artalejo et al., 1995). However, as with all such capacitance experiments no spatial information is gained whether recapture occurs at the same or adjacent to the corresponding fusion site of the parent vesicle.

In the secretory cell line INS-1 the group of Rutter has used GFP to label the granule membrane protein phogrin (Tsuboi et al., 2000). After membrane fusion, detected by the concomitant release of acridine orange and GFP dequenching, the membrane signal remained visible, moving away from the site of exocytois. These findings led the authors to suggest a "kiss and glide" model for secretory granules i.e. after fusion vesicle collapse is retarded and the empty vesicle defuses from the site of exocytosis. However, the authors were unable to determine the extent to which the fusion pore expanded or if it had remained open. Again using a microscopic approach Barg and colleagues (2002) demonstrated that large peptidergic secretory markers (modelled using GFP fusion proteins) undergo a slow, delayed, release after fusion pore opening. Granule fusion resulted in a transient increase in GFP intensity preceding its partial or complete loss. Thus, the initial size of the fusion pore is sufficient for an exchange of protons, but further dilation is required before GFP can escape. Together, these finding raise several interesting questions: Do the vesicles need to undergo full fusion during peptidergic release? Does the fusion pore remain open or can granules reseal (endocytosis)? What molecular mechanisms are involved?

Such questions have been addressed mainly using electrophysiological methods such as capacitance patch clamping and amperometry. However, approaches that combine both temporal and spatial read-outs together with the chance to do biochemical experiments have not yet been applied.

3.5 A model system for investigating life at the plasma membrane

As a topic for this thesis, it was chosen to study the exocytosis of single secretory granules *in-vitro*. Although numerous investigators have extensively addressed many aspects of secretory granule exocytosis by a variety of techniques, none have used an *in-vitro* approach that simultaneously provided both spatial and temporal resolution together with a simplified cellular and defined biochemical environment. Dr Julia Avery previously developed such an assay in this laboratory. Dr. Avery used a simple method for producing plasma membrane sheets from PC12 cells grown on poly-L-lysine coated coverslips – a preparation that allows spatio-temporal resolved observation with a microscope together with access for biochemical probes. The cells were submerged in an ice-cold buffer and subjected to a brief pulse of ultrasound generated with a standard tip sonifier. When the cells were treated prior to sonification with the vital dye acridine orange numerous membrane sheets where found to possess bound fluorescent spots. Further morphological and physiological

analysis revealed that these objects were secretory granules and that the membrane sheets were devoid of nuclei and other organelles (Fig. 3).

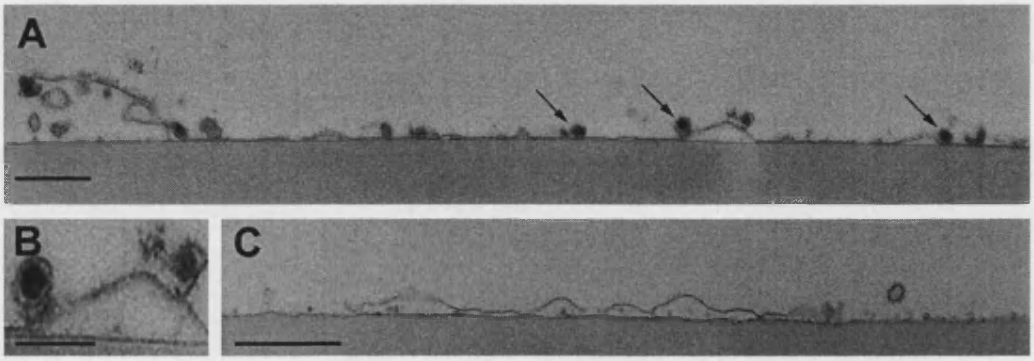

▲ ***Figure 3. Cross sections of membrane patches analysed by electron microscopy***

(A) Membrane sheet incubated under control condtions. Several secretory granules (arrows) are attached to the cytoplasmic face of the plasma membrane. (B) Two secretory granules at higher magnification. (C) For comparison a membrane sheet incubated with calcium prior to fixation. Bars: (A and C) 0.5 µm; (B) 0.25 µm (by kind permission of Dr. Dietmar Riedel).

Dr. Avery was able to observe and quantify that these secretory granules were capable of undergoing exocytosis in a manner dependent on micromolar concentrations of Ca^{2+}, MgATP and cytosol. These measurements were made by looking into the microscope with the naked eye and counting the fluorescent signals resulting from escape of the acridine orange dye upon exocytosis (see also Avery et al., 2000).

In collaboration with Dr. Avery (and as part of a joint publication, Avery et al., 2000) it was possible to improve this assay by introducing

digital imaging to monitor and quantify secretion, and to investigate other biological aspects of the preparation (e.g. toxin sensitivity, secretion rates) which are presented here. In addition, a semi-automated image-processing algorithm was developed for the impartial and rapid processing of image data. The initial findings of this approach are also presented here.

As an alternative to acridine orange, Green fluorescent protein (GFP) was fused to the *c*-terminus of human neuropeptide Y. PC12 cells were transiently transfected with this construct. Neuropeptide Y labelled with GFP has previously been demonstrated to be correctly expressed and sorted by PC12 cells and can be used as a fluorescent marker to monitor secretory granule exocytosis (Lang et al., 1997). It was possible to produce membrane sheets from cells expressing this marker and to stimulate and monitor exocytosis in the same manner as with acridine orange. However, whereas acridine orange was observed to escape completely during fusion, the stimulation of granules labelled with GFP revealed a striking pattern of fluorescent intensity changes. In fact granules were not only observed to lose their fluorescence, but were also seen to get brighter or dimmer. These findings are presented in the second part of this thesis and form the major biological insights of this study (Holroyd et al., 2002).

4. Part I – An *in-vitro* cell-free assay for monitoring exocytosis

4.1 Introduction

One approach to try and clarify the sequence of events before during and after membrane fusion is to develop *in-vitro* cell-free assays (for review see Avery et al., 1999). Systems for studying fusion of intracellular trafficking vesicles are commonly available. As a read out the mixing of lumenal content markers allows vesicle fusion to be monitored. Recently, this method has been developed further with green fluorescent protein (GFP) and microscopy providing spatial information about pre and post fusion events (Wang et al., 2002). However, during exocytosis a secretory vesicle fuses with the flat plasma membrane, releasing its contents into the surrounding medium. This precludes the use of content mixing assays. To circumvent this problem it is possible to use cracked or permeablised cell preparations which allow access to the cytoplasm via holes in the plasma membrane. Biochemical methods can then be used to study secretion, for example small molecules or antibodies can be added and their effects on secretion monitored. A progressive loss of the exocytotic response to Ca^{2+} is observed in such systems, probably due to the slow wash out of cytosolic components required to maintain a secretory response. Adding back cytosolic fractions can restore secretion, this allows the identification of cytosolic proteins that are involved in exocytosis.

Although instrumental in the identification of several soluble factors required for exocytosis (Hay and Martin, 1993; Linial and Parnas, 1996; Ann et al., 1997), permeabilised and cracked cells are not ideal systems for studying secretion. Firstly, variability in the rates at which cytosolic constituents are washed out may differ between experimental situations and individual proteins. Secondly, the only function that can be assayed is the bulk release of granule content because there is no direct experimental access to the participating membranes. Thirdly, it is difficult to distinguish between effects that are essential for exocytosis and those that have purely regulatory roles, or are involved in earlier steps of the secretory process such as cytoskeletal rearrangements or secretory vesicle transport. Fourthly, measurements of compensatory endocytosis are not possible. Finally, the temporal resolution is too crude to clearly identify individual steps leading to exocytosis, and no spatial information is gained.

True cell-free preparations in which a secretory vesicle fuses with plasma membrane fragments have only been described for a limited number of specialised systems. These include the sea urchin egg (Vacquier, 1975; Baker and Whitaker, 1978; Crabb and Jackson, 1985) and the mammalian exocrine pancreas (Maclean and Edwardson, 1992). More recently, Martin and Kowalchyk (1997) have described a plasma membrane enriched fraction isolated from PC12 cell homogenates. Secretory vesicles remaining attached to these membranes were found to release their content under the appropriate conditions, suggesting that the

preparation retained exocytotic competence during isolation. However, even though these systems are considerably minimalist, they continue to suffer from similar drawbacks to those described above for permeabilised cells.

Dr. Avery developed a novel *in vitro* assay for regulated exocytosis in PC12 cells that has a good temporal and spatial resolution. Sonification of PC12 cells grown on poly-L-lysine coated glass coverslips results in the generation of flat, inside-out membrane sheets that remain attached to the coverslip. These structures are devoid of nuclei and other organelles. However, in some cases membrane sheets are generated with docked secretory granules. Ca^{2+} causes the exocytotic fusion of these vesicles, which can be monitored by fluorescence microscopy at the single vesicle level (Avery et al., 2000).

4.2 Results and analysis 1 – Further characterisation of an *in-vitro* cell-free assay for regulated exocytosis

The generation of carrier supported plasma membranes with attached secretory granules from PC12 cells grown on coated coverslips was established in this laboratory by Dr. Julia Avery. Analysis by a combination of atomic force, electron and fluorescence microscopy revealed that these structures were devoid of nuclei and other cytoplasmic structures. The granules attached to these membranes are conveniently labelled with the fluorescent dye acridine orange. This dye, due to its acidophilic nature accumulates into acidic organelles, such as secretory granules, where it becomes protonated and is rendered membrane impermeable. The concentration of the dye is such that it forms dimers or higher aggregates, which cause quenching of its fluorescence at 530 nm (Plamgren, 1991). Thus, because of the dyes emission spectra, granules can be observed as brightly fluorescent orange spots. Exocytosis of granules labelled in this manner is observed as a transient flash of fluorescent light (due to dilution dependent fluorescent de-quenching of dye molecules upon escaping the granule) with the subsequent disappearance of the spot. These events could be counted by eye within a given field of the microscope. Exocytosis was shown to be dependent on micromolar concentrations of Ca^{2+} MgATP, and rat brain cytosol. Extending the incubation time resulted in a gradual run down of the exocytotic signals despite the continued presence of cytosol and MgATP

(Avery et al., 2000). Together these findings were in line with previous reports on exocytosis in permeabilised PC12 cells (reviewed by Martin and Kowalchyk, 1997; Avery et al., 1999). In collaboration with Dr. Avery it was possible to improve this assay by introducing digital imaging to monitor and quantify secretion. Other biological aspects of the preparation were also investigated though the use of these new methods. The results of these efforts are presented below.

4.2.1 Exocytosis on membrane sheets can be quantified and characterised using digital imaging

As described above, exocytosis from membrane sheets was shown to dependent on micromolar Ca^{2+}, MgATP and rat brain cytosol, with individual exocytotic events been counted by eye in a semi quantitative manner. To improve this a cooled slow scan CCD camera was used to record the distribution of acridine orange labelled vesicles on membrane sheets before and after a 1 min stimulus with 0.5 µM Ca^{2+} (Fig. 4.). Typically, membrane sheets used for these experiments were found to have an average area of 40 ± 3.5 μm^2 (n=39) and an acridine orange stained granule density of 0.9 ± 0.05 granules/μm^2.Before stimulation, the membrane sheets were incubated for 2 min with 5 mg/ml rat brain cytosol and 2 mM MgATP in the absence of Ca^{2+} to fully prime the vesicles.

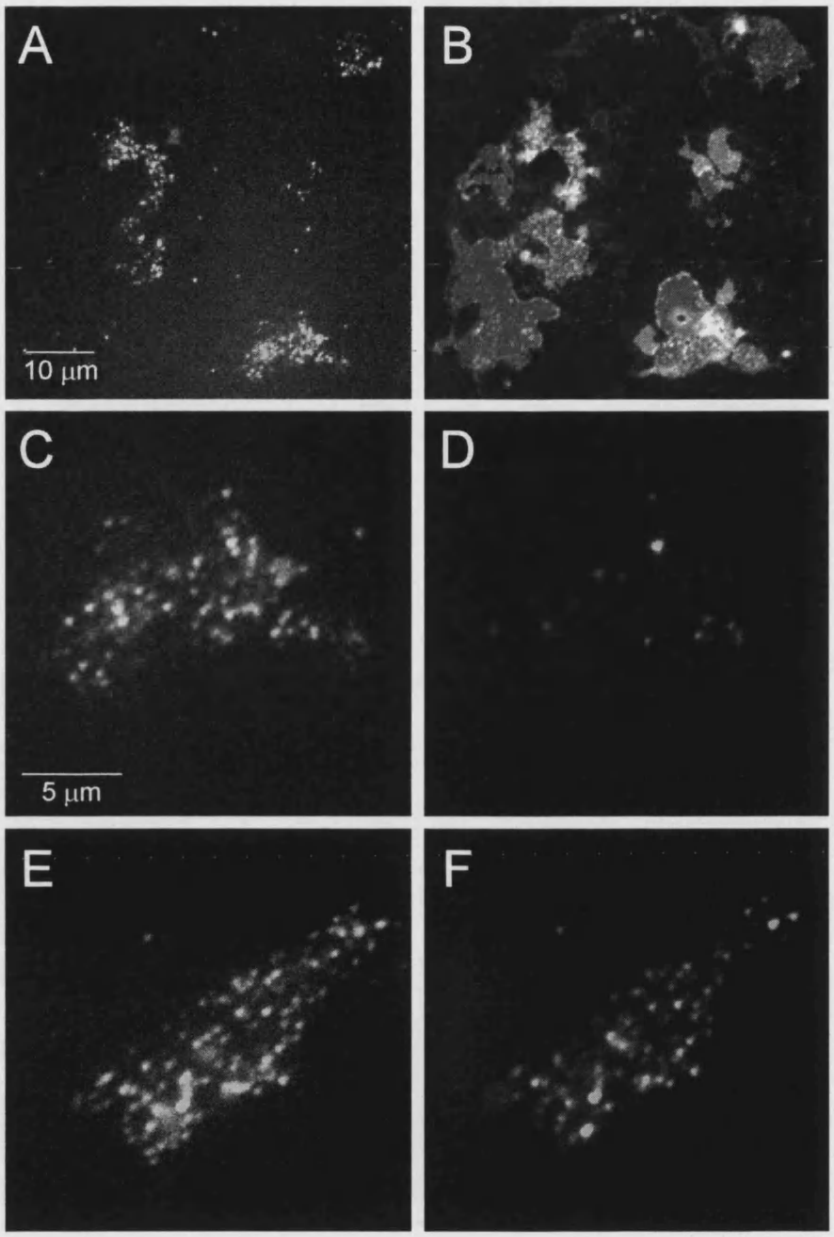

▲ ***Figure 4. Disappearance of acridine orange labelled particles after Ca^{2+} stimulation***

Membrane patches were prepared from cells preloaded with 10 µM acridine orange and imaged in incubation buffer containing 5 mg/ml rat brain cytosol and ATP. (A) Lower magnification of labelled membrane patches. (B) Same field as in (A) but stained with FM1-43 at the end of the experiment in order to visualise all phospholipid membranes. (C-F) High magnification of membrane patches before (C & E) or after a 1 min treatment with 0.5 µM Ca^{2+} (D) or control buffer (F).

Under control conditons, numerous fluorescent spots were visible (Fig. 4 A, C, & E). Addition of Ca^{2+} led to a reduction in the number of spots (compare Fig 4. C & D), which was not observed when EGTA was, used instead (Fig.4 E & F). To assess this effect more precisely, the disappearance of spots was quantified from a series of membrane sheets. The reduction was 58.5 ± 5.6 % upon stimulation with 0.5 µM Ca^{2+} (n=17) and 16.5 ± 5,4 % for control (un-stimulated) membrane sheets incubated in parallel (n=12).

4.2.2 The disappearance of granules from membrane sheets is a SNARE dependent process

To confirm that the disappearance of acridine orange labelled granules is due to exocytosis, membrane sheets were pre-treated for 10 min with Tetanus toxin light chain before the addition of cytosol, MgATP and Ca^{2+} (Fig. 5).

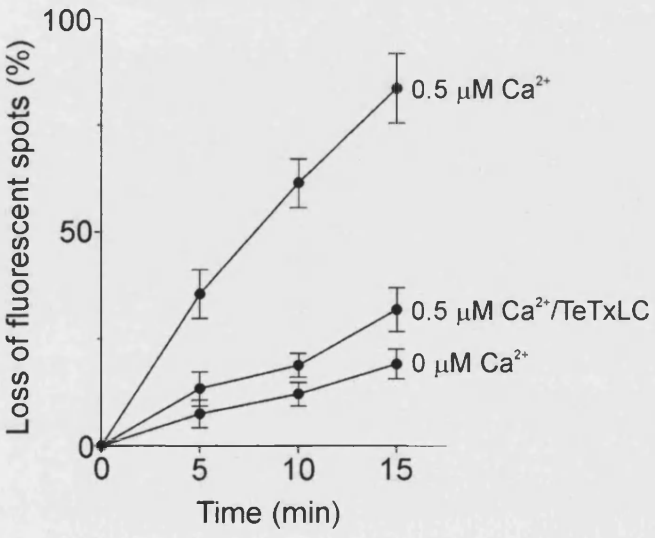

◄***Figure 5. Ca^{2+}-dependent disappearance of labelled particles is blocked by pre-incubation of the membrane sheets with Tetanus toxin light chain***

At the times indicated, the membrane sheets were imaged and the loss of particles was determined by counting. Note that in this

experiment MgATP was added together with 0.5 μM Ca^{2+} and 2.5 mg/ml cytosol. Note that the concentration of cytosol was lower than that shown in figure 5 resulting in a slower rate of exocytosis. Each data point represents the mean value of 15-20 membrane sheets obtained from six independent preparations, with the exception of the 15 min data points for which 4-8 membrane sheets were used.

As expected for exocytosis, toxin pre-treatment largely prevented the disappearance of acridine orange labelled spots regardless of whether Ca^{2+} was elevated. In this experiment, MgATP was added together with Ca^{2+} and the pre-incubation with concentrated cytosol was omitted, resulting in a slower time course of exocytosis than that described above.

4.2.3 Exocytosis can be monitored with both high temporal and spatial resolution by video rate microscopy

In addition to the assay described above, it was possible to make use of the self quenching properties of acridine orange to monitor single, calcuim dependent exocytotic events in real time. This was achieved using a cooled, video rate (25 frames/s) intensified CCD camera (V/ICCD, Princeton Instruments Inc.). Again the distribution of single acridine orange labelled vesicles was observed and it was possible to record their exocytotic response to calcium as a release of the dye (Fig. 6). Such events were seen as bright, transient flashes of light due to the dilution dependent dequenching of acridine orange at 530 nm. The fluorescence intensity increased sharply and then gradually decayed with a time constant in the range of 150 ms.

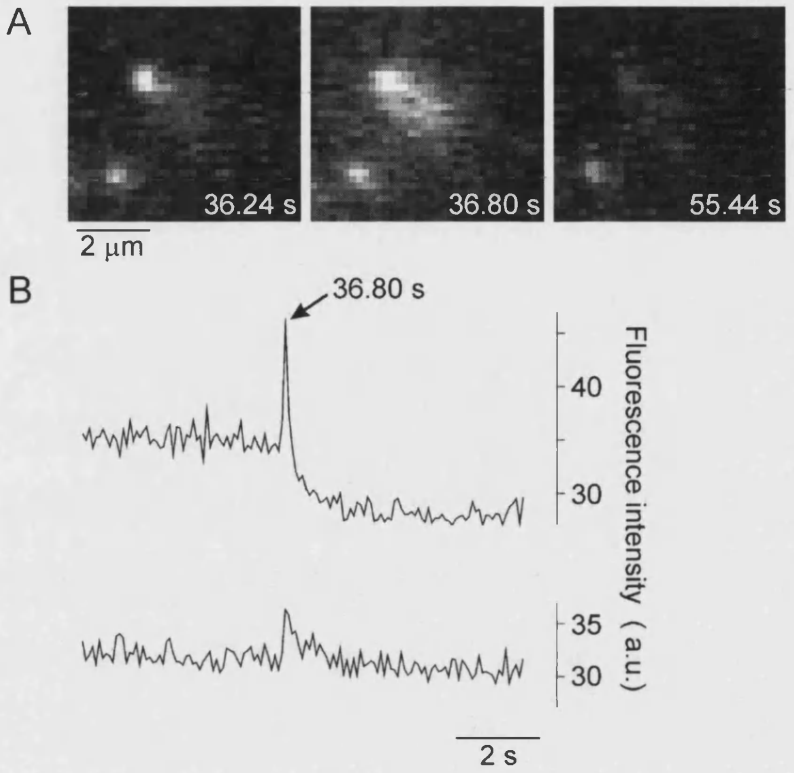

▲ ***Figure 6. Dequenching flash caused by exocytosis of an acridine orange loaded secretory granule, imaged by video microscopy at a rate of 25 Hz***

(A) Sequence of video images showing a typical dequenching flash arising from a fluorescent spot (upper left). The time delay after the addition of 0.5 µM Ca^{2+} *is indicated. Note that after the flash the spot is largely diminished whereas a second spot (lower left) remains unchanged. (B) Fluorescence intensity profile of the dequenching flash shown in the sequence. A circular mask with a diameter of 10 pixels was centred over both spots. The average intensity was determined for every second frame over the sequence and plotted against time. The blip in the intensity profile of the lower spot is caused by a spill-over of acridine orange during exocytosis of the upper spot. a.u., arbitrary units.*

Figure 7 shows the intensity trace averaged from 24 such flashes. When closely examined frame by frame, some individual flash sequences displayed a distinct horizontal stripe pattern in the frame were the flash first became visible (data not shown). These stripes occurred in every second line of pixels throughout the flash "cloud". This can be attributed to the read-out mechanism of the camera CCD array. The array is divided into horizontal, paired lines of pixels that run across it. When the chip is read-out, information from one of each paired lines of pixels is collected. This is followed by the information from the second line of every pair. These two striped, half images are then combined by the camera electronics to give 1 frame every 40 ms. Thus, flashes in which such striped patterns were seen represent events with a rise time of less than 40 ms.

◄ ***Figure 7. Averaged dequenching flash caused by exocytosis of acridine orange loaded secretory vesicles, imaged by video microscopy***
A circular mask with a diameter of 10 pixels was placed over individual flashes. The average intensity was determined for each frame of the sequence. These data were then normalised, averaged for 24 such events and plotted against time as shown.

4.2.4 Analysis of video sequences reveals distinct phases of vesicle exocytosis

Regulated secretion in neuroendocrine cells is known to occur in distinct phases. These are readily defined by their kinetics when granule fusion is monitored by electrophysiological methods. The different kinetic phases of exocytosis have been assigned to represent different hypothetical pools of granules within the cell. These pools represent granules in differing states of release competence, with those most able to exocytose upon triggering assigned to the fastest kinetic phase of the response. While these vesicle pools are kinetically well defined, their location (distance from sites of Ca^{2+} influx, docked at or close to the membrane, within the cytosol) and the biochemical composition of their fusion machinery are mostly unknown.

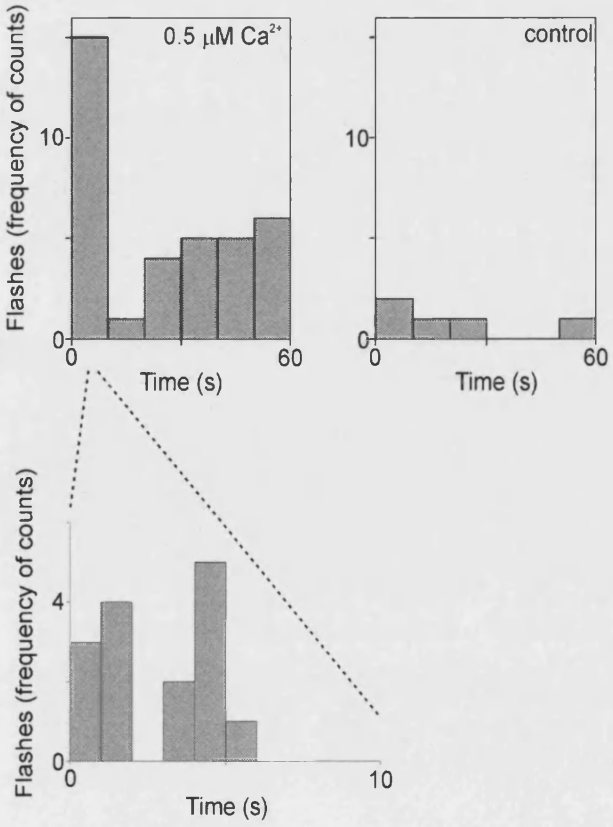

◄ ***Figure 8. Histograms showing the time distribution of exocytic events recorded by video microscopy***

Cells were prepared as described and incubated in buffer containing rat brain cytosol and MgATP before treatment with 0.5 μM Ca^{2+}, n=7 membrane sheets, (A) or control buffer, n=5 membrane sheets, (B). Time 0 represents buffer exchange with events occurring

afterwards been placed into ten second bins. (C) Breakdown of the first 10 s from (A) showing the distribution of events in 1 sec bins

The granules found upon membrane sheets appear to be tightly bound to the plasma membrane and probably represent vesicles from the morphologically docked vesicle pool (Parsons et al., 1995). After a 2 minute pre-incubation in 2.5 mg/ml rat brain cytosol membrane sheets with acridine orange loaded granules were stimulated with 0.5 μM Ca^{2+} and monitored by video rate imaging for 1 min. Subsequently, flash events were counted and the time of the event after the start of stimulation recorded. This information is shown in figure 8 as a histogram with the number of events placed into 10 or 1 sec bins and reveals a distinct burst of exocytosis occurring in the first 10 s. This is followed by slower but, sustained activity throughout the remaining 50 s. A further breakdown of the first 10 s bin into a histogram of 1 s bins shows that most of the burst events occur in the first 5 s after application of the Ca^{2+}.

4.2.5 A comparison of Phallodin green staining of filamentous actin in fixed cells and on membrane sheets

The role of the actin cortex in exocytosis is unclear. In some models it forms a barrier to vesicles moving to the membrane, while according to others it assists their movement to it. In whole cells filamentous actin forms a sub-plasmalemma layer or cortex that acts as a dynamic scaffold, allowing for rapid changes in cell shape.

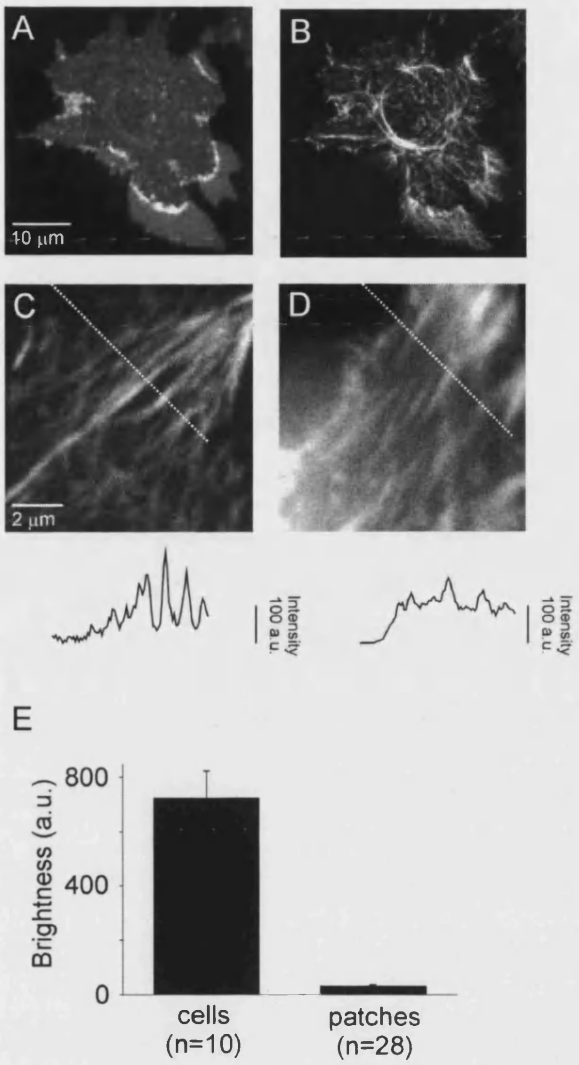

◄ ***Figure 9. Staining of filamentous actin on membrane sheets***

(A & B) Filamentous actin localises to membrane sheets as seen in these two images. Freshly prepared patches were stained with Phalloidin-Oregon green 488 (B) followed by FM1-43 (A) to visualise the entire membrane patch. High magnification images of typical Phalloidin staining on a fixed patch (C) and a fixed cell (D). Note the absence of actin between the large actin bundles in (C). This is more clearly demonstrated by a line scan (traced with the dotted line in C & D) plotted below each image. The thinning or loss of fine filaments is seen as deep troughs in the line scan from (C). (E) Quantification of the amounts of actin in fixed cells (n=10) and on patches (n=28). In cells the cortex was found to be a factor of 22 times brighter than on patches. Values given as mean ± sem.

The thickness of this cortex in cultured cells is greatest at their base, where it appears to facilitate adhesion. Thus, as membrane sheets are derived from the base of cells it was prudent to characterise and quantify the extent to which the actin cortex remains intact. The fungal reagent Phallodin binds specifically to filamentous actin. Thus using a fluorescently labelled derivative of this reagent it was possible to make a

comparison of the amounts of actin in the cortex of whole PC12 cells at the cell-glass interface and that on membrane sheets.

In an initial experiment un-fixed membrane sheets were stained with Phalloidin to examine the distribution of actin to FM1-43 labelled membrane (Fig. 9 A & B). The staining was localised and specific. The pattern suggested that most of the fine meshwork of filaments had de-polymerised, while larger stress fibres appeared to have remained intact. To quantify this the bases of 10 fixed PC12 cells stained with Phalloidin were compared to 28 fixed membrane sheets (Fig. 9 C, D, & E). Approximately 4 % of the actin found in the base of whole cells remained on membrane sheets. Most of this residual actin is represented by stress fibres (Fig. 9 C & D). This is clearly illustrated by performing line scans of fluorescence intensity (Fig. 9 C & D, lower panels). On membrane sheets this reveals a pattern of high peaks and deep troughs which represent individual stress fibres and the empty spaces between them. In whole cells a similar pattern of peaks can be found, but these stress fibre peaks protrude from an even plateau of stained actin filaments. It is important to note that this does not represent fluorescence from other focal planes, as the actin cortex has a maximum thickness of 2 µM in this part of the cell (Lang et al., 2000).

4.3 Results and analysis 2 – An algorithm for the semi-automated analysis of *in-vitro* exocytosis assay image sequences

As described above the exocytotic loss of acridine orange labelled granules from membrane sheets can be quantified using a simple before and after imaging procedure. This method generates small amounts of image data (in the case of the slow scan CCD camera used here a single image has a size of approximately 1 megabyte), which can be rapidly analysed manually. The specimen is also subjected to low levels of photo-toxic stress allowing images to be captured over long time periods (for example, up to fifteen minutes in the Tetanus toxin experiment). However, this method does not provide sufficient temporal information for an assessment of phenomena that have a dynamic nature. On the other hand a single video rate image sequence of 2 min generates 3000 images (or approximately 500 megabytes of image data) requiring a laboriously long image processing procedures in order to extract data. The specimen is also constantly under illumination resulting in rapid bleaching, a loss of signal to noise ratio and poorer resolution. However, the temporal information allows different biological questions to be addressed.

Thus, given that both these methods have significant drawbacks a new approach combining the positive qualities of both was needed, namely: (i) A possibility to monitor secretion over periods of 5 minutes or longer, with sufficient time resolution to assess the rate of exocytosis. (ii) Photo-toxic stress and bleaching to be kept to a minimum. (iii) Storage

requirement/ processing time minimised for image data without a compromise of the information content. (iv) In addition, an impartial method for the assessment of the data that does not rely on a slow and subjective manual quantification was needed.

To tackle these problems a new method was implemented. The better signal to noise ratio of a slow scan CCD camera for longer exposures (1 sec or more) was combined with time lapse imaging at a rate of 0.5 Hz to reduce photo-toxic stress (by illuminating the specimen only during camera exposure). This allowed the exocytotic response to be recorded for up to 5 min and generated 150 images. The imaging rate was such that exocytosis was seen simply as the abrupt loss of acridine orange labelled spots. The corresponding de-quenching flashes observed by video microscopy were rarely captured.

Given that the loss of acridine orange dye from individual granules was recorded an all or nothing event (a binary read out), it was possible to speed up the analysis of these data sets by developing a semi-automated image processing algorithm. This essentially enabled the Metamorph software to quantify the number of acridine orange labelled granules per image. This also avoided the inconsistency problems associated with manually processing image data. The algorithm was based on the following principles: (i) raw data were to be used as a direct input, (ii) each image was to be analysed independently from that preceding or following it in the sequence and (iii) the output would be a simple count of the number of acridine orange stained spots per frame (per sheet).

To tackle this problem the convenient system of "journal" editing integrated into the Metamorph imaging sofware was used to build a simple algorithm. In an initial step to reduce the size of the data set and computing time, individual membrane sheets (as judged by FM1-43 staining) were cut as complete sequences from each recording. This was also required to separate the output data for the individual membrane sheets. The data was then treated as follows for every image in the sequence (see also figure 10):

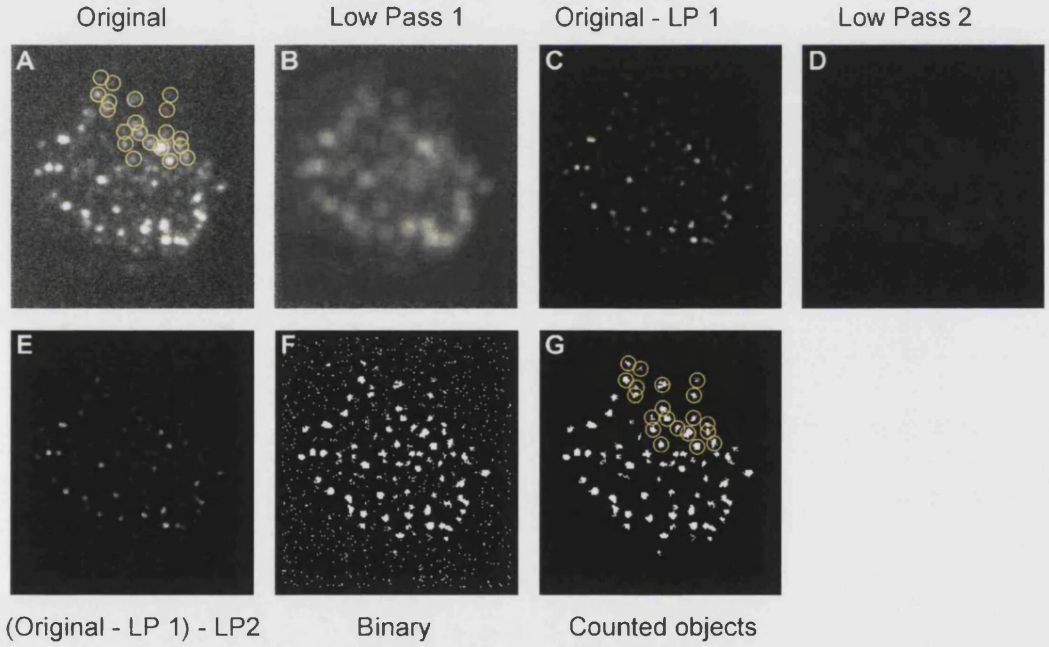

▲ ***Figure 10. Individual steps in the image analysis algorithm for the counting of acridine orange labelled spots***

(A) Single frame of the original image stack. The yellow circles represent individual fluorescent objects. (B) A copy of the original image after the low pass filtering results in a strongly convolved image. The quadratic form of the blurred fluorescent spots is due the square shape of the filter. (C) Result of subtracting the

filtered image from the original. Note the overall loss of intensity, but a gain in signal to noise ratio (~10-20 fold). (D) Low pass filter of the image shown in (C), and (E) result of subtracting this from (C). (F) A binary image produced from (E) produced by setting a low intensity threshold (≤ 15 arbitrary units) for pixels. (G) Objects identified in (F) by the size exclusion filter. The yellow circles represent the fluorescent spots seen in the original image (A).

- Double low pass filtering and subtraction. The signal to noise ratio and the spatial resolution of each original image (Fig. 10 A) was improved by using a low pass filter (10 x 10 pixel matrix) to produce a convolved copy (Fig. 10 B) which was subtracted from the original (Fig. 10 C). This result was low pass filtered again (Fig. 10 D) and subtracted from the starting image to produce a double low pass filtered subtracted image (Fig. 10 E). This method is well documented and is essentially a method for high pass spatial filtering of images i.e. it enhances the high frequency information content. Although the subtraction results in an overall reduction of the intensity, the signal to noise ratio is improved for individual objects by around 10 - 20 fold. This process enhances the spatial resolution, especially in areas where the intensity changes swiftly from one pixel to the next e.g. the rapid change on moving from pixels of background intensity onto the edge of a bright object (in this case an acridine orange labelled granule). The effects of the low pass filtering and subtraction are shown more clearly in figure 11.

- Conversion to binary images. In order to count the objects within the image, the pixel intensity values within it must be converted to binary (Fig. 10 F). This is achieved by setting a threshold for pixels of low intensity values. An intensity threshold of 15 arbitrary units gave the best results under these conditions. The resulting image appears noisy (single white pixels in Fig. 10 F) with bright objects appearing as groups of white pixels. The effect of changing the binary threshold is discussed later.

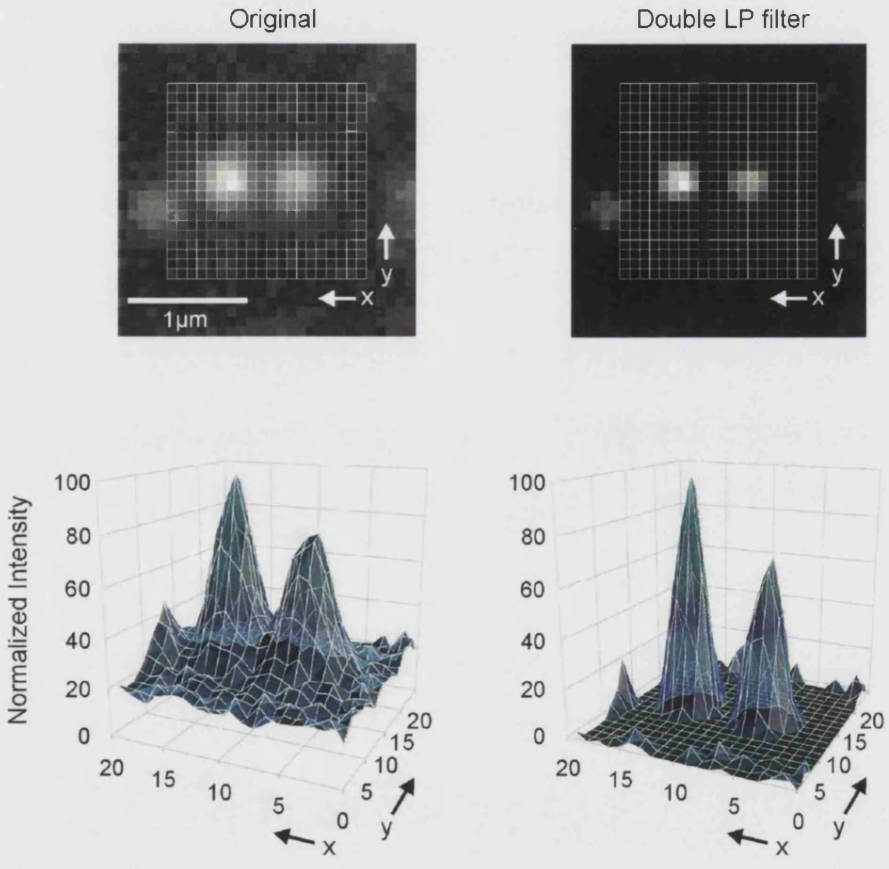

▲ ***Figure 11. Example of the result of using a double low pass filter protocol***

The original image (top left) shows two resolved but partially overlapping fluorescent signals. The white grid shows the individual pixels that make up the image; their intensities are plotted as a 3D surface map (bottom left). Note the

level of background and the clear overlap of the signals. The result of double low pass filtering (top right) on the same two objects and again plotted as 3D surface intensity map (bottom right). Background signal has been reduced to zero and the objects are clearly separated from one another. In all cases intensity has been normalised to aid comparison.

- Object counting. A second filter defines the objects within the binary image that the Metamorph software counts. Objects were defined as groups of 5 or more white pixels having direct contact to one another via edges or corners. A typical result of applying this size exclusion filter to a binary image is shown in figure 10 G. Note that the background noise has been removed. The remaining number of objects corresponds well with the acridine orange labelled structures seen in the original image (compare Fig. 10 A with G, note the excellent overlap of the yellow circles in both images). The number of objects is then recorded for later analysis. Effects of changing the size exclusion filter are discussed below.

The effects of varying the binary and size exclusion thresholds on the number of objects counted in an image are demonstrated in figure 12. For convenience the same image analysed in figure 10 is used. In the first two image columns of the effect of changing the binary threshold whilst maintaining an object size exclusion threshold of ≥ 5 pixels can be clearly seen. When the binary threshold is too low (e.g. 5 a.u.), pixels of background intensity are not excluded and are of sufficient number and density to form "pseudo" objects. Alternatively, when the binary threshold

is too high (e.g. 25 a.u.) pixels or groups of pixels belonging to objects are excluded leading to an under estimate of their numbers. In addition a bias towards brighter objects/granules is observed. In the upper row of images the effects of varying the size exclusion filter are shown. In this case the effects are similar - a too high threshold leads to an under estimate of object numbers and vice versa.

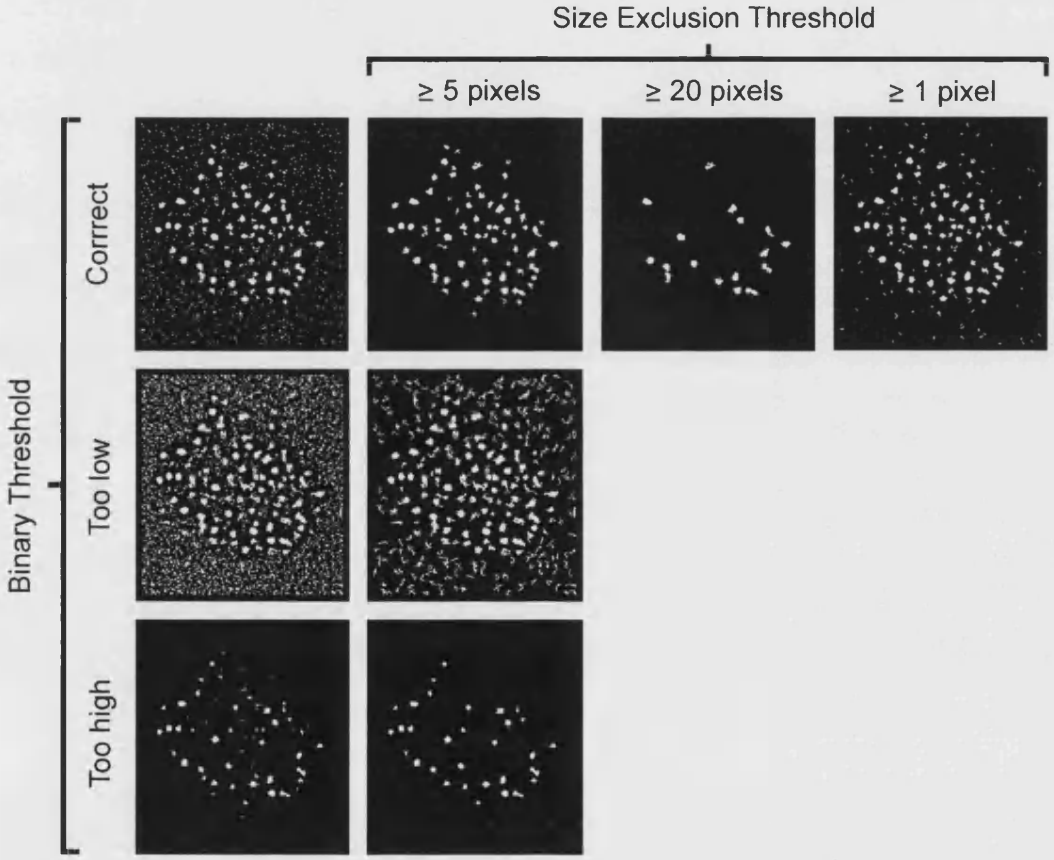

▲ ***Figure 12. The effects of varying the binary and size exclusion thresholds on the number of objects counted in an image***

The results of varying the binary threshold (first column) on the number of objects counted can be clearly seen (second column). The effects of changing the size exclusion threshold are also demonstrated (top row of images). Note that for convenience that same image as in figure 10 is used.

Initial experiments in which this system was used to estimate the rates of exocytosis (as a loss of acridine orange labeled particles) proved to be very successful. However, insufficient data has been gathered for a fully quantitative assessment and only some preliminary data is presented here. This is shown in figure 13.

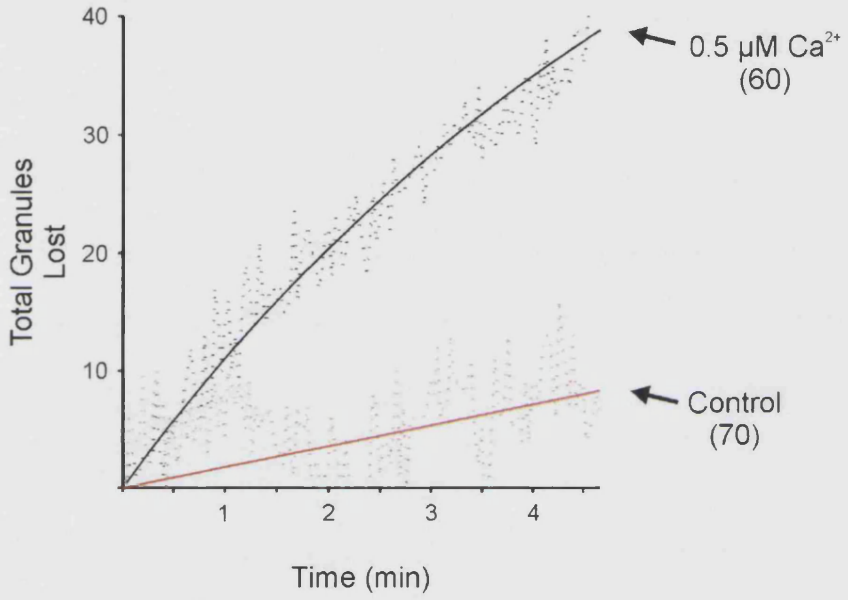

▲ ***Figure 13. Traces produced from an experiment to estimate exocytosis by semi automated image analysis***

Excyotosis is plotted as a loss of granules (fluorescent spots) over time for a membrane sheet incubated with Ca^{2+} (black) or under control conditions (red). The raw data (counting output) is shown as a dotted line in both cases. The numbers in brackets represent the number of objects counted in the first frame of each sequence. The data shown here is typical of one preliminary experiment.

Stimulation of a membrane sheet with 0.5 µM Ca^{2+} results in a loss of acridine orange labelled spots that is fit well by a single exponential. Under control conditions, as expected, only a slow linear background loss

of spots is seen. Note that in both cases the dotted line represents the values determined by the algorithm for individual images of the time-lapse sequence. These values are noisy due to fluctuations in the fluorescent intensity caused by small changes in the focal position during the measurement.

4.4 Results and analysis 3 – GFP labelled neuropeptide Y as a fluorescent marker for monitoring exocytosis on membrane sheets

The use of acridine orange as a fluorescent marker for monitoring secretory granule exocytosis is well documented (see for example Steyer and Almers, 1997; Avery et al, 2000). However, the use of this fluorescent dye has several drawbacks. First, it is non-specific and labels all acidic organelles. Second, it bleaches in a rapid and non-linear manner making it unsuitable for extended observations. Third, compartments strongly labelled with the dye display a tendency to undergo photolysis when exposed to excitation light of high intensity (J. Avery, personal communication). Forth, upon illumination it forms highly reactive radicals, which are damaging to biological material.

Thus, as an alternative to acridine orange, GFP fused to the *c*-terminus of neuropeptide Y was transiently tranfected into PC12 cells from which it was subsequently possible to produce membrane patches loaded with GFP labelled secretory granules. GFP labelled neuropeptide Y has been previously shown to be correctly sorted and expressed in this cell

line, and can be used a fluorescent marker to monitor exocytosis (Lang et al., 1997). In addition to a specific labelling of secretory granules, GFP is more photo-stable and bleaches in a relatively linear manner. In comparison to acridine orange it is also benign to the cell. GFP is also a pH sensitive fluorophore and can be used to monitor rapid changes in organelle acidity (for review of GFP properties see Patterson et al., 1997).

The characteristics of membrane sheets produced from GFP neuropeptide Y transfected PC12 cells are similar to those of acridine orange labelled cells. With an average area of decorated membrane sheet of 52 $\mu m^2 \pm 19$ (n=17) and a granule density of $0.75/\mu m^2 \pm 0.24$ the preparations are comparable to those labelled with acridine orange (see 4.2.1).

When such GFP labelled membrane sheets were stimulated for exocytosis, initial experiments revealed a surprising pattern of fluorescence intensity changes (Fig. 14, overleaf). Although a uniform abrupt loss of intensity was observed like with acridine orange (F_{lost}), dimming (F_{down}) and also brightening (F_{up}) of secretory granules were also seen.

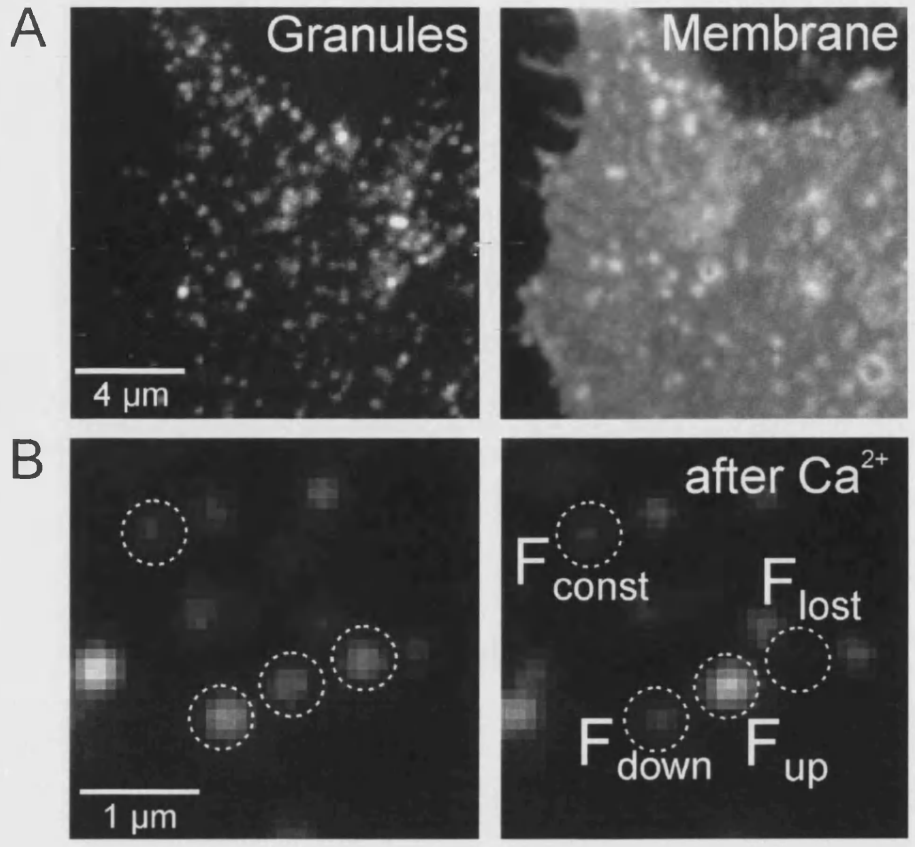

▲ Figure 14. Secretory granules labelled with neuropeptide Y GFP bound to membrane sheets prepared from a transiently transfected PC12 cell

(A) Overview of a membrane sheet generated from a PC12 cell transiently transfected with neuropeptide Y GFP. The membrane is counted stained with TMA-DPH. (B) A group of GFP labelled secretory granules that resided on a membrane sheet before (left panel) and after stimulation with 0.5 µM Ca^{2+}. Three of those granules highlighted by the dashed circles undergo abrupt changes in flourescent intensity. The data shown are typical for the observations made in 10 separate experiments.

4.5 Discussion

In this section the further characterisation of a cell free assay for exocytosis in PC12 cells is described. This system allows a study of the membrane fusion of single secretory granules at high spatial and temporal resolution. Previously, exocytosis in this system was shown to be dependent on micromolar Ca^{2+}, MgATP and cytosol (Avery et al., 2000) in a manner that resembles exocytosis in permeabilised cells (Martin, 1997).

In this assay system, carrier supported plasma membranes with attached secretory granules are derived from PC12 cells grown on coated coverslips. Methods for the production of such preparations are well established (reviewed by Heuser, 2000), but limited to a small number of suitable cell shearing techniques. Here, ultrasonic pressure waves (generated with a standard tip sonifier) propagated through a suitable buffer were used to disrupt cells. This occurs such that the cell body, together with the nucleus and associated organelles are removed leaving the glass attached plasma membrane "footprint" of the cell behind. These are in some cases found to have numerous bound secretory granules. Thus a balance must be struck between efficient production of membrane sheets and blasting away of the secretory granules. Using the current method, it appears that no clear optimum has been found for this buffer system and PC12 cell clone. This method also gives variable results between coverslips, probably as a consequence of numerous uncontrollable factors in the plating and cultivation of cells. However, the

process was sufficient to perform the experiments described in both this and the following section. In the future it will probably be possible to increase the success and efficiency of membrane sheet production by performing this step with a smaller sonifier mounted directly on the microscope stage. This would facilitate through-put by allowing several attempts per coverslip at producing a suitable membrane sheet and would reduce the time required to locate such specimens.

The sub-plasmalemma region were a cultured neuro-endocrine cell adheres to a coated glass substrate might represent an area of the cell that has become specialised for adhesion. This is further emphasised by the finding that the actin cortex is thicker in this area (Lang et al., 2000). Does this have an influence on exocytosis in this part of the cell? Thus, for the membrane sheet preparation described here this represents a pertinent question. However, evidence presented here and in numerous publications strongly suggests that this is not the case. In particular, studies using evanescent wave and confocal microscopy (Steyer et al., 1997; Lang et al., 1997; Steyer and Almers, 1999; Tsuboi et al., 2000; Barg et al., 2002) have shown exocytosis to occur with similar frequency and characteristics to that monitored in other parts of the cell. The densities of granules that appear to be docked at the plasma membrane are also similar to those seen in other regions ~ 1 granule/μm^2. Indeed these findings are also confirmed by electron microscopic studies (Parsons et al., 1995; Plattner et al., 1997; D. Riedel, unpublished observations). In the membrane sheet preparation described here the

absolute rate of exocytosis is approximately 8-10 times slower than that measured in whole PC12 cells (D. Schutz personal communication). However, the density of docked granules is comparable to that found in whole cells by the methods described above.

In PC12 cells the sub-plasmalemma is characterised by a thick pad of filamentous actin, forming a dynamic meshwork that underlies the entire cell periphery. Before they can dock at the plasma membrane secretory granules must traverse this actin cortex. The ultrasonic disruption of PC12 cells to produce membrane sheets results in a sever thinning of the actin cortex. In fact, the remaining actin accounts for only 4 % of that in the cortex of whole cells and is composed mainly of large actin stress fibres. This finding is, in itself, not surprising, given that the steady state between globular and fibrous actin has been destroyed, or that other cortex remodelling factors have been lost. However, it may help to explain the slow, steady loss of granules observed under control conditions in the exocytosis assay. In whole cells, those granules not tethered to the membrane directly are probably restricted by a cage of actin in which they are embedded (Steyer and Almers, 1999; Lang et al., 2000). Thus it is not possible for them to retreat back into the cytosol. However, on membrane sheets this restricting mesh of actin is no longer in place. Hence, this might be one factor contributing to the small but steady loss of granules observed under control conditions.

While the de-polymerisation of a restricting actin meshwork may contribute to and accelerate the background loss of granules, several

other possibilities might also be considered. A slow wash out of controlling factors leads to a lack of regulation resulting in higher rates of Ca^{2+} independent fusion or un-tethering of granules allowing them to defuse away. It is also possible that some granules lost their membrane pH gradient, indeed treatment of membrane sheets with $(NH_4)_2SO_4$ leads to a rapid escape of acridine orange from granules (data not shown). Finally, organelles strongly labelled with acridine orange have a tendency to photolyse when the intensity of the excitation light is too high (J. Avery, personal communication). This phenomenon has also been observed by other groups studying exocytosis using acridine orange as a marker (Johns et al., 2001). In fact acridine orange, although it is a simple, bright and rapid vital stain, has several other drawbacks which should be mentioned here. Firstly it is non specific and labels all acidic organelles. Secondly, it bleaches in a rapid, highly non-linear manner. Thirdly, upon illumination it forms highly reactive radical species, which are damaging to biological material.

Three imaging methods are described here for monitoring the *in-vitro* exocytotic loss of the acidophilic dye acridine orange from secretory granules. All methods take advantage of the lack of out of focus fluorescence in this preparation and hence image membrane bound particles at the full resolution afforded by a NA 1.4 objective. The simplest of these uses a before and after image principle to relate exocytosis to the total pool of membrane bound granules at the beginning of the experiment. While not suited to investigating questions of a dynamic

nature, this method provides a simple tool to document some of the basic characteristics of membrane sheet morphology and physiology (see above). At the other extreme, it was possible to image exocytosis over short periods at video rate (40 Hz), but with a poorer signal to noise ratio. Finally, the third method is a compromise taking advantage of the better signal to noise ratio of a cooled slow scan CCD camera during longer exposures, combined with time lapse imaging and a semi-automated image analysis algorithm for data analysis.

Video rate imaging combined with acridine orange dye labelling again allows observation of single granule distribution but, in addition individual excytotic events are recorded as dye dequenching flashes. Such events display striking resemblance in their intensity-time traces to the current-time spikes detected by carbon fibre amperometry from PC12 cells. However, as described in the results, these events have rise times that are beyond the time resolution of the camera system. Thus, it is not possible to make conclusive statements about the fusion kinetics of single vesicles based on these data.

Capacitance measurements of exocytosis in chromaffin cells show that the response follows distinct kinetic phases (Parsons et al., 1995; Mennerick and Mathews, 1996; Voets et al., 1999). These are believed to represent distinct, interconnected granule pools within the cell, with the release kinetics related to the exocytotic competence of the granules within the pool. The relative size of the pools can also be estimated. However, these methods provide no spatial information about individual

vesicles. Steyer and Almers (1997, 1999) have shown chromaffin cells (observed by evanescent wave microscopy) to have a large pool of granules close to or tethered at the plasma membrane. Turnover is slow with new granules taking an average of 6 min to arrive at the membrane. Thus, those granules belonging the faster phases seen in the capacitance measurements are most likely part of this membrane anchored/proximal population. The granules seen on PC12 membrane sheets probably represent those that are anchored at the membrane. When stimulated and imaged at 25 Hz for 2 min, two distinct phases of exocytosis were observed. The burst-like phase seen in the first 10 s most likely represents a sub-population of tethered granules that are more competent, and exocytose earlier upon addition of Ca^{2+}. Neher and co-workers have suggested that release competence and local Ca^{2+} gradients (produce by the influx of Ca^{2+} via ion channels and distribution of native Ca^{2+} binding entities, for review see Neher, 1998) play a role in the multi-phasic responses found in chromaffin cells. It has been further suggested that a sub-population of granules be directly coupled to Ca^{2+}-channels via a syntaxin-mediated interaction (Rettig et al., 1997). In the experiments described here it is highly unlikely that Ca^{2+} gradients play a role in the secretory response. Thus the release competence of individual granules on membrane sheets is due to or limited by other unknown factors.

While the time resolution of video microscopy is not comparable to those available to electrophysiological studies of exocytosis, it is a great leap forward from *in-vitro* assays based on cracked or permeabilised cells,

and equal to or better than that obtained in fluorometric systems (e.g. that described for the exocrine pancreas by Maclean and Edwardson). However, for many experiments such a level of time resolution is not required or unnecessary, much more useful is the spatial information and the biochemical access facilitated by the open nature of the preparation. Video microscopy also has the disadvantage that the specimen is under constant illumination. This leads to rapid bleaching of the sample, reducing both the resolution, through a loss of signal to noise ratio, and hence the time available for imaging.

To minimise these problems, a time lapse-imaging method was employed which enabled secretion to be monitored for up to 5 min. The advantage of this method is a reduced rate of photo-bleaching which maintains the signal to noise ratio and hence the ability to resolve objects over longer periods. This imaging protocol was combined with a semi-automated image analysis algorithm. This was implemented to speed the analysis of image data sets (~150 images/membrane sheet), while providing a consistent, impartial way of assessing secretion rates.

Finally, as an alternative to acridine orange GFP labelled neuropeptide Y can be used as a specific fluorescent marker for secretory granules. It was also possible to produce membrane sheets with bound GFP labelled granules from cells transiently transfected with this construct. These have a similar size and density of granules to those found in the acridine orange labelled membrane sheet preparations. However, the signal to noise ratio is improved due to the specificity of the labelling and

the fluorescent properties of the GFP fluorophore. More interesting are the striking fluorescence intensity changes displayed by individual granules upon stimulation of exocytosis. In addition to the uniform loss of intensity that is observed exclusively with acridine orange, granules also became brighter and dimmer. In some cases two changes were observed. These findings suggest that GFP is incompletely released from some granules during exocytosis. An in depth quantification, investigation and discussion of this phenomena and the possible molecular mechanisms behind it are the subject of the second part of this thesis.

5. Part II – Fates of secretory granules following exocytosis investigated using an *in-vitro* cell-free assay

5.1 Introduction

Neurones and neuroendocrine cells release hormones and neurotransmitters by Ca^{2+}-dependent exocytosis from storage vesicles. After exocytosis, the membranes of fusing vesicles are recovered by endocytosis. Thus a net equilibrium is maintained between membrane addition and membrane removal from the plasma membrane. Much of the history, development and debate surrounding investigations into this process were introduced at the beginning of this thesis. In this section, data will be presented that tries to address some of the biological questions put forward there.

A technically improved version of the *in-vitro* approach described in Part I of this thesis was used. Several major improvements have been introduced: (i) Secretory granules were labelled specifically using a fusion protein of human neuropeptide Y (NPY) and the enhanced green fluorescent protein (GFP, introduced at the end of part I). This was introduced to the cells by transient transfection and has been previously shown to be correctly expressed and targeted by this cell line (Lang et al., 2001). (ii) Images were recorded using a frame transfer camera with back illuminated CCD with up to 90 % quantum efficiency. (iii) The focal position was maintained using a piezo electric device. (iv) A xenon arc lamp was used as the illuminating light source for more efficient excitation of GFP

fluorescence. (v) An electronic shutter device coupled to the trigger of the camera improved the ability to control illumination of the specimen. These improvements enabled an extended 15 min imaging protocol to be used.

5.2 Results and analysis

5.2.1 Transient exocytosis of secretory granules in a cell-free preparation

When neuropeptide Y-GFP (Lang et al., 2001) was used a content marker for secretory granules in this preparation, a surprising pattern of fluorescence intensity changes was observed that was different from the uniform dye loss observed with acridine orange (Fig. 15A & B). In addition to abrupt loss of fluorescent intensity (F_{lost}) dimming (F_{down}) and also brightening (F_{up}) of secretory granules were observed (Fig. 15B & D). Occasionally, granules were observed that underwent two consecutive fluorescence changes e.g. brightening, followed by dimming or loss (see e.g. Fig 16). All changes in fluorescence intensity were dependent on calcium, and there was not strong preference for the one or the other mode over a broad range of calcium concentrations (Fig. 15F, see also Fig. 17, lower panel). In addition, there was no correlation between changes in fluorescence and the initial fluorescence intensity of a granule (data not shown). It was also not possible to exclude if some of those granules seen to undergo F_{down} or F_{lost} events underwent a prior change in intensity due to the time resolution used (2 frames/min). However, recording at higher speeds results in more rapid bleaching of granules

such that it becomes difficult to distinguish between F_{lost} and F_{down} changes (data not shown).

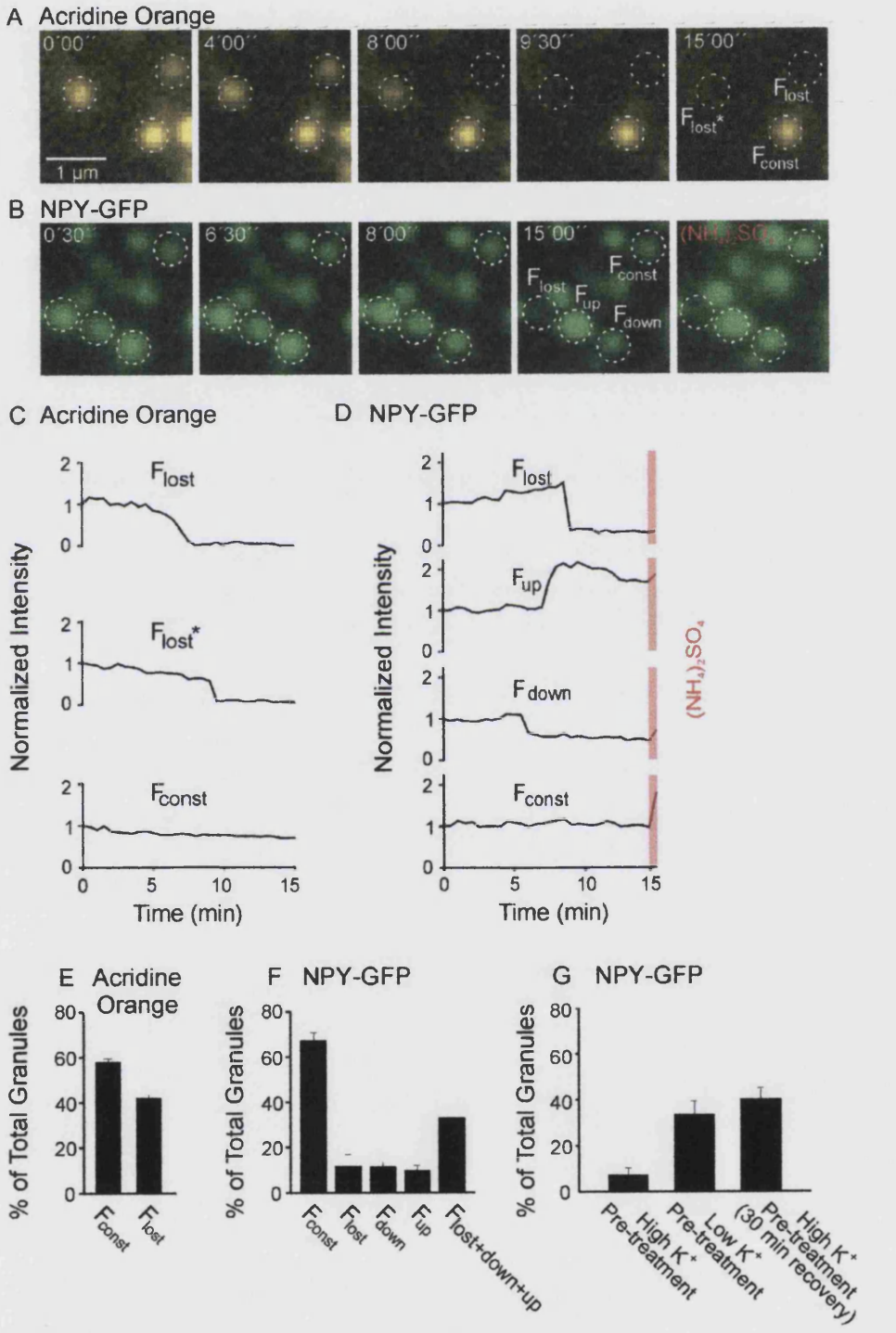

◄ ***Previous page, Figure 15. Ca^{2+} -dependent exocytosis of secretory granules in a cell free preparation, monitored by time lapse microscopy using either acridine orange or NPY-GFP as content marker***

Membrane sheets with attached secretory granules labelled either by the acidophilic dye acridine orange (A) or by expression of the secretory granule marker NPY-GFP (B) were incubated in a solution containing 0.5 µM free calcium, 0.5 mg/ml rat brain cytosol and 2 mM MgATP to stimulate exocytosis. Images were taken every 30 s for 15 min, and the fluorescence intensity of individual granules was measured (see Methods). (C and D) Exemplary intensity traces of those granules shown in A and B. Intensity values were corrected for local background, normalised to initial intensity, and plotted against time. (C) When acridine orange was used, granules either lost their fluorescence (F_{lost}) or were slowly bleached (F_{const}). (D) Changes in fluorescence intensity of granules labelled with NPY-GFP. Granules disappeared (F_{lost}), became brighter (F_{up}), dimmer (F_{down}) or did not change in fluorescence intensity (F_{const}). Orange bars; fluorescence intensity after addition of 20 mM $(NH_4)_2SO_4$ which abolishes the pH-gradient across the granule membrane. (E and F) Relative abundance (percent of total) of granules classified according to their fluorescence intensity changes as described above. For acridine orange 4 membrane sheets were analysed, for NPY-GFP 10 membrane sheets. (G) Exocytosis of NPY-GFP labelled secretory granules from membrane sheets derived from intact cells pre-treated with high K^+ or control buffers for 2 min at 37 °C in the presence of 20 µM sulforhodamine. Membrane sheets were prepared immediately after such treatment or after a 30 min recovery at 37 °C. Membrane sheets were then stimulated as described above. The values indicate mean values ± sem (n =6-10 membrane sheets for each condition).

GFP fluorescence is known to be quenched at low pH, with a 50 % reduction in intensity when the pH is shifted from 7.5 to 5.5 (Patterson et al., 1997). Thus, the increase in fluorescence intensity may be due to a pH increase of the acidic granule interior. To test for this possibility $(NH_4)_2SO_4$

was added to neutralise the pH-gradient across the vesicle membrane. As shown in figure 15D granules that did not exhibit a fluorescent change during stimulation (F_{const}) increased 72 ± 7 % (n=134 granules) in intensity, confirming that GFP is indeed quenched to a low intra-granular pH. F_{up} granules also increased in brightness but to a lesser extent (22 ± 5 %, n=44 granules), and there was a significant fraction in which no increase was observed after addition of $(NH_4)_2SO_4$. F_{down} granules also showed an increase (46 ± 10 %, n=18 granules). To exclude that $(NH_4)_2SO_4$ has a direct effect on GFP-fluorescence, membrane sheets from cells expressing syntaxin 1A-GFP (Lang et al., 2001) were exposed to a final concentration of 20 mM in K-Glu buffer. No change of fluorescence was observed.

These observations could be explained by a transient fusion of secretory granules, followed by its re-capture at the site of exocytosis. Since fusion allows neutralisation of the vesicle interior due to exposure to extracellular buffer, the increase in fluorescence (F_{up}) is probably due to vesicles that had undergone transient fusion for a period sufficient for content neutralisation, but not sufficient for GFP to escape. That such events were transient is further supported by the observation that some F_{up} granules are capable of re-acidification. This results in a slow, but significant decrease in their fluorescent intensity after fusion (see F_{up} granule Fig 15D), which can be reversed by the addition of $(NH_4)_2SO_4$. Furthermore, granules were also seen that increased in fluorescent intensity before undergoing an intensity loss after short delay (e.g. see Fig.

16 $F_{up+down}$). F_{down}-granules would represent those that had lost part of their GFP content during transient fusion. Thus, transient fusion would be of sufficient duration for the small dye molecules of acridine orange to escape into the medium. In contrast, depending on the open time and diameter of the fusion pore, the larger GFP protein would be released only incompletely, with some granules retaining most of the marker and others releasing it in full (see also Barg et al., 2002).

If secretory granules indeed undergo transient fusion, their interiors are expected to be temporally accessible to membrane-impermeant molecules that are present in the medium. To test this hypothesis, exocytosis was stimulated in the presence of bromophenol blue, a dye that reversibly quenches GFP fluorescence (Choi et al., 2001b). As a result, only F_{lost} granules were observed (data not shown) indicating that bromophenol blue had access to the GFP labelled cores of F_{down} and F_{up} granules. Removal of the quencher led to a re-appearance of GFP fluorescence. However, quantification was made difficult due to a retarded diffusion of bromophenol blue across the granule membrane. This leads to disappearance of all granules within 5-10 min. In a second approach, it was attempted to label re-captured secretory granules directly be the uptake of a fluorescent fluid phase marker. GFP-labelled granules were stimulated for exocytosis in the presence of 5 µM sulforhodamine-101, a membrane impermeant red fluorescent dye that is not detectable in the GFP-channel of the microscope. At the end of the stimulation excess sulforhodamine was removed by extensive washing with K-Glu buffer. As

shown in figure 16, red fluorescent spots were observed that precisely co-localised with secretory granules, with a strong preference for granules that had undergone intensity changes in the GFP channel during the preceding stimulation period (Fig. 16). In addition red-labelled structures were observed that had a more irregular shape and did not co-localise with green labelled structures. These probably represent components of the endosomal pathway.

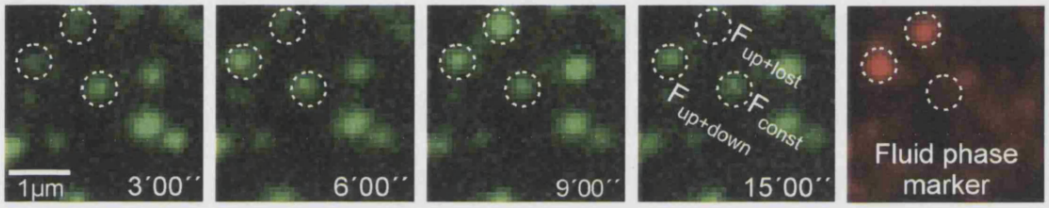

Figure 16. Endocytotic capture of the fluid phase marker sulforhodamine by secretory granules following stimulation of exocytosis and its dependence on calcium

Membrane sheets with docked NPY-GFP-labelled secretory granules were stimulated for exocytosis (as in Fig. 15) in the presence of 5 µM sulforhodamine and imaged as before. Exemplary images from the sequence in the GFP-channel are shown. After 15 min, sulforhodamine was washed out, and images were acquired in the red and the green channel. Two red spots are visible that are concentric with secretory granules that have undergone exocytosis ($F_{up+lost}$ and $F_{up+down}$), whereas an inactive granule (F_{const}) has no corresponding signal.

To quantify this uptake of fluid phase marker, circles were superimposed on active granules (or in the case of F_{lost} granules, centred at the point where the granule disappeared in the sequence) and transferred to identical pixel locations of the corresponding fluid phase

marker uptake-image. Granules were rated to have undergone endocytosis (re-capture) when the two signals were concentric to within 150 nm (~2 pixels with this camera at 160 x magnification). To correct for accidental co-localisation, statistical overlap was calculated for each experiment using a fixed grid of circles placed randomly onto the membrane sheet of interest (see methods). This background ranged between 3 and 5 %. As shown in figure 17 (middle panel) more than 30 % of the active granules (F_{lost}, F_{down}, and F_{up}) were labelled with sulforhodamine. In contrast, sulforhodamine was only rarely seen in F_{const} granules (4.3 ± 2.4 %, n=339 from 7 membrane sheets).

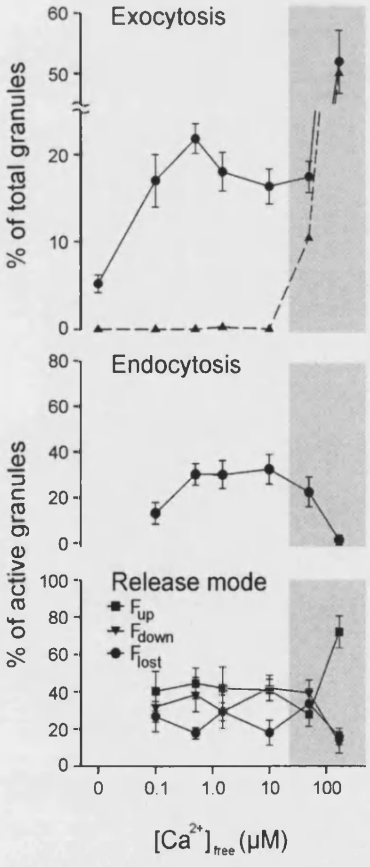

◄ ***Figure 17. Endocytotic capture of the fluid phase marker sulforhodamine by secretory granules following stimulation of exocytosis and its dependence on calcium***

Calcium dependence of exocytosis, endocytosis and the individual release modes. For each calcium concentration 5-9 membrane sheets were analysed. Rates of endocytosis were corrected for random overlap as described in the methods section. The grey box indicates calcium concentrations at which the assay allows no evaluation of the data since secretory granules not associated with the membrane sheets but attached to the glass also display changes in fluorescence intensity (triangles, upper panel). Values are given as mean ± sem (n = 5 - 9 membrane sheets).

The proportion of granules undergoing such endocytic re-capture was lower at 0.1 µM free calcium, but did not vary significantly between 0.5 µM and 50 µM. At calcium concentrations higher than 50 µM (shaded area in Fig. 17) no reliable data could be obtained. This was because changes in GFP-fluorescence were also observed on washed out granules that were bound to the surrounding glass surface (triangles in Fig. 17 upper panel). There was no correlation between one of the release modes (F_{lost}, F_{down}, and F_{up}) and endocytic uptake of sulforhodamine (data not shown).

If secretory granules undergo transient exocytosis, that is they are re-captured at the site of exocytosis, are they capable of undergoing a second round of exocytosis. To investigate this possibility membrane sheets were prepared from cells that were stimulated for 2 min with high-K^+ Ringer buffer in the presence of 20 µM sulforhodamine. Immediately, after stimulation, membrane sheets were prepared by sonification. Although such sheets contained both GFP- and GFP/sulforhodamine labelled secretory granules (data not shown), exocytosis could not be stimulated beyond background levels (Fig 15G). This suggests that the preparation was refractory to further stimulation. If cells were incubated for 30 min in culture media after the 2 min stimulation with high-K^+ Ringer buffer, membrane sheets prepared thereafter still contained both GFP and GFP/sulforhodamine positive granule populations. When these sheets were stimulated, normal rates of exocytosis were observed (Fig. 15G), with no difference between single and double-labelled granules.

5.2.2 Stimulus-dependent labelling of secretory granules with fluid phase markers in intact PC12 cells

In an independent approach the stimulus dependent uptake of fluid phase marker by secretory granules was studied in intact PC12 cells by cryo-electron microscopy. Intact cells were stimulated for 2 min by high K^+ depolarisation in the presence of the fluid phase marker horseradish-peroxidase (HRP). Cells were then washed, fixed and reacted with diamino benzidine. From this ultra-thin cryo-sections were then prepared and analysed by transmission election microscopy in collaboration with Dr. Dirk Wenzel. HRP labelling was observed in small un-coated round and elongated membrane profiles that probably represent early endosomal structures (Fig. 18G, H, see also De Wit et al., 1999 for comparison). However, labelling was also detected in vesicles with morphological features (size, shape, lack of internal membranes) indistinguishable from secretory granules (Fig.18A – D). Often these profiles were seen in close proximity to the plasma membrane. Labelled vesicles were not confined to zones of surface or cell-cell contact excluding that granule recapture is caused by the inability of membranes to move laterally due to substrate attachment i.e. as in the case of carrier supported membrane sheets.

To document that the high electron density of these granules is indeed a result of HRP uptake and not due to density variations of granule cores, the intensity distribution was profiled. The cores of granules from cells stimulated in the presence and absence of HRP were. Secretory granules were easily identified due to their round shape, size (a diameter

of around 120 nm in this clone, Tooze et al., 1991) and the presence of a clearly visible dense core devoid of internal membrane. The relative granule density was determined by placing a line scan through the centre of the secretory granule. The average intensity of the core was then related to the density of the surrounding cytosol. In the presence of HRP, two peaks of relative core densities were identified, one at around 20 % and the other at around 45 % (Fig. 18J). In the absence of HRP only one peak at 20 % density was found (Fig. 18I) Non-stimulated cells processed in parallel also displayed some HRP-labelled secretory granules, but to a much lower extent (data not shown).

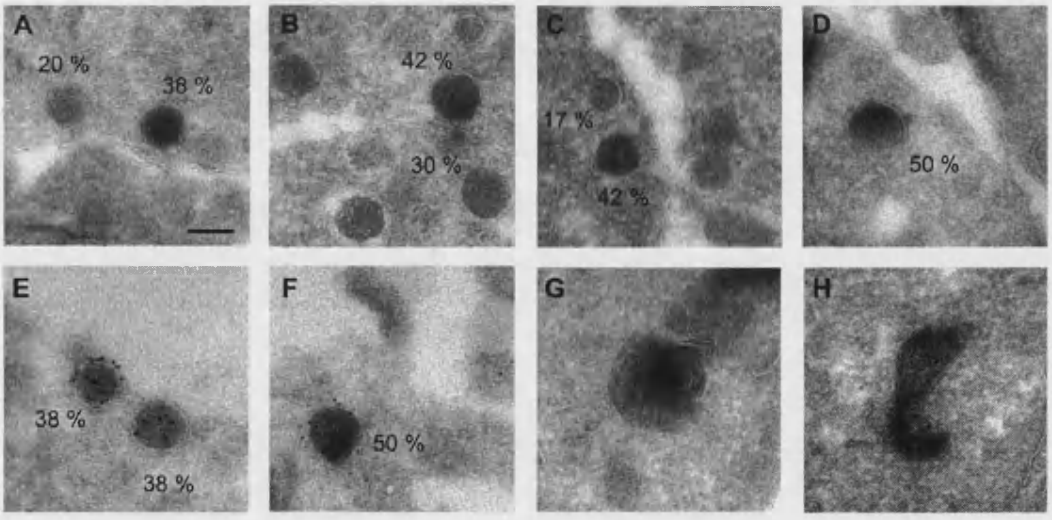

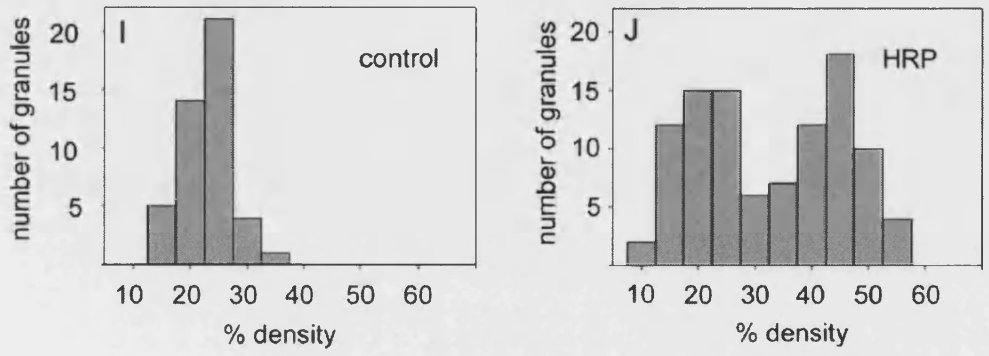

◄ ***Previous page, Figure 18. Gallery of electron micrographs showing organelles sequestering horseradish peroxidase (HRP) after 2 min high K^+-stimulation of intact PC12 cells***

Organelles that have taken up HRP appear more electron dense. To quantify HRP uptake, line scans were performed through the centre of the labelled structure, measuring its average intensity ($gran_{int}$) and the intensity of the surrounding cytosol (cyt_{int}). The density was calculated according to: % density = (1-$gran_{int}/cyt_{int}$) x 100. (A-D) Organelles classified as secretory granules (numbers indicate % density, (see text)). (E, F) Double labelling of secretory granules from NPY-GFP transfected cells containing GFP (immunogold labelling) and trapped HRP after stimulation of intact cells. (G, H) HRP-labelled organelles probably representing endosomes. (I, J) Histograms showing the % density distribution of secretory granules in stimulated cells in the absence (I, n=45 granules) and presence (J, n=101 granules) of HRP. Scale bar, 100 nm.

Despite the morphological similarity of the labelled vesicles with bona-fide secretory granules it cannot be excluded that these vesicles represent endosomal structures rather than re-captured granules retaining part of their protein cargo. Therefore, HRP labelling was performed of PC12 cells that were transfected with the secretory granule marker NPY-GFP. The resulting sections were then immunogold-labelled for GFP using a GFP specific antibody. As shown in figure 18E and F, numerous vesicles with morphological characteristics of secretory granules were observed that were labelled both for GFP and for the extracellular marker. No gold label was found in un-transfected cells with or without HRP labelling (data not shown).

5.2.3 Retrieval of secretory granules depends on dynamin function

The results described so far suggest that a sizeable portion (~30 %) of all secretory granules undergoing exocytosis on membrane sheets are recaptured by a spatially coupled, direct retrieval mechanism rather than by the well established pathway of clathrin mediated endocytosis. The question then arises as to whether the molecular mechanism involved in retrieval is a reversal of fusion (as implicated in the kiss and run model, Fesce and Meldolesi, 1999) or else, if a different and independent mechanism is involved. The latter was suggested by capacitance patch clamping experiments in which rapid and reactive endocytosis was at least partially inhibited by the PH-domain of dynamin (Artalejo et al., 1997). Dynamin is a GTPase that forms rings around the necks of coated pits and has recently been suggested to play a crucial function in the nano-mechanics of membrane fission (Dinino and Hinshaw, 2001; Marks et al., 2001).

To examine whether dynamin is involved in the re-capture of secretory granules, it was first investigated if dynamin is present at sites of secretory granule attachment on membrane sheets, and secondly whether there is a correlation between the presence of dynamin and granule re-capture. Membrane sheets from cells containing GFP labelled granules were fixed and immuno-stained for dynamin (Fig. 19A). About 12 % of all granules co-localised with dynamin, with no significant change after stimulation of exocytosis (Fig. 19B). However, when dynamin co-localisation was determined with granules that had sequestered fluid

phase marker during stimulation, the degree of overlap was significantly higher (more than 30 %, Fig. 19B). The same was true for GFP/sulforhodamine labelled granules on membrane sheets derived from cells pre-loaded with fluid phase marker by depolarisation induced stimulation for 2 min (Fig. 19B). These numbers are probably underestimated because dynamin staining needed to be corrected for crosstalk from the sulforhodamine channel. Thus, the sensitivity for dynamin detection was reduced. Furthermore, it is possible that dynamin dissociates from the retrieval site after fission of the membranes (Sever et al., 2000; Tsuboi et al., 2002). Thus, it would no longer to be possible to detect it at the time of fixation.

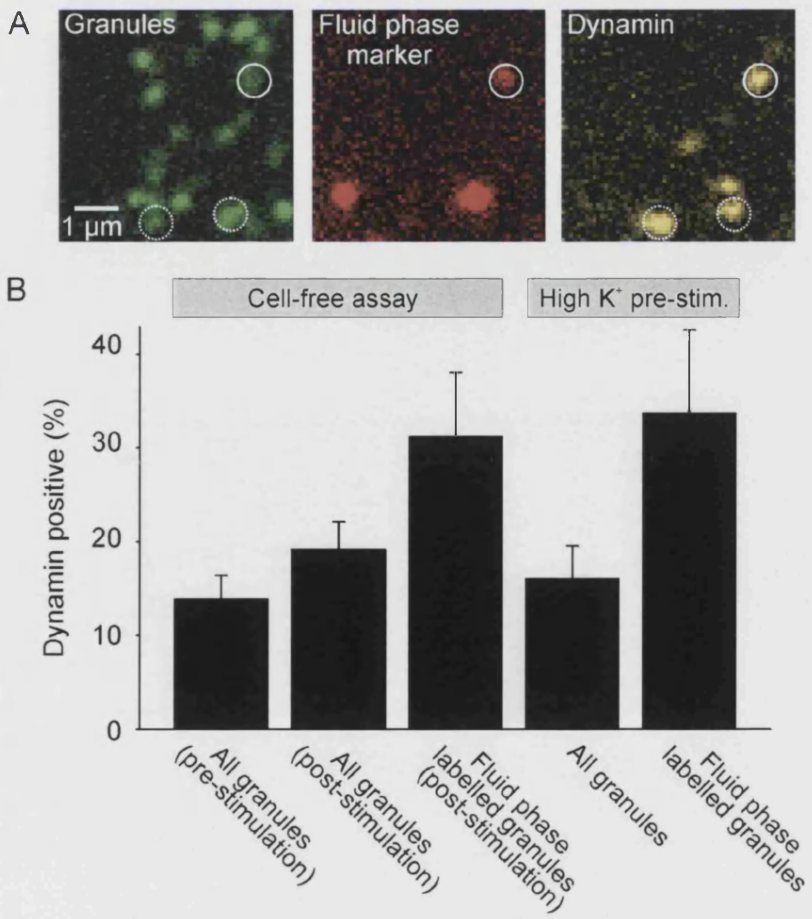

◄ ***Previous page, Figure 19. Association of secretory granules with dynamin***

(A) Triple-labelling of membrane sheets that were stimulated for exocytosis as in Fig. 15 and then fixed. The position of secretory granules was visualised by NPY-GFP (green channel). Granule re-capture was monitored by sulforhodamine uptake (red channel, see Fig. 16). Dynamin was localised by immunocytochemistry (far-red channel, displayed as yellow). (B) Percentage of granules co-localised with dynamin immunoreactivity. The first column is derived from experiments in which membrane sheets were prepared, immediately fixed and stained for dynamin. For the second and third columns membrane sheets were prepared, stimulated for exocytosis with 0.5 µM $[Ca^{2+}]_{free}$, 2 mM MgATP, and 0.5 mg/ml rat brain cytosol in the presence of 5 µM sulforhodamine, followed by washing, fixation, immuno-labelling and imaging. The last two columns are derived from experiments in which intact PC12 cells were pre-stimulated by high K^+ for 2 min in the presence of 20 µM sulforhodamine. This was immediately followed by generation of membrane sheets, fixation and immunostaining for dynamin. In all cases association of granules with dynamin was corrected for channel cross talk as well as for random association (see methods). For every condition 12 membrane sheets were analysed. Values are given as mean ± sem.

To further investigate a possible role of dynamin in the recapture of secretory granules, a series of functional studies were performed. This was done by introducing several factors established to interfere with dynamin function *in-vivo* and *in-vitro* to the membrane sheet exocytosis assay. Firstly, the non-hydrolysable analogue GTPγS was tested. GTPγS is known to lock dynamin into an oligomeric state (Stowell et al., 1999; Takei et al., 1995), preventing closure of the pore and membrane fission in clathrin-mediated endocytosis. Indeed, GTPγS inhibited recapture of secretory granules by almost 60 % whereas GTP had no effect (Fig. 20A, lower panel).

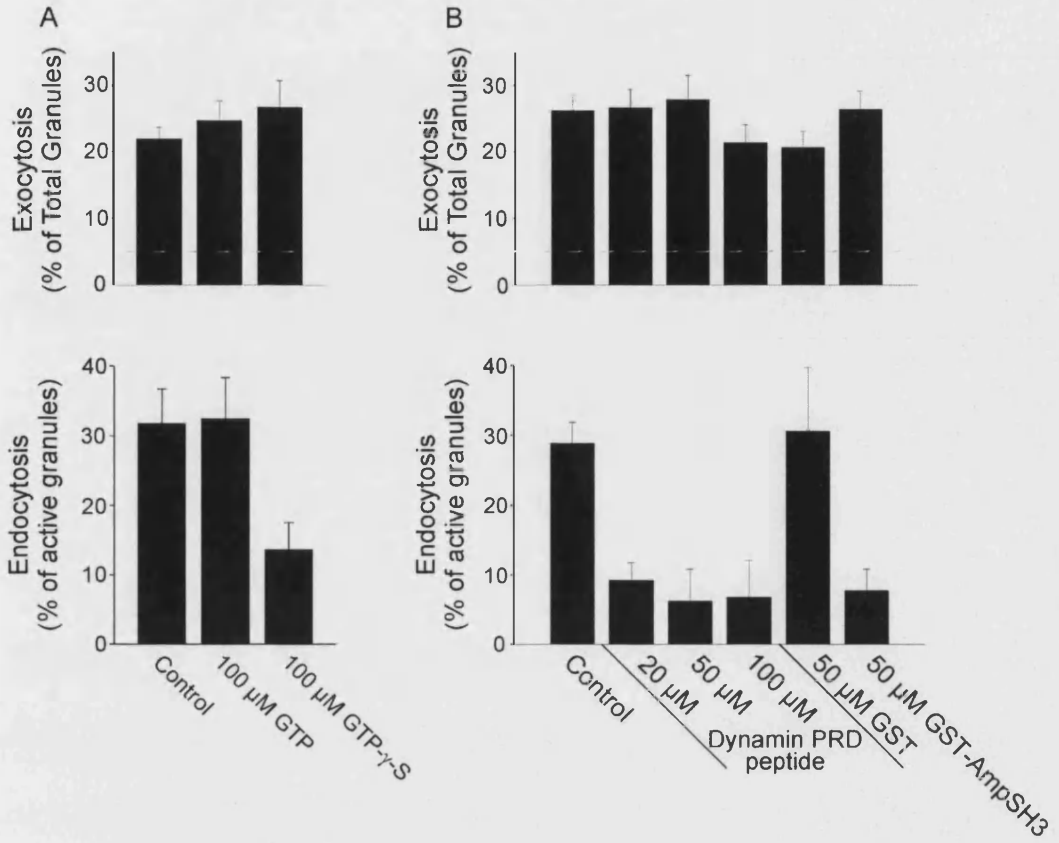

▲ ***Figure 20. Inhibition of granule re-capture by guanine nucleotides and by peptides known to interfere with dynamin function***

(A) Upper panel, effect of GTP and GTPγS on the exocytosis of secretory granules as measured by in-vitro assay. Lower panel, effect of GTP and GTPγS on endocytosis of secretory granules measured by sulforhodamine uptake. (B) Effects of a peptide corresponding to the proline-rich domain of dynamin (dynamin PRD peptide) and a GST fusion protein corresponding to the SH3-domain of amphiphysin on exocytosis (upper panel) and endocytosis (lower panel) of secretory granules. Note that experiments shown in (B) were performed in the absence of cytosol to avoid interference with cytosolic proteins. Values are given as mean ± sem (n= 6-11 membrane sheets for each condition).

Secondly, it was investigated whether granule recapture is prevented by two peptides that are known to block the action of dynamin

in endocytosis by interfering with the function of its proline-rich domain (Shupliakov et al., 1997). The first corresponds to residues 828 to 842 of dynamin. The second is a purified GST fusion protein containing the SH3 domain of amphiphysin (Grabs et al., 1997). To exclude interference by cytosolic factors, these experiments were performed in the absence of cytosol that in the in-vitro assay was not essential for the enhancement of endocytosis (compare control columns in Fig. 20A and B, lower panels). A strong inhibition of granule recapture was observed with the dynamin peptide that was almost complete at the maximal concentration (Fig. 20B, lower panel). Addition of 50 µM of the amphiphysin SH3 domain caused a similarly strong inhibition, whereas GST alone had no effect (Fig. 20B, lower panel). No significant change in the rates of exocytosis was observed in the presence of any of the peptides or of the guanine nucleotides (Fig. 20A and B upper panels) in agreement with the recent findings of Graham et al. (2002). Together, these data suggest that retrieval of secretory granules by recapture is dependent on dynamin.

5.3 Discussion

Using PC12 cells as model for a neuroendocrine cell, here it is shown that up to a third of all secretory granules undergoing stimulus-dependent exocytosis are re-captured at the site of exocytosis without undergoing full fusion. Re-capture was observed in surface-attached membrane sheets as well as in intact cells. Furthermore, re-capture is dependent on dynamin documenting that exocytosis and endocytotic re-capture follow different biochemical pathways.

The classical "kiss-and-run" model was originally developed in order to explain the fast recycling rate of synaptic vesicles and the presumed lack of correlation between exocytosis and the appearance of clathrin-coated vesicles in nerve terminals (Ceccarelli and Hurlbut, 1980, Heuser, 1989). Furthermore, neurotransmitter was suggested to be released only partially (Choi et al., 2000a) which, due to fast diffusion of small transmitter molecules, implies opening and closure of fusion pores in the sub-millisecond range. The presence of amperometric "foot"-signals suggested that exocytosis of secretory granules is preceded by the opening of a fusion pore that may remain arrested for some time before full fusion (Chow et al., 1992, Neher, 1993) and that occasionally may re-close without undergoing fusion (Bruns and Jahn, 1995). This experimental set-up does not allow for such high time resolution. However, it is possible that the secretory granules remain open for some time (second range) before re-capture for the following reasons. First, acridine orange, a low

molecular weight dye is invariably lost during exocytosis. This agrees with recent amperometric data in which no evidence for partial release of transmitter was obtained (Bruns et al., 2000). Second, labelling of secretory granules with sulforhodamine was generally quite homogeneous indicating that the open time of the granule suffices for dye equilibration. Third, at least some of the re-captured granules stayed open long enough to admit access of the protein horseradish peroxidase to the granule interior. Finally, sulforhodamine uptake was also observed in granule populations that had undergone full discharge of the slowly diffusing NPY-GFP. A wide variation in the open time is also suggested by capacitance patch clamping experiments, and more recently also by amperometry (Elhamdani et al., 2001), but, as pointed out in the introduction, the origin of the endocytosed material remains uncertain in such experiments.

Is there any exchange of membrane constituents between the granule and the plasma membrane during the time the granule stays open? Although some membrane lipids may diffuse across the neck of the granule, it is less likely that membrane proteins "mix" into the plasma membrane. Their lateral diffusion is often impeded due to oligomerization or cluster formation, and the highly curved neck of the granule may form an additional barrier. Indeed, in the chromaffin cell, granule membrane proteins were shown to remain concentrated at the site of membrane fusion after exocytosis (Patzak et al., 1984).

Several previous studies dealt with the endocytotic pathway in neuroendocrine cells including PC12 cells. In a recent study by De Wit, the

consecutive passage of endocytotic markers through organelles involved in exocytosis has been analysed by quantitative electron microscopy using bovine serum albumin with bound nanogold particles as tracer (De Wit et al., 1999). Early endocytotic structures including coated vesicles, small round vesicles, and elongated cisternae were observed. Such structures were also seen in the analysis presented here, but apparently no evidence for labelling of secretory granules was obtained by De Wit and co-workers. However, this is not surprising as uptake was performed under non-stimulating conditions. It is also possible that BSA-gold is too large to enter the granule during transient fusion, or else, that it is prevented from uptake by the flow of ongoing protein discharge which would be less of a problem for smaller molecules that diffuse much more readily. Thus, it is possible to further exclude that the HRP labelled secretory granules seen in these studies represent classical structures of the endocytotic pathway.

Interestingly, re-capture of secretory granules was postulated many years ago based on an electron microscopic analysis of organelles labelled with extracellular tracers (Sawano et al., 1986), and stimulus-dependent labelling of secretory granules has also been observed in a more recent study (Henkel et al., 2001a). However, like in the capacitance experiments it is not possible to spatially correlate exocytosis with endocytosis in such approaches.

The requirement of dynamin for granule re-capture, at least for a significant sub-population of such events, provides firm evidence that the molecular mechanisms of exocytosis and endocytosis are different. This

agrees with the concept that fusion and fission are irreversible biochemical reactions. As outlined in Fig. 21, exocytosis requires SNAREs to convert from "trans" to "cis" complexes, a reaction that is thought to drive membrane merger. SNARE assembly follows a steep energy gradient and is essentially irreversible (Fasshauer et al., 2002). Disassembly requires the efforts of the chaperone-like ATPase NSF and is presumably a relatively slow reaction (Morgan et al., 1994).

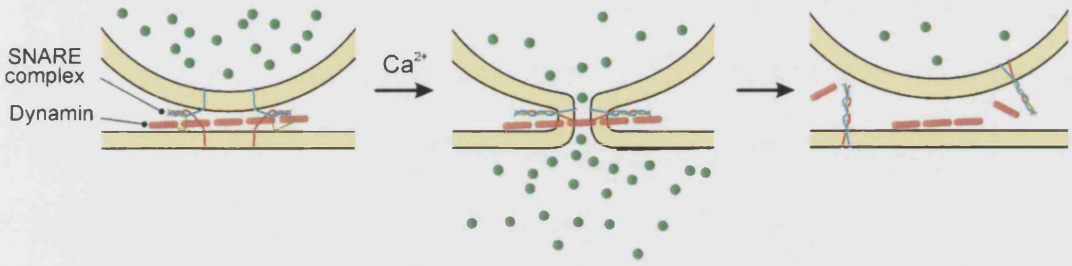

▲ ***Figure 21. Model describing the molecular steps involved in secretory granule exocytosis and re-capture***

Individual components are drawn to scale using the following dimensions: NPY-GFP, 2.4 x 4.2 nm (here represented as a sphere 3 nm in diameter), fusion pore diameter, 4 nm, dynamin ring (depicted here with five subunits), 45 nm, SNARE-complex, 12 nm, membrane thickness, 5 nm, granule diameter, 100 nm.

The data presented here suggest that dynamin assembles at the site of release before the granule fuses and is thus in place for mediating re-capture as soon as exocytosis occurs. Endocytosis thus does not require active SNAREs or disassembly of SNARE complexes. After recapture is complete dynamin probably begins to dissociate into monomers, diffusing away from the site of action (Fig. 21) (Sever et al.,

2000). Recent observations with green fluorescent-protein labelled dynamin in PC12 cells have revealed the dynamic shifting nature of dynamin localisation between the cytosol and the plasma membrane (Tsuboi et al., 2002). Dynamin is presently the best candidate for catalysing the fission reaction (Danino and Hinshaw, 2001, Marks et al., 2001), thus performing the task in endocytosis that is carried out by the SNAREs in exocytosis.

Dynamin belongs to a family of GTPases that are involved both in membrane fission and in signalling events (Danino and Hinshaw, 2001, Di Fiore and De Camilli, 2001). While dynamin is best characterised for its crucial role in the pinching off of clathrin-coated vesicles, dynamin family members are also invoked in fission events of other trafficking steps. Presently, we cannot exclude that clathrin is involved in granule re-capture. However, re-captured granules are morphologically indistinguishable from normal secretory granules (see Fig. 18) that are distinguished from clathrin-coated vesicles both by their larger size and by the presence of an electron-dense core. It remains to be established to which extent other proteins involved in endocytosis are required such as endophilin, amphiphysin (as suggested by our peptide inhibition results, see Fig. 20), intersectin, synaptojanin, or syndapin. As recently proposed by Jarousse and Kelly (2001) it is conceivable that for such "kiss-and-run" events only those proteins are needed that are required for membrane constriction and membrane fission, whereas proteins required for membrane invagination are expendable. It should be noted that it is not

possible to exclude the presence of additional pathways for membrane retrieval after transient fusion. "Kiss-and-run" events at synapses are believed to be fast (ms-range) and it is conceivable that alternative mechanisms are involved.

The fate of re-captured granules will require further investigations. Since membrane-attached granules are refractory when cells are stimulated immediately prior to membrane sheet preparation, it was not possible to determine whether re-captured granules are able to undergo a second round of exocytosis. Rather, it is probable that in intact cells they are eventually removed from the plasma membrane and enter the endocytotic pathway involving fusion with other intracellular organelles. However, it was also observed that granules labelled with fluid phase marker during a first round of exo-endocytosis regained competence for exocytosis after 30 min of recovery. The label may have reached the granules via endocytic uptake and equilibration with the Trans Golgi network. Yet, it cannot be excluded that a sub-population of re-captured granules remains stationary after re-capture and undergoes re-priming and activation, enabling them to fuse again after a refractory period. Hopefully, future experiments will resolve whether secretory granules can be re-used for several rounds of exocytosis while retaining their identity or whether they need to undergo membrane recycling and thus intermingle with the secretory pathway before being regenerated.

5.4 Possible future investigation

The fate of secretory granule membrane markers after exocytosis has been previously investigated in chromaffin cells using immuno-gold labelling to follow the distribution of these labels (see for example Paztak et al., 1984). The author proposed to address this question using the membrane sheet assay. To do this it was intended to again make use of fluorescent protein (FP) labelling to monitor secretory granule exocytosis with a lumenal content marker (npy). In addition, the c-terminal end of synaptobrevin can be FP labelled, and using a double transfection protocol it might be possible to monitor granule content and membrane marker using two channel fluorescent imaging. The fusion of FP to the c-terminus of synaptobrevin has been used to monitor rounds of exocytosis and endocytosis in cultured neurons (Sankaranarayanan & Ryan, 2000). However, this study did not follow the process at the level of single vesicles. In PC12 cells Tsuboi and co-workers used a c-terminal FP labelled synaptobrevin as a secretory granule marker together with FP labelled dynamin (Tsuboi, et al., 2002). However, they were not able to identify secretory granules specifically, as the labelled synaptobrevin could reside in the plasma membrane as clusters (Lang et al., 2001) or within compartments of the endosomal pathway (De Wit et al., 1999). In the proposed scheme, this problem would be avoided by the use of the npy-GFP used thus far. Hence, it would be possible to identify secretory granules labelled by both npy and synaptobrevin. The next step would be

to stimulate exocytosis, and observe what happens to the FP labelled synaptobrevin resident in the granule membranes. There would be several difficulties associated with this approach. For example, there would be an inherent uncertainly in identifying the dual labelled granules due to the diffraction-limited resolution of the microscope i.e. it would not be possible to say that overlapping FP signals from the two channels represent the same or two objects. However, one might partially avoid this problem by using a pH-sensitive FP for the synaptobrevin label. Thus, plasma membrane resident synaptobrevin would be visible throughout the experiment, while that confined within the acidic lumen of secretory granules would be quenched. This would become visible simultaneously with the occurrence of calcium dependent exocytosis of the granules.

A further avenue of investigation, which was initiated in research published in 2001 (Lang et al., 2001), could also be of further interest. The spatial relationship of sites of exocytosis to clusters of plasma membrane bound or membrane associated proteins (for example; syntaxin, Munc18, or complexin) may reveal something about the biochemical maturity of secretory granules or about the sites at which they are attached and fuse to the membrane. The membrane sheet assay would enable one to approach both these aspects. Labelling of proteins might be achieved through fluorescent dye coupled antibodies (as in Lang et al., 2001) or by making FP chimeras of the protein of interest and co-expression with npy-FP.

6. Methods

6.1 General Methods

6.1.1 Cell Culture

PC12 cells (clone 251; Heumann et al. 1983) were maintained in 75 cm^2 un-coated tissue culture flasks containing growth medium (DMEM with 4.5 g/l glucose, 10 % horse serum, 5 % foetal calf serum, 4 mM L-glutamine, 60 U/ml penicillin, 60 U/ml streptomycin) at 37 °C in 10 % CO_2 at 95 % relative humidity under sterile conditions. For experiments cells were split onto glass coverslips. One flask of confluent cells (2.4 x 10^5 cells/cm^2) was used. Media was decanted followed by 2 x washes with PBS (2.7 mM KCl, 1.5 mM KH_2PO_4, 137 mM NaCl, 8 mM Na_2HPO_4, pH 7.3). Cells were detached from the substrate with 3 ml trypsin/EDTA (GibcoBRL) for 1 min. Trypsin was then inhibited by the addition of 30 ml of growth media. The suspension was centrifuged at 1000 rpm for 5 min at RT. Media was decanted and the cells re-suspended give a final concentration of approximately 600,000 cells/ml. 500 µl of this suspension (3 x 10^4 cells/cm^2) were evenly plated onto each 25 mm ∅ (diameter) poly-L-lysine coated coverslip. Coverslips were prepared two hours prior to plating the cells. Coverslips were cleaned in absolute ethanol and sterilised by brief flaming. 500 µl of a 100 µg/ml poly-L-lysine (Sigma P-1399) solution was placed evenly onto each coverslip and incubated for 20 min at RT. This was followed by washing 1x with 2 ml sterile ddH_2O.

Coverslips were then air dried at RT for 2 hours. After plating, cells were allowed to settle onto the coverslips for 20 min. 2.5 ml of medium were then added. Cells were used for experiments 48 hr after plating.

6.1.2 Preparation of rat brain cytosol

Cytosol was prepared from the brains of freshly killed male Wistar rats (after Martin, 1989). The cerebellum and brain stem were first removed. Brains were placed into 1 ml ice cold isotonic buffer/brain (130 mM NaCl, 2 mM EGTA, 50 mM PIPES, pH 6.8, 0.1 mM PMSF, 1 µg/ml leupeptin, 1 µg/ml pepstatin A) and homogenised with 1 slow and 3 fast strokes of a Teflon homogeniser running at 800-1000 rpm at 4 °C. Larger debris was removed by centrifugation at 14500 x g_{av} (SS-34 rotor, Sorval) for 15 min at 4 °C. The supernatant was collected and centrifuged at 128000 x g_{av} (TLA 100.3 rotor, Beckman) for 60 min, 4 °C to remove myelin and mitochondria. The second supernatant was then dialysed (dialysis tubing 6000-8000 MW cut off) into 1 litre of ice cold KGlu buffer (120 mM potassium glutamate, 20 mM potassium acetate, 20 mM HEPES pH 7.2) for 4 hr at 4 °C. Buffer was exchanged every hour. Cytosol was then aliquoted, flash frozen in liquid N_2 and stored at -80 °C. Protein concentration was determined by Bradford assay (typically 12 mg/ml).

6.1.3 Determination of protein concentration

Cytosol was first diluted 1:100 in ddH_20. 10, 25, 50, 75, and 100 µl of this were diluted to 200 µl with ddH_2O in 1.5 ml tubes (Eppendorf) and

centrifuged at 13000 rpm for 3 min in a bench top centrifuge. Samples were transferred to new tubes and 800 µl of Bradford reagent was added followed by incubation for 5 min at room temperature. Absorbance was measured at 595 nm and the concentration determined from values for a BSA standard curve prepared in the same manner (1 to 6 µg BSA in ddH_2O).

6.1.4 Preparation of membrane sheets

For preparation of membrane sheets, cells were grown on poly-L-lysine coated coverslips as described and disrupted using a 100 ms ultrasound-pulse (Sonifier 450, Branson Ultrasonics Corp.) in K-Glu-EGTA buffer (20 mM Hepes, pH 7.2, 120 mM potassium glutamate, 20 mM potassium acetate, 10 mM EGTA, 2 mM MgATP and 0.5 mM dithiothreitol). For sonification, a tip diameter of 2.5 mm, a coverslip-to-tip clearance of 12 mm, and a duty cycle of 100 ms were used as standard with the power setting used as a variable. Each coverslip was exposed to a single cycle (100 ms ultrasound pulse). These preparations were then used as described. See also appendix for description of terms.

6.1.5 Flurometric calibration of calcium buffers

EGTA and DPTA calcium buffers were calibrated as follows using 1 µM Fura-2 or 10 µM Mag-Fura-2 (Molecular Probes Inc., Eugene, OR) ratio metric dyes respectively. A standard curve was generated using known concentrations of $CaCl_2$ in calibration buffer (10 mM Tris-HCl, pH

7.2, 0.3 mM $MgCl_2$) produced by serial dilution of a 2 M stock solution. Measurements were performed in a fluorometer (Fluoromax2, Jovinspex) with values expressed as a ratio of the emission at two differing excitation wavelengths. EGTA and DPTA calcium buffers were prepared in KGlu buffer containing 2 mM MgATP, 0.5 mM DTT. EGTA/DPTA and $CaCl_2$ were added from 25x stock solutions to give a working concentration of 10 mM chelator and the corresponding concentration of free calcium ions. Cytosol was omitted for the calibration because the resulting strong auto-fluorescence interfered with the measurements, but for experiments a final concentration 0.5 mg/ml was used.

6.2 Part I specific methods

6.2.1 Microscopy & high resolution digital Imaging

All microscopy was performed with a Zeiss Axiophot-2 microscope and 100x 1.4 NA Plan-apochromat objective. Images were acquired using Metamorph 3.5 (Universal Imaging Corp.) from a cooled slow scan CCD (charge coupled device) camera (Princeton Instruments Inc.) with 6.8 μm^2/pixel. Acridine orange fluorescence was detected using Zeiss filter set 09 (excitation filter BP 450-490, BS 510, emission filter LP 520) at 20 % lamp intensity (100 W HBO) and various combinations of neutral density filters. FM1-43 fluorescence was detected using Zeiss filter set 10 (excitation filter BP 450-490, BS 510, emission filter BP 515-565), 50 % lamp intensity and various neutral density filters.

6.2.2 Acridine orange staining

Cells were stained with acridine orange prior to sonification by pre-incubation for 5 min in medium supplemented with 10 µM acridine orange (Molecular Probes). Cells were sheared by sonification as described. The coverslip was rapidly mounted into ice cold K-Glu-EGTA buffer. Preparations were then taken directly to the microscope for imaging.

6.2.3 Phalloidin green staining of filamentous actin in fixed cells and membrane sheets

Membrane sheets were prepared as described and fixed in cytoskeleton buffer (137 mM NaCl, 5 mM KCl, 1.1 mM Na_2HPO_4, 0.4 mM KH_2PO_4, 4 mM $NaHCO_3$, 5 mM Glucose, 2 mM $MgCl_2$, 2 mM EGTA, 5 mM PIPES, pH 6.05) (Small et al., 1981) containing 4 % PFA and 320 mM sucrose for 20 min. Whole cells were washed twice with 1 ml TBS II buffer (150 mM NaCl, 20 mM Tris, pH 7.4) and fixed as described for membrane sheets. All samples were then washed 2 x with 1.5 ml TBS II followed by permeabilisation in TBS II + 0.5 % Triton X-100 with 50 mM NH_4Cl for 10 min. Samples were stained with 420 nM Oregon Green 488 Phalloidin in TBS II + 0.1 % Triton X-100 for 10 min turned over on parafilm. Finally, samples were washed 2 x 10 min in TBS II + 0.1 % Triton X-100. Membrane sheets and cells were then imaged using Zeiss filter set 10 (excitation filter BP 450-490, BS 510, emission filter BP 515-565). All images were taken on a Zeiss Axiophot 2 microscope mounted with a cooled, slow scan CCD camera (Princeton Instruments Inc.) with 6.8

μm^2/pixel using a 100x 1.4 NA objective. Identical illumination intensities were used such that a direct comparison of the amounts of actin present could be made.

6.2.4 Stimulation of membrane sheet preparations with Ca^{2+}

Membrane sheets were prepared as described above and were mounted in "priming" buffer (K-Glu buffer containing 2 mM MgATP, 0.5 mM DTT and 5 mg/ml rat brain cytosol). Photo bleaching and photo-damage to the preparation were minimised by using a lamp intensity of 20 % and various neutral density filters. Within the first 2 min of illumination, a membrane sheet (or preferentially a group of membrane sheets) with brightly fluorescent orange granules was located. This was then imaged with a single 800 ms exposure. The chamber solution was then carefully exchanged with either 500 nM free Ca^{2+} or 0 µM free Ca^{2+} solutions (K-Glu buffer containing 2 mM MgATP, 0.5 mM DTT, 0.5 mg/ml rat brain cytosol and 0.5 or 0 µM EGTA buffered free [Ca^{2+}]). The preparation was then incubated for 1 minute followed by a second imaging. This second exposure was for 3 s to counteract the effect of photo bleaching. Changes in the number of spots after buffer exchange were quantified by manually counting the spots. Finally, each preparation was stained with FM1-43 and imaged as described above.

6.2.5 Tetanus toxin light chain treatment of membrane sheets

For pre-treatment of membrane sheets with tetanus toxin, cells were sonified and incubated for 10 min at 37°C in KGlu buffer containing 1.7 µM acridine oranged and 8 µM tetanus toxin light chain (kind gift of Dr. Martin Margittai) as indicated. The coverslips were then mounted on the microscope and an area containing between 1 and 5 membrane sheets with secretory granules was imaged. The solution was exchanged by capillary action and replaced with KGlu buffer containing 2 mM MgATP, 0.5 mM DTT, 0.5 mg/ml rat brain cytosol and 0.5 or 0 µM EGTA buffered free $[Ca^{2+}]$. At the times indicated pictures of the selected area were taken. Images were high pass filtered with a spatial frequency of 1/500 nm. Changes in the number of spots after buffer exchange were quantified by manually counting the spots.

6.2.6 Video rate microscopic fluorescent dequenching assay

Membrane sheets were prepared as described. Coverslips were rapidly mounted into an open chamber and incubated in "priming" buffer (as above, but 2.5 mg/ml rat brain cytosol). Samples were illuminated with a 100 W HBO lamp set to 20 % light intensity on a Zeiss Axiovert 100 TV microscope. The intensity of incident light was further reduced with combined 3 % and 1 % neutral density filters. Fluorescence was excited and detected using Zeiss filter set 09 (excitation filter BP 450-490, BS 510, emission filter LP 520). All images were taken with a 100x 1.4 NA objective and collected with a video intensified CCD camera (V/ICCD,

Princeton Instruments Inc.) mounted on the vertical ocular port of the microscope. Camera settings: none-integration mode, CCD gain 5, intensifier setting 5.0 - 9.9, offset 0. Images were collected at a rate of 25 Hz by the frame grabber of a personal computer and stored directly onto the hard-drive. A region containing several membrane sheets with 15 or more brightly fluorescent orange granules was selected as quickly as possible and within 2 minutes of the first illumination. A 2 minute recording was started, the shutter opened and 500 nM free calcium solution (KGlu buffer containing 2 mM MgATP, 0.5 mM DTT, 0.5 mg/ml rat brain cytosol and 0.5 or 0 μM EGTA buffered free [Ca^{2+}]) added to the chamber. For control experiments the same buffer was used omitting Ca^{2+}. Sub-second exchange of the priming buffer could be observed by a rapid reduction in background fluorescence (caused by auto-fluorescence of the rat brain cytosol). At the end of the recording membrane sheets were stained with FM1-43 and single images were captured using filter set 09.

6.2.7 Reduction of video sequence file size

Raw video images were first converted into sequential tif files using a simple editing program (Media studio 2.5). Taking only every second image, such tifs were loaded as stacks of 50-100 images into Metamorph 3.5 (Universal Imaging Corp.) and colour decoded. Regions of interest were defined using the FM1-43 image and used to generate smaller stacks from the colour-decoded data sets.

6.3 Part II specific methods

6.3.1 Plasmids

The Plasmid encoding a fusion protein of human neuropeptide Y (previously used in Lang et al., 1997, but re-cloned for this study from the original Lang et al. construct) with EGFP was constructed by inserting the corresponding cDNA into the multi cloning site of the EGFP containing mammalian expression vector pEGFP-N1 (Clonetech Lab., Heidelberg, Germany). The neuropeptide Y cDNA was modified by PCR to introduce restriction sites that allowed subsequent cloning in-frame with the N-terminal end of EGFP. Both constructs were verified by restriction analysis and DNA sequencing. Plasmid DNA was isolated from overnight cultures of *E. coli* XL-1 blue bacteria (Stratagene, Heidelberg), grown from a single colony of transfected cells, using the Qiagen Maxi and Giga systems according to the manufacturer instructions. Purified plasmid was re-suspended in Tris buffer (10 mM Tris-HCl, pH 8.0, 1 mM EDTA). A small aliquot was diluted 1:50 in Tris buffer to photometrically determine yield and purity (10 mm path-length Quartz cuvette, Genequant photometer, Pharmacia Biotech). Plasmid DNA was then diluted to a final concentration of 1 µg/µl and stored as 50 µl aliquots at -20 °C.

6.3.2 Transient transfection of PC12 cells

Cells were passaged as above, but after trypsin treatment were re-suspended in cytomix buffer (van den Hoff et al., 1992; 120 mM KCl, 10

mM KH_2PO_4, 10 mM K_2HPO_4, 0.15 mM $CaCl_2$, 2 mM EGTA, 5 mM $MgCl_2$, 2 mM ATP, 5 mM Glutathione and 25 mM HEPES-KOH, pH 7.7, sterile filtered) at a density of 6 x 10^6 cells/ml. ATP and Glutathione were added to the cytomix shortly before re-suspension. 350 µl of cell suspension together with 50 µg of NPY-EGFP plasmid DNA were mixed in an electroporation cuvette (2 mm electrode gap, Biorad). An electric pulse was applied using a Biorad Genepulser II (settings: potential difference - 1.15 kV, resistance - 24 Ω, capacitance - 50 µF) and the cells allowed to stand at RT for 15 min. The contents of the cuvette were then diluted with 2.7 ml DMEM growth media. 500 µl of the resulting suspension were plated onto poly-L-lysine coated coverslips as described for un-transfected cells. Cells prepared in this manner were used for experiments 36 to 48 hrs after transfection.

6.3.3 Fluorescence microscopy

Membrane sheets were analysed using a Zeiss Axiovert 100 TV fluorescence microscope with a 100x 1.4 NA plan apochromat objective. For imaging a back-illuminated frame transfer CCD-camera (2x 512 x 512-EEV chip, 13 x 13 µm pixel size, Princeton Instruments Inc.) was used with a magnifying lens (1.6x Optovar) to avoid spatial under-sampling by the larger pixels. The focal position of the objective was controlled throughout all experiments using a low voltage piezo translator driver and a linear variable transformer displacement sensor/controller (Physik Instrumente, Waldbronn, Germany). EGFP fluorescence was detected

using Zeiss filter set 10 (excitation filter BP 450-490, BS 510, emission filter BP 515-565), whereas for acridine orange this filter was modified to Zeiss filter set 09 by exchange of the emission filter (LP 520). For Cy5 Chroma filter set HQ41008 was taken (excitation filter BP 590-650, BS 660, emission BP 662-738). TMA-DPH fluorescence was detected using Zeiss filter set 02 (excitation filter G 365, BS 395, emission LP 420). Images were analysed with Metamorph (Universal Imaging Corporation, West Chester, PA). Background correction was then performed according to the following formula: Real colocalization (a.u.) = (measured colocalization – background colocalization) /(1 – accidental colocalization/100). This algorithm takes into account that the contribution of accidental colocalization is inversely related to the real colocalization.

6.3.4 Standard *in-vitro* exocytosis – recapture assay

Membrane sheets with 15 or more brightly fluorescent granules were located within ten minutes of preparation (when otherwise indicated). Exocytosis was stimulated after ten minutes using the indicated $[Ca^{2+}]_{free}$ in KGlu buffer containing of 2 mM MgATP, 0.5 mg/ml rat brain cytosol (omitted where indicated, prepared according to Martin, 1989), 0.5 mM DTT and 5 µM sulforhodamine-101 (Molecular Probes Inc., Eugene, OR). After addition of Ca^{2+} membrane sheets were imaged every 30 s for 15 mins using a 1 second exposure. At the end of this period the preparation was washed twice for 5 min K-Glu buffer to remove excess sulforhodamine-101. Finally, membranes were visualised using TMA-DPH

(Molecular Probes Inc., Eugene, OR). 0.1 and 0.5 µM $[Ca^{2+}]_{free}$ were buffered using 10 mM EGTA, while 1.5, 10, and 50 µM $[Ca^{2+}]_{free}$ buffers used 10 mM DPTA (see above under general methods)

6.3.5 Immunostaining for dynamin

Rabbit polyclonal sera for dynamin was obtained from Synaptic Systems, Göttingen, Germany, (Cat#115002). Before immunostaining of the membrane sheets, all antibodies were diluted 100-fold into PBS (150 mM NaCl, 10 mM Na_2HPO_4, 10 mM NaH_2PO_4, pH 7.4) containing 1% (w/v) BSA, incubated for 45 min at room temperature and centrifuged for 10 min at 13000 x g_{av}. Membrane sheets were fixed for 30 min at room temperature in 4 % paraformaldehyde in PBS, quenched for 20 min in PBS containing 50 mM NH_4Cl and washed 3 times in PBS for 10 min each. They were then incubated for 15 min with the primary antibody. Subsequently, sheets were washed 3 times in HS-PBS (500 mM NaCl, 20 mM Na_2HPO_4, 20 mM NaH_2PO_4, pH 7.4) for 15 min each, followed by a 15 min incubation with the secondary antibody (Cy5-coupled goat-anti-rabbit, Dianova, Hamburg, Germany) diluted 1:100 in PBS containing 1% BSA. Before imaging, membrane sheets were washed 3 times in HS-PBS for 15 min and once for 10-40 min in PBS.

6.3.6 Expression and purification of GST fusion protein

The cDNA encoding the SH3 domain of amphiphysin (aa 545-695, Grabs et al., 1997) was cloned in frame into the pGEX-6P vector

(Amersham pharmacia) as a C-terminal fusion to glutathione-S-transferase (GST). For expression, *E.coli* BL-21 cells were grown at 37 °C to a density of A_{600} 0.8 in LB media (170 mM NaCl, 0.5 % (w/v) yeast extract, 1 % (w/v) bactotryptone) supplemented with 100 µg/ml amphicillin. Cells were then induced with 0.25 mM isopropyl-1-thio-ß-D-galactopyranoside at 20 °C for 3 hrs. Cells were harvested, re-suspended and disrupted by sonification in lysis buffer (300 mM NaCl, 50 mM Tris, pH 8.0, 1 % Triton-X-100, 5 mM EDTA, 1mM DTT, and Complete protease inhibitor cocktail (Roche, Mannheim, Germany)) and spun at 35,000 x *g*. Supernatant was incubated with 1 ml glutathione Sepharose beads (Amersham Pharmacia Biotech, Freiburg, Germany) per 15 ml lysate for 1 hr at 4 °C on a rotating bed. Beads were then washed 3 times in lysis buffer followed by 3 washes in lysis buffer without Triton-X-100 and transferred to 10 ml columns (Bio-Rad Labs., CA). GST-fusion protein was eluted in elution buffer (150 mM NaCl, 50 mM Tris, pH 8.0, 15 mM glutathione) and dialysed into KGlu buffer (as for rat brain cytosol) then further concentrated using a Centricon. Finally the sample was analysed by SDS-PAGE (purity typically > 80 %) and the protein concentration determined by Bradford assay. GST-amp-SH3 prepared in this manner was used at a final concentration of 50 µM in the standard in-vitro exocytosis – recaputure assay.

6.3.7 HRP uptake and subsequent electron microscopy of ultra-thin cryo-sections

PC12 cells were maintained as described above on 10 cm ∅ culture dishes. Before uptake cells were washed twice in pre-warmed PBS (2.7 mM KCl, 1.5 mM KH_2PO_4, 137 mM NaCl, 8 mM Na_2HPO_4, pH 7.3) followed by a 2 min stimulation in high K^+ Ringer buffer (50 mM NaCl, 80 mM KCl, 5 mM $CaCl_2$, 1 mM $MgCl_2$, 48 mM glucose, 10 mM Hepes-NaOH pH 7.4) with 1 mg/ml horse radish peroxidase (EC 1.11.1.7) at 37 °C. Cells were then washed twice with PBS. For preparation of Ultrathin cryo-sections (after Tokuyasu, 1973) PC12 cells were then immeadiately fixed with 2 % paraformaldehyde and 0.1 % glutaraldehyde in a 1:1 mixture of 0.1 M sodium phosphate (pH 7.4) and DMEM culture media for 30 min at room temperature directly on cell culture dishes. After removal of the fixation solution cells were postfixed with 4% paraformaldehyde and 0.1% glutaraldehyde in 0.1 M sodium phosphate (pH 7.4) for 2 hr on ice. Cells were then removed with a cell scraper from the dishes. After washing with phosphate buffer, cells were embedded in 10% gelatine, cooled on ice and cut into small blocks. For diamino benzidine (DAB) labelling blocks were incubated with 1 mg/ml DAB and 0.01 % H_2O_2 in TBS (20 mM Tris pH 7.4, 150 mM NaCl) for 1 hr at RT. After washing in 0.1 M sodium phosphate the blocks were infused with 2.3 M sucrose at 4°C overnight, mounted on small metal pins, frozen and stored in liquid nitrogen, until cryo-ultramicrotomy. Ultrathin cryo sections were cut at -120 °C using a diamond knife (Diatome Cryo-P, 35° knife angle) in an ultracryomicrotome

(Leica) and collected using a 1:1 mixture of 1.8% methyl-cellulose and 2.3 M sucrose and deposited on formvar and carbon coated nickel grids (Liou et al., 1996). After washing, sections were incubated with uranyl acetate/methyl-cellulose on ice and embedded in a mixture of methyl-cellulose and uranyl acetate (Tokuyasu, 1978) and examined with a Phillips CM120 electron microscope. Immunogold labeling of cyro-sections was performed as previously described (Lang et al., 2001) using a 1:40 dilution of a polyclonal anti-GFP antibody (kind gift of Dr. I. Majoul).

7. References

Albillos, A., Dernick, G., Horstmann, H., Almers, W., Alvarez de Toledo, G., Lindau, M. (1997) The exocytotic event in chromaffin cells revealed by patch amperometry. Nature *389*, 509-512

Ales, E., Tabares, L., Poyato, J.M., Valero, V., Lindau, M. and Alvarez de Toledo, G. (1999). High calcium concentrations shift the mode of exocytosis to the kiss-and-run mechanism. Nat Cell Biol *1*, 40-44

Alvarez de Toledo, G., Fernandez-Chacon, R., Fernandez, J.M. (1993) Release of secretory products during transient vesicle fusion. Nature *363*, 554-558

Angleson, J.K., Cochilla, A.J., Kilic, G., Nussinovitch, I., Betz, W.J. (1999) Regulation of dense core release from neuroendocrine cells revealed by imaging single exocytic events. Nat Neurosci *2*, 440-446

Ann, K., Kowalchyk, J.A., Loyet, K.M., Martin, T.F.J. (1997) Novel Ca^{2+}-binding protein (CAPS) related to UNC-31 required for Ca^{2+}-activated exocytosis. J Biol Chem *272*, 19637-19640

Artalejo, C.R., Lemmon, M.A., Schlessinger, J., Palfrey, H.C. (1997) Specific role for the PH domain of dynamin-1 in the regulation of rapid endocytosis in adrenal chromaffin cells. EMBO J *16*, 1565-1574

Artalejo, C.R., Henley, J.R., McNiven, M.A., Palfrey, H.C. (1995) Rapid endocytosis coupled to exocytosis in adrenal chromaffin cells involves Ca2+, GTP, and dynamin but not clathrin. Proc Natl Acad Sci U S A *92*, 8328-8332

Avery, J., Ellis, D.J., Lang, T., Holroyd, P., Riedel, D., Henderson, R.M., Edwardson, J.M., Jahn, R. (2000) A cell-free system for regulated exocytosis in PC12 cells. J Cell Biol *148*, 317-324

Avery, J., Jahn, R., Edwardson, J.M. (1999) Reconstitution of regulated exocytosis in cell-free systems: a critical appraisal. Annu Rev Physiol *61*, 777-807

Balch, W.E., Dunphy, W.G., Braell, W.A., and Rothman, J.E. (1984) Reconstitution of the transport of protein between successive compartments of the Golgi measured by the coupled incorporation of N-acetylglucosamine. Cell *39*, 405-416

Baker, P.F. and Whitaker, M.J. (1978) Influence of ATP and calcium on the cortical reaction in sea urchin eggs. Nature *276*, 513-515

Barg, S., Olofsson, C.S., Schriever-Abeln, J., Wendt, A., Gebre-Medhin, S., Renstrom, E., Rorsman, P. (2002) Delay between fusion pore opening and peptide release from large dense-core vesicles in neuroendocrine cells. Neuron *33*, 287-299

Betz, A., Thakur, P., Junge, H.J., Ashery, U., Rhee, J.S., Scheuss, V., Rosenmund, C., Rettig, J., Brose, N. (2001) Functional interaction of the active zone proteins Munc13-1 and RIM1 in synaptic vesicle priming. Neuron *30*, 183-196

Block, M.R., Glick, B.S., Wilcox, C.A., Wieland, F.T., and Rothman, J.E. (1988) Purification of an N-ethylmaleimide- sensitive protein catalyzing vesicular transport. Proc Natl Acad Sci USA *85*, 7852-7856

Brodin, L., Low, P., Shupliakov, O. (2000) Sequential steps in clathrin-mediated synaptic vesicle endocytosis. Curr Opin Neurobiol *10*, 312-320

Brose, N., Petrenko, A.G., Südhof, T.C. and Jahn, R. (1992) Synaptotagmin: a calcium sensor on the synaptic vesicle surface. Science *256*, 1021-1025

Brose, N., Rosenmund, C., Rettig, J. (2000) Regulation of transmitter release by Unc-13 and its homologues. Curr Opin Neurobiol *10*, 303-311

Bruns, D. and Jahn, R. (1995) Real-time measurement of transmitter release from single synaptic vesicles. Nature *377*, 62-65

Bruns, D., Riedel, D., Klingauf, J., Jahn, R. (2000) Quantal release of serotonin. Neuron *28,* 205-220

Bruns, D. and Jahn, R. (2002) Molecular determinants of exocytosis. Pflugers Arch *443*, 333-338

Burgess, T.L. and Kelly, R.B. (1987) Constitutive and regulated secretion of Proteins. Annu Rev Cell Biol *3*, 243-293

Carr, J.F. and Hinshaw, J.E. (1997) Dynamin assembles into spirals under physiological salt conditions upon the addition of GDP gamma phosphate analogues. J Biol Chem *272*, 28030-28035

Ceccarelli, B. and Hurlbut, W.P. (1980) Vesicle hypothesis of the release of quanta of acetylcholine. Physiol Rev *60*, 396-441

Chamberlain L.H., Burgoyne R.D., Gould G.W. (2001) SNARE proteins are highly enriched in lipid rafts in PC12 cells: implications for the spatial control of exocytosis. Proc Natl Acad Sci U S A *98,* 5619-5624

Chapman, E.R., Hanson, P.I., An, S., and Jahn, R. (1995) Ca^{2+} regulates the interaction between synaptotagmin and syntaxin 1. J Biol Chem *270*, 23667-23671

Cheek, T.R. and Burgoyne, R.D. (1986) Nicotine-evoked disassembly of cortical actin filaments in adrenal chromaffin cells. FEBS letters *207*, 110-114

Chen, Y.A. and Scheller, R.H. (2001) SNARE-mediated membrane fusion. Nat Rev Mol Cell Biol *2*, 98-106

Chen, Y.A., Scales, S.J., Scheller, R.H. (2001) Sequential SNARE assembly underlies priming and triggering of exocytosis. Neuron *30*, 161-170

Choi, S., Klingauf, J. and Tsien, R.W. (2000a) Postfusional regulation of cleft glutamate concentration during LTP at silent synapses. Nat Neurosci *3*, 330-336

Choi, S., Harata, N., Pyle, J., Tsien, R.W. (2000b) Monitoring exocytosis by quenching of green fluorescent protein fluorescence in the lumen of synaptic vesicles. Soc Neurosci Abstracts Vol *26*, 34.6

Chow, R.H., von Ruden, L., Neher, E. (1992) Delay in vesicle fusion revealed by electrochemical monitoring of single secretory events in adrenal chromaffin cells. Nature *356*, 60-63

Crabb, J.H. and Jackson, R.C. (1985) In vitro reconstitution of exocytosis from plasma membrane and isolated secretory vesicles. J Cell Biol *101*, 2263-2273

Cremona, O. and De Camilli, P. (2001) Phosphoinositides in membrane traffic at the synapse. J Cell Sci *114*, 1041-1052

Cremona, O., Di Paolo, G., Wenk, M.R., Luthi, A., Kim, W.T., Takei, K., Daniell, L., Nemoto, Y., Shears, S.B., Flavell, R.A., McCormick, D.A., De Camilli, P. (1999) Essential role of phosphoinositide metabolism in synaptic vesicle recycling. Cell *99*, 179-188

Danino, D. and Hinshaw, J.E. (2001) Dynamin family of mechanoenzymes. Curr Opin Cell Biol *13*, 454-460

David, C., McPherson, P.S., Mundigl, O., De Camilli, P. (1996) A role of amphiphysin in synaptic vesicle endocytosis suggested by its binding to dynamin in nerve terminals. Proc Natl Acad Sci U S A *93*, 331-335

Davis, A.F., Bai, J., Fasshauser, D., Wolowick, M.J., Lewis, J.L. and Chapman, E.R. (1999) Kinetics of synaptotagmin responses to Ca^{2+} and assembly with the core SNARE complex onto membranes. Neuron *24*, 363-376

De Wit, H., Lichtenstein, Y., Geuze, H.J., Kelly, R.B., van der Sluijs, P. and Klumperman, J. (1999) Synaptic vesicles form by budding from tubular extensions of sorting endosomes in PC12 cells. Mol Biol Cell *10*, 4163-4176

Del Castillo, J., and Katz, B. (1954) Quantal components of the end plate potential. J Physiol *124*, 560-573

Di Fiore, P.P. and De Camilli, P. (2001) Endocytosis and signalling: an inseparable partnership. Cell *106*, 1-4

Elhamdani, A., Palfrey, H.C., Artalejo, C.R. (2001) Quantal size is dependent on stimulation frequency and calcium entry in calf chromaffin cells. Neuron *31*, 819-830

Fasshauer, D. Otto, H., Eliason, W.K., Jahn, R., and Brünger, A.T. (1997b) Structural changes are associated with soluble N-ethylmalemide-sensitive fusion protein attachment protein receptor complex formation. J Biol Chem *272*, 28036-28041

Fasshauer, D., Antonin, W., Subramaniam, V., Jahn, R. (2002) SNARE assembly and disassembly exhibit a pronounced hysteresis. Nat Struct Biol 9, 144-151

Ferro-Novick, S. and Jahn, R. (1994) Vesicle fusion from yeast to man. Nature *370*, 191-193

Fesce, R. and Meldolesi, J. (1999) Peeping at the vesicle kiss. Nature Cell Biol *1*, E3-E4

Fiebig, K.M., Rice L.M., Pollock, E., Brunger, A.T. (1999) Folding intermediates of SNARE complex assembly. Nat Struct Biol *6*, 117–123

Ford, M.G., Pearse, B.M., Higgins, M.K., Vallis, Y., Owen, D.J., Gibson, A., Hopkins, C.R., Evans, P.R., McMahon, H.T. (2001) Simultaneous binding of PtdIns(4,5)P2 and clathrin by AP180 in the nucleation of clathrin lattices on membranes. Science *291*, 1051-1055

Gad, H., Ringstad, N., Löw, P., Kjaerulff, O., Gustafsson, J., Wenk, M., Di Paolo, G., Nemoto, Y., Crum, J., Ellisman, M.H., De Camilli, P., Shupliakov, O., and Brodin, L. (2000) Fission and uncoating of synaptic clathrin-coated vesicles are perturbed by disruption of interactions with the SH3 domain of endophilin. Neuron *27*, 301-12

Gepppert, M. and Südhof, T.C. (1998) Rab3 and synaptotagmin: the yin and yang of synaptic membrane fusion. Ann Rev Neurosci *21*, 75-95

Glick, B.S., and Rothman, J.E. (1987) Possible role for fatty acyl-coenzyme A in intracellular protein transport. Nature *326*, 309-312

Gonzalez-Gaitan, M. and Jackle, H. (1997) Role of Drosophila alpha-adaptin in presynaptic vesicle recycling. Cell *88*, 767-776

Grabs, D., Slepnev, V.I., Songyang, Z., David, C., Lynch, M., Cantley, L.C., De Camilli, P. (1997) The SH3 domain of amphiphysin binds the proline-rich domain of dynamin at a single site that defines a new SH3 binding consensus sequence. J Biol Chem *272*, 13419-13425

Graham, M.E., O'Callaghan, D.W., McMahon, H.T., Burgoyne, R.D. (2002) Dynamin-dependent and dynamin-independent processes contribute to the regulation of single vesicle release kinetics and quantal size. Proc Natl Acad Sci U S A *99*, 7124-7129

Harlow, M.L., Ress, D., Stoschek, A., Marshall, R.M., McMahan, U.J. (2001) The architecture of active zone material at the frog's neuromuscular junction. Nature *409*, 479-484

Hata, Y., Slaughter, C.A., Südhof, T.C. (1993) Synaptic vesicle fusion complex contains unc-18 homologue bound to syntaxin. Nature *366*, 347-351

Hay, J.C. and Martin, T.F. (1993) Phosphatidylinositol transfer protein required for ATP-dependent priming of Ca^{2+}-activated secretion. Nature *366*, 572-575

Henkel, A.W., Horstmann, H., Henkel, M.K. (2001a) Direct observation of membrane retrieval in chromaffin cells by capacitance measurements. FEBS Lett *505*, 414-418

Henkel, A.W., Kang, G., Kornhuber, J. (2001b) A common molecular machinery for exocytosis and the "kiss-and-run" mechanism in chromaffin cells is controlled by phosphorylation. J Cell Sci *114*, 4613-4620

Heumann, R., Kachel, V., Thoenen, H. (1983) Relationship between NGF-mediated volume increase and "priming effect" in fast and slow reacting clones of PC12 pheochromocytoma cells. Role of cAMP. Exp Cell Res *145*, 179-190

Heuser, J.E. (2000) Production of cell cortices for light and electron microscopy. Traffic *1*, 545-552

Heuser, J.E. (1989) The role of coated vesicles in recycling of synaptic vesicle membrane. Cell Biol Int Rep *13*, 1063-1076

Heuser, J.E., and Reese, T.S. (1973) Evidence for recycling of synaptic vesicle membrane during transmitter release at the frog neuromuscular junction. J Cell Biol *57*, 315-344

Hille, B., Billiard, J., Babcock, D.F., Nguyen, T., and Koh, D.S. (1999) Stimulation of exocytosis without a calcium signal. J Physiol *250*, 23-31

Hinshaw, J.E. and Schmid, S.L. (1995) Dynamin self assembles into rings suggesting a mechanism for coated vesicle budding. Nature *374*, 190-192

Hinshaw, J.E. (2000) Dynamin and its role in membrane fission. Annu Rev Cell Dev Biol *16*, 483-519

Holroyd, P., Lang, T., Wenzel, D., De Camilli, P., and Jahn, R. (2002) Imaging direct, dynamin-dependent re-capture of fusing secretory granules on plasma membrane lawns from PC12 cells. Proc Natl Acad Sci USA *99*, 16806-16811

Hua, S.Y., and Charlton, M.P. (1999) Activity dependent changes in partial VAMP complexes during neurotransmitter release. Nat Neurosci *2*, 1078-83

Jahn, R., and Südhof, T.C. (1999) Membrane fusion and exocytosis. Annu Rev Biochem *68*, 863-911

Jahn, R. and Niemann, H. (1994) Molecular mechanisms of clostridial neurotoxins. Ann NY Acad Sci *733*, 245-255

Jarousse, N., and Kelly, R.B. (2001) Endocytotic mechanisms in synapses. Curr Opin Cell Biol *13*, 461-469

Johns, L.M., Levitan, E.S., Sheldon, E.A., Holz, R.W., Axelrod, D. (2001) Restriction of secretory granule motion near the plasma membrane of chromaffin cells. J Cell Biol 153, 177-190

Kim, T., Tao-Cheng, J., Eiden, L.E., and Peng Loh, Y. (2001) Chromogranin A, an "on/off" switch controlling dense core secretory granule biogenesis. Cell *106*, 499-509

Kirchhausen, T. (2000) Three ways to make a vesicle. Nat Rev Mol Cell Biol *2*, 216

Kleinchin, V.A., Kowalchyk, J.A., Martin, T.F. (1998) Large dense-core vesicle exocytosis in PC12 cells. Methods *16*, 204-208

Klingauf, J., Kavalali, E.T., Tsien, R.W. (1998) Kinetics and regulation of fast endocytosis at hippocampal synapses. Nature *394*, 581-585

Koenig, J.H., Saito, K., Ikeda, K. (1983) Reversible control of synaptic transmission in a single gene mutant of Drosophila melanogaster. J Cell Biol *96*, 1517-1522

Kosaka, T., and Ikeda, K. (1983) Possible temperature-dependent blockage of synaptic vesicle recycling induced by a single gene mutation in Drosophila. J Neurobiol *14*, 207-225

Lang, T., Bruns, D., Wenzel, D., Riedel, D., Holroyd, P., Thiele, C., Jahn, R. (2001) SNAREs are concentrated in cholesterol-dependent clusters that define docking and fusion sites for exocytosis. EMBO J *20*, 2202-2213

Lang, T., Wacker, I., Wunderlich, I., Rohrbach, A., Giese, G., Soldati, T., Almers, W. (2000) Role of actin cortex in the subplasmalemmal transport of secretory granules in PC-12 cells. Biophys J *78*, 2863-2877

Lang, T., Wacker, I., Steyer, J., Kaether, C., Wunderlich, I., Soldati, T., Gerdes, H.H., Almers, W. (1997) Ca2+-triggered peptide secretion in single cells imaged with green fluorescent protein and evanescent-wave microscopy. Neuron *18*, 857-863

Lindau, M., and Almers, W. (1995) Structure and function of fusion pores in exocytosis and ectoplasmic membrane fusion. Curr Opin Cell Biol *7*, 509-517

Linial, P., and Parnas, D. (1996) Deciphering neuronal secretion: tools of the trade. Biochem Biophys Acta *1286*, 117-152

Liou, W., Geuze, H.J., Slot, J.W. (1996) Improving structural integrity of cyrosections for immunogold labeling. Histochem Cell Biol *106*, 41-48

Maclean, C.M., and Edwardson, J.M. (1992) Fusion between rat pancreatic zymogen granules and pancreatic plasma membranes. Modulation by a GTP binding protein. Biochem J *286*, 747-753

Margittai, M., Fasshauer, D., Pabst, S., Jahn, R., Langen, R. (2001) Homo- and heterooligomeric SNARE complexes studied by site-directed spin labelling. J Biol Chem *276*, 13169–13177

Marks, B., Stowell, M.H., Vallis, Y., Mills, I.G., Gibson, A., Hopkins, C.R., McMahon, H.T. (2001) GTPase activity of dynamin and resulting conformation change are essential for endocytosis. Nature *410*, 231-235

Martin, T.F. (2002) Prime movers of synaptic vesicle exocytosis. Neuron *34*, 9-12

Martin, T.F. (1997) Stages of regulated exocytosis. Trends Cell Biol *7*, 271-276

Martin, T.F., and Kowalchyk, J.A. (1997) Docked secretory vesicles undergo Ca2+ activated exocytosis in a cell free system. J Biol Chem *272*, 14447-14453

Martin, T.F. (1989) Cell cracking: permeabilizing cells to macromolecular probes. Methods Enzymol *168*, 225-233

Maruyama, I. N., and Brenner, S. (1991) A phorbol ester/diacylglycerol-binding protein encoded by the unc-13 gene of Caenorhabditis elegans. Proc Natl Acad Sci U S A *88*, 5729-5733

McMahon, H.T., Wigge, P., Smith, C. (1997) Clathrin interacts specifically with amphiphysin and is displaced by dynamin. FEBS Lett *413*, 319-322

McPherson, P.S., Garcia, E.P., Slepnev, V.I., David, C., Zhang, X., Grabs, D., Sossin, W.S., Bauerfeind, R., Nemoto, Y., De Camilli, P. (1996) A presynaptic inositol-5.phosphatase. Nature *379*, 353-357

Mennerick, S., and Mathews, G. (1996) Ultrafast exocytosis elicited by calcium current in synaptic terminals of retinal bipolar neurones. Neuron *17*, 1241-1249

Montecucco, C., and Schiavo, G. (1994) Mechanism of action of tetanous and botulinum neurotoxins. Mol Microbiol *13*, 1-8

Morgan, A., Dimaline, R., Burgoyne, R.D. (1994) The ATPase activity of N-ethylmaleimide-sensitive fusion protein (NSF) is regulated by soluble NSF attachment proteins. J Biol Chem *269*, 29347-29350

Murthy, V.N., and Stevens, C.F. (1998) Synaptic vesicles retain their identity through the endocytic cycle. Nature *392*, 497-501

Neher, E. (1998) Vesicle pools and calcium microdomains: new tools for understanding their roles in neurotranmitter release. Neuron *20*, 389-399

Neher E. (1993) Secretion without full fusion. Nature *363*, 497-498

Neher, E., and Zucker, R.S. (1993) Multiple calcium-dependent processes related to secretion in bovine chromaffin cells. Neuron *10*, 21-30

Newmyer, S.L., and Schmid, S.L. (2001) Dominant-interfering Hsc70 mutants disrupt stages of the clathrin-coated vesicle cycle in vivo. J Cell Biol *152*, 607-620

Nickel, W., Weber, T., McNew, J.A., Parlati, F., Sollner, T.H., and Rothman, J.E. (1999) Content mixing and membrane integrity during membrane fusion driven by pairing of isolated v-SNAREs and t-SNAREs. Proc Natl Acad Sci USA *96*, 12571-12576

Palmgren, M.G. (1991) Acridine orange as a probe for measuring pH gradients across membranes: mechanism and limitation. Anal Biochem *192*, 316-321

Parsons, T.D., Coorssen, J.R., Horstmann, H., Almers, W. (1995) Docked granules, the exocytic burst, and the need for ATP hydrolysis in endocrine cells. Neuron *15*, 1085-1096

Patterson, G.H., Knobel, S.M., Sharif, W.D., Kain, S.R., Piston, D.W. (1997) Use of the green fluorescent protein and its mutants in quantitative fluorescence microscopy. Biophys J *73*, 2782-2790

Patzak, A., Bock, G., Fischer-Colbrie, R., Schauenstein, K., Schmidt, W., Lingg, G., Winkler, H. (1984) Exocytotic exposure and retrieval of membrane antigens of chromaffin granules: quantitative evaluation of immunofluorescence on the surface of chromaffin cells. J Cell Biol *98*, 1817-1824

Perin, M.S., Freid, V.A., Mignery, Jahn, R., and Südhof, T.C. (1990) Phospholipid binding by a synaptic vesicle protein homologous to the regulatory region of protein kinase C. Nature *345*, 260-263

Perin, M.S., Johnston, P.A., Ozcelik, T., Jahn, R., Francke, U., and Südhof, T.C. (1991) Structural and functional conservation of synaptotagmin (p65) in Drosophila and humans. J Biol Chem *266*, 615-622

Peters, C., Bayer, M.J., Buhler, S., Andersen, J.S., Mann, M., Mayer, A. (2001) Trans-complex formation by proteolipid channels in the terminal phase of membrane fusion. Nature *409*, 581-588

Phillips, G.R., Huang, J.K., Wang, Y., Tanaka, H., Shapiro, L., Zhang, W., Shan W.S., Arndt, K., Frank, M., Gordon, R.E., Gawinowicz, M.A., Zhao, Y. Colman, D.R. (2001) The presynaptic particle web: ultra-structure, composition, dissolution, and reconstitution. Neuron *32*, 63-77

Plattner, H., Artelejo, A.R., Neher, E. (1997) Ultrastructural organization of bovine chromaffin cell cortex-analysis by cryofixation and morphometry of aspects pertinent to exocytosis. J Cell Biol *139*, 1709-1717

Rettig. J., Heinemann, C., Ashery, U., Sheng, Z.H., Yokoyama, C.T., Catterall, W.A., Neher, E. (1997) Alteration of Ca2+ dependence of neurotransmitter release by disruption of Ca2+ channel/syntaxin interaction. J Neurosci *17*, 6647-6656

Rhee, J.S., Betz, A., Pyott, S., Reim, K., Varoqueaux, F., Augustin, I., Hesse, D., Sudhof, T.C., Takahashi, M., Rosenmund, C., Brose, N. (2002) Beta phorbol ester- and diacylglycerol-induced augmentation of transmitter release is mediated by Munc13s and not by PKCs. Cell *108*, 121-133

Richmond, J.E., Weimer, R.M., and Jorgensen, E.M. (2001) An open form of syntaxin bypasses the requirement for UNC-13 in vesicle priming. Nature *412*, 338-341

Ringstad, N., Gad, H., Low, P., Di Paolo, G., Brodin, L., Shupliakov, O., De Camilli, P. (1999) Endophilin/SH3p4 is required for the transition from early to late stages in clathrin-mediated synaptic vesicle endocytosis. Neuron *24*, 143-154

Roos, J. and Kelly, R.B. (1999) The endocytic machinery in nerve terminals surrounds sites of exocytosis. Curr Biol *9*, 1411-1414

Rossi, G., Salminen, A., Rice, L.M., Brünger, A.T. and Brennwald, P. (1997) Analysis of a yeast SNARE complex reveals remarkable similarity to the neuronal SNARE complex and a novel function for the C-terminus of the SNAP-25 homolog, Sec9. J Biol Chem *272*, 16610-16617

Sankaranarayanan, S., Ryan, T.A. (2000) Real time measurements of vesicle-SNARE recycling in synapses of the central nervous system. Nat Cell Biol *2*, 197-204

Sawano, F., Ravazzola, M., Amherdt, M., Perrelet, A., Orci, L. (1986) Horseradish peroxidase uptake and crinophagy in insulin-secreting cells. Exp Cell Res *164*, 174-182

Scales, S.J., Chen, Y.A., Yoo, B.Y., Patel, S.M., Doung, Y.C., Scheller, R.H. (2000) SNAREs contribute to the specificity of membrane fusion. Neuron *26*, 457–464

Schiavo, G., Stenbeck, G., Rothman, J.E., and Söllner, T.H. (1997) Binding of the synaptic vesicle v-SNARE, synaptotagmin, to the plasma membrane t-SNARE, SNAP-25, can explain docked vesicles at neurotoxin-treated synapses. Proc Natl Acad Sci USA *94*, 997-1001

Schiavo, G., Matteoli, M. and Montecucco, C. (2000) Neurotoxins affecting neuroexocytosis. Physiol Rev *80*, 717-766

Schmidt, A., Wolde, M., Thiele, C., Fest, W., Kratzin, H., Podtelejnikov, A.V., Witke, W., Huttner, W.B., Soling, H.D. (1999) Endophilin I mediates synaptic vesicle formation by transfer of arachidonate to lysophosphatidic acid. Nature *401*, 133-141

Sever, S., Muhlberg, A.B., Schmid, S.L. (1999) Impairment of dynamins GAP domain stimulates receptor mediated endocytosis. Nature *398*, 481-486

Sever, S., Damke, H., Schmid, S.L. (2000) Garrotes, springs, ratchets, and whips: putting dynamin models to the test. Traffic *1*, 385-392

Shupliakov, O., Low, P., Grabs, D., Gad, H., Chen, H., David, C., Takei, K., De Camilli, P., Brodin, L. (1997) Synaptic vesicle endocytosis impaired by disruption of dynamin-SH3 domain interactions. Science *276*, 259-263

Slepnev, V.I., Ochoa, G.C., Butler, M.H., Grabs, D., De Camilli, P. (1998) Role of phosphorylation in regulation of the assembly of endocytic coat complexes. Science *281*, 821-824

Slepnev, V.I., Ochoa, G.C., Butler, M.H., De Camilli, P. (2000) Tandem arrangement of the clathrin and AP-2 binding domains in amphiphysin 1 and disruption of clathrin coat function by amphiphysin fragments comprising these sites. J Biol Chem *275*, 17583-17589

Slepnev, V.I., and De Camilli, P. (2000) Accessory factors in clathrin dependent synaptic vesicle endocytosis. Nat Rev Neurosci *1*, 161-172

Small, J.V. (1981) Organisation of actin in the leading edge of cultured cells: influence of osmium tetroxide and dehydration on the ultra-structure of actin meshworks. J Cell Biology *91*, 695-705

Smith, C., and Neher, E. (1997) Multiple forms of endocytosis in bovine adrenal chromaffin cells. J Cell Biol *139*, 885-894

Sontag, J.M., Aunis, D., Bader, M.F. (1986) Peripheral actin filaments control calcium-mediated catecholamine release from streptolysin-O-permeabilized chromaffin cells. Eur J Cell Biol *46*, 316-326

Söllner, T., Whiteheart, S.W., Brunner, M., Erdjument-Bromage, H., Geromanos, S., Tempst, P., and Rothman, J.E. (1993a) SNAP receptors implicated in vesicle targeting and fusion. Nature *362*, 318-324

Söllner, T., Bennett, M.K., Whiteheart, S.W., Scheller, R.H., and Rothman, J.E. (1993b) A protein assembly-disassembly pathway *in vitro* that may correspond to sequential steps of synaptic vesicle docking, activation, and fusion. Cell *75*, 409-418

Steyer, J.A., and Almers, W. (1999) Tracking single secretory granules in live chromaffin cells by Evanescent-field fluorescence microscopy. Biophys J *76*, 2262-2271

Steyer, J.A., Horstmann, H., Almers, W. (1997) Transport, docking and exocytosis of single secretory granules in live chromaffin cells. Nature *388*, 474-478

Stowell, M.H., Marks, B., Wigge, P., McMahon, H.T. (1999) Nucleotide-dependent conformational changes in dynamin: evidence for a mechanochemical molecular spring. Nat Cell Biol *1*, E8-9

Sutton, B., Fasshauer, D., Jahn, R., Brunger, A.T. (1998) Crystal structure of a SNARE complex involved in synaptic exocytosis at 2.4 A resolution. Nature *395*, 347-353

Sweitzer, S.M., and Hinshaw, J.E. (1998) Dynamin undergoes a GTP-dependent conformation change causing vesiculation. Cell *93*, 1021-1029

Takei, K., McPherson, P.S., Schmid, S.L., De Camilli, P. (1995) Tubular membrane invaginations coated by dynamin rings are induced by GTP-gamma S in nerve terminals. Nature *374*, 186-190

Takei, K., Slepnev, V.I., Haucke, V., De Camilli, P. (1999) Functional partnership between amphiphysin and dynamin in clathrin-mediated endocytosis. Nat Cell Biol *1*, 33-39

Taraska, J.W., Perrais, D., Ohara-Imaizumi, M., Nagamtsu, S., Almers, W. (2003) Secretory granules are recaptured largely intact after stimulated exocytosis in cultured endocrine cells. Proc Natl Acad Sci U S A *100*, 2070-2075

Thiele, C., Hannah, M.J., Fahrenholz, F., Huttner, W.B. (2001) Cholesterol binds to synaptophysin and is required for biogenesis of synapic vesicles. Nat Cell Biol *2*, 42-49

Tokuyasu, K.T. (1978) A study of positive staining of ultrathin frozen sections. J Ultrastruct Res *63*, 287-307

Tokuyasu, K.T. (1973) A technique for ultracryotomy of cell suspensions and tissues. J Cell Biol *57*, 551-565

Toomre, D., Steyer, J.A., Keller, P., Almers, W., Simons, K. (2000) Fusion of constitutive membrane traffic with the cell surface observed by evanescent wave microscopy. J Cell Biol *149*, 33-40

Tooze S.A., Martens G.J., Huttner W.B. (2001) Secretory granule biogenesis: rafting to the SNARE. Trends Cell Biol *11*, 116-122

Tooze, S.A., Flatmark, T., Tooze, J., Huttner, W.B. (1991) Characterization of the immature secretory granule, an intermediate in granule biogenesis. J Cell Biol *115*, 1491-1503

Tsuboi, T., Terakawa, S., Scalettar, B.A., Fantus, C., Roder, J., Jeromin, A. (2002) Sweeping model of dynamin activity: Visualisation of coupling between exocytosis and endocytosis under an evanescent wave microscope with green fluorescent proteins. J Biol Chem *277*, 15957-15961

Tsuboi, T., Zhoa, C., Terakawa, S., Rutter, G.A. (2000) Simultaneous evanescent wave imaging of insulin vesicle membrane and cargo during a single exocytotic event. Curr Biol *10*, 1307-1310

Turner K.M., Burgoyne, R.D., Morgan, A. (1999) Protein phosphorylation and the regulation of synaptic membrane traffic. Trends Neurosci *22*, 459-464

Ungermann, C., Wickner, W., Xu, Z. (1999) Vacuole acidification is required for trans-SNARE pairing, LMA1 release, and homotypic fusion. Proc Natl Acad Sci USA *96*, 11194-11199

Vacquier, V. (1975) The isolation of intact cortical granules from sea urchin eggs: calcuim ions trigger granule discharge. Dev Biol *43*, 62-74

Van den Hoff, M.J., Moorman, A.F., Lamers, W.H. (1992) Electroporation in "intracellular" buffer increases cell survival. Nucleic Acids Res *20*, 2902

Verstreken, P., Kjaerulff, O., Lloyd, T.E., Atkinson, R., Zhou, Y., Meinertzhagen, I.A., Bellen, H.J. (2002) Endophilin mutations block clathrin-mediated endocytosis but not neurotransmitter release. Cell *109*, 101-112

Vitale, M.L., Rodriguez Del Castillo, A., Tchakarov, L., Trifaro, J.M. (1991) Cortical filamentous actin disassembly and scinderin redistribution during chromaffin cell stimulation precede exocytosis, a phenomenon not exhibited by gelsolin. J Cell Biol *113*, 1057-1067

Voets, T., Neher, E., Moser, T. (1999) Mechanisms underlying phasic and sustained secretion in chromaffin cells from mouse adrenal slices. Neuron *23*, 607-615

Wakeham, D.E., Ybe, J.A., Brodsky, F.M., Hwang, P.K. (2000) Molecular structures of proteins involved in vesicle fusion. Traffic *1*, 474-479

Wang, L., Seeley, E.S., Wickner, W., Merz, A.J. (2002) Vacuole fusion at a ring of vertex docking sites leaves membrane fragments within the organelle. Cell *108*, 357-369

Wang, L.H., Südhof, T.C., Anderson, R.G. (1995) The appendage domain of alpha-adaptin is a high affinity binding site for dynamin. J Biol Chem *270*, 10079-10083

Warnock, D.E., and Schimid, S.L. (1996) Dynamin GTPase, a force generating molecular switch. Bioassays *18*, 885-893

Waters, M.G. and Hughson, F.M. (2000) Membrane tethering and fusion in the secretory and endocytic pathways. Traffic *1*, 588-597

Weber, T., Zemelman, B.V., McNew, J.A., Westermann, B., Gmachl, M., Parlati, F., Sollner, T.H., Rothman, J.E. (1998) SNAREpins: minimal machinery for membrane fusion. Cell *92*, 759–772

Whiteheart, S.W, Griff, I.C., Brunner, M., Clary, D.O., Mayer, T., Buhrow, S.A., and Rothman, J.E. (1993) Nature *362*, 353-355

Williams, R., and Webb, W.W. (2000) Single granule pH cycling in antigen-induced mast cell secretion. J Cell Sci *113*, 3839-3850

Xu, T., Rammner, B., Margittai, M., Artalejo, A.R., Neher, E., Jahn, R. (1999) Inhibition of SNARE complex assembly differentially affects kinetic components of exocytosis. Cell *99*, 713–722

Yang, B., Steegmaier, M., Gonzalez, L.C., Scheller, R.H. (2000) nSec1 binds a closed conformation of syntaxin1A. J Cell Biol *148*, 247-252

Zhang, J.Z., Davletov, B.A., Sudhof, T.C., Anderson, R.G. (1994) Synaptotagmin I is a high affinity receptor for clathrin AP-2: implications for membrane recycling. Cell *78*, 751-60

8. Appendix

Sonification apparatus: Diagram and explanation of terms

Ultrasound generator: Model 450 sonifier, Branson Ultrasonics Corp.

Duty cycle: defines the duration of ultrasound emission

Power level: the amplitude or peak to peak motion of the ultrasonic vibrations

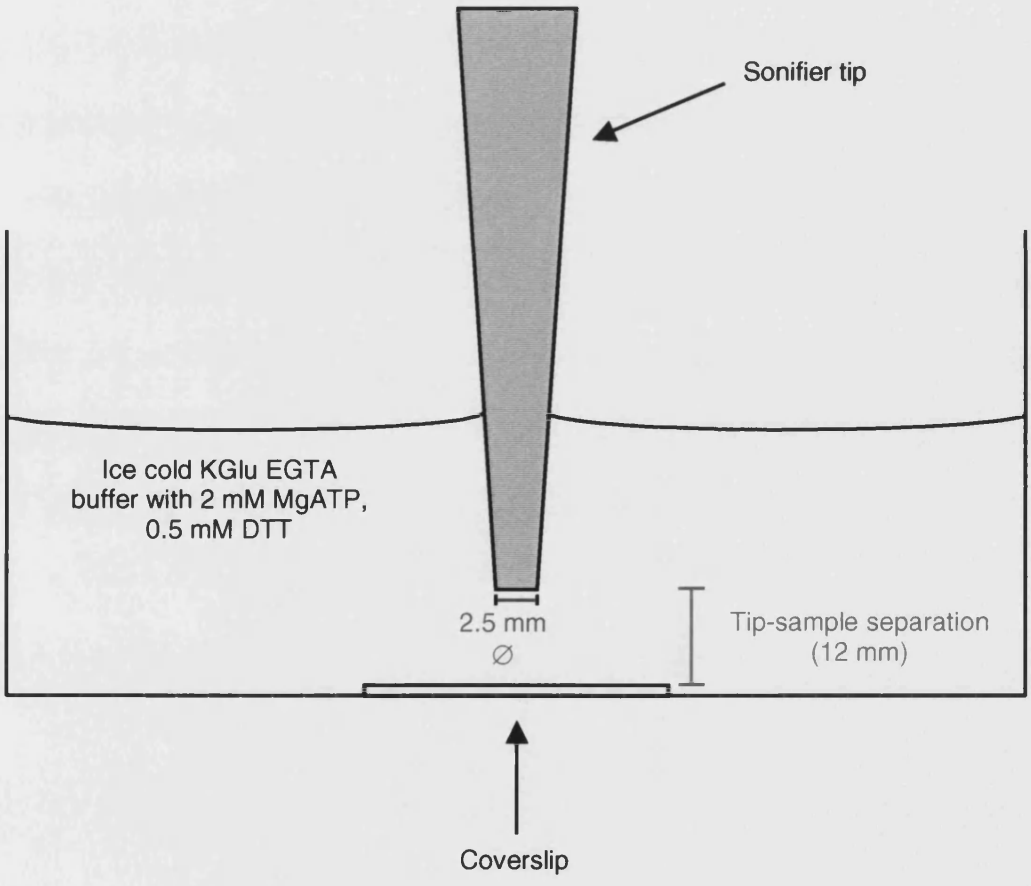

9. Acknowledgements

I would like to express my profound gratitude to Prof. Dr. Reinhard Jahn for the opportunity to perform my PhD within this department, for his patience, understanding and constant support and enthusiasm throughout. Dr. Thorsten Lang deserves special thanks for providing a guiding and experienced hand at all times. One could not have wished for a more committed source of ideas and guidance during his PhD. Many thanks!

I should like to thank Dr. Barbara Reaves for administering the Bath connections on my behalf, and for her kindness and generosity during all of my visits back to base.

I should also like to acknowledge the kindness and support of several lab members past and present: Wolfram Antonin, Stefan Pabst and Dietmar Riedel for many a shared joke and beer that have made the whole Göttingen experience much more memorable! Gottfried Mieskes for his kindness and wisdom without whom none of this would ever have been accomplished! Shigeo Takamori and Dieter Bruns for their countless hours of enchanting scientific discussion and input. And to all those that deserve to be thanked for behind the scenes activity that have somehow helped me in one way or another.

Finally, I wish to thank my wife and family for constant support, (moral and financial) patience, and encouragement throughout my PhD and previous studies.